

Georgia State University

**ScholarWorks @ Georgia State University**

---

Biology Dissertations

Department of Biology

---

Spring 5-7-2011

## **Control of Secondary Granule Release in Neutrophils by Ral GTPase**

Xiaojing Chen

Follow this and additional works at: [https://scholarworks.gsu.edu/biology\\_diss](https://scholarworks.gsu.edu/biology_diss)

---

### **Recommended Citation**

Chen, Xiaojing, "Control of Secondary Granule Release in Neutrophils by Ral GTPase." Dissertation, Georgia State University, 2011.

doi: <https://doi.org/10.57709/1997601>

This Dissertation is brought to you for free and open access by the Department of Biology at ScholarWorks @ Georgia State University. It has been accepted for inclusion in Biology Dissertations by an authorized administrator of ScholarWorks @ Georgia State University. For more information, please contact [scholarworks@gsu.edu](mailto:scholarworks@gsu.edu).

# CONTROL OF SECONDARY GRANULE RELEASE IN NEUTROPHILS BY RAL GTPASE

by

XIAOJING CHEN

Under the Direction of Yuan Liu, MD., Ph.D.

## ABSTRACT

Neutrophil (PMN) inflammatory functions, including cell adhesion, diapedesis, and phagocytosis, are dependent on the mobilization and release of various intracellular granules/vesicles. In this study, I found that treating PMN with damnacanthal, a Ras family GTPase inhibitor, resulted in a specific release of secondary granules, but not primary or tertiary granules, and caused dysregulation of PMN chemotactic transmigration and cell surface protein interactions. Analysis of the activities of Ras members identified Ral GTPase as a key regulator during PMN activation and degranulation. In particular, Ral was active in freshly isolated PMN, while chemoattractant stimulation induced a quick deactivation of Ral that correlated with PMN degranulation. Overexpression of a constitutively active Ral (Ral23V) in PMN inhibited chemoattractant-induced secondary granule release. By subcellular fractionation, I found that Ral, which was associated

with the plasma membrane under the resting condition, was redistributed to secondary granules after chemoattractant stimulation. Blockage of cell endocytosis appeared to inhibit Ral translocation intracellularly. In conclusion, these results demonstrate that Ral is a critical regulator in PMN that specifically controls secondary granule release during PMN response to chemoattractant stimulation.

INDEX WORDS: Neutrophil (PMN), Ral, Degranulation, Secondary granules, Transmigration

CONTROL OF SECONDARY GRANULE RELEASE IN NEUTROPHILS BY RAL GTPASE

by

XIAOJING CHEN

A Dissertation Submitted in Partial Fulfillment of the Requirements for the Degree of

Doctor of Philosophy

in the College of Arts and Sciences

Georgia State University

2011

Copyright by  
Xiaojing Chen  
2011

CONTROL OF SECONDARY GRANULE RELEASE IN NEUTROPHILS BY RAL GTPASE

by

XIAOJING CHEN

Committee Chair: Yuan Liu, MD., Ph.D.

Committee: Deborah Baro, Ph.D.

Zhi-Ren Liu, Ph.D.

Electronic Version Approved:

Office of Graduate Studies

College of Arts and Sciences

Georgia State University

May 2011

## **DEDICATION AND ACKNOWLEDGEMENTS**

This dissertation is dedicated to all the people who have helped me and guided me over the obstacles during my Ph.D. training at Georgia State.

I feel great honor to have Dr. Deborah Baro, Dr. Yuan Liu, and Dr. Zhi-Ren Liu in my committee. They have been constantly helping me in my scientific development.

In addition, I am truly thankful for the financial support provided to me by the Molecular Basis for Disease program at Georgia State.

Dr. Yuan Liu has truly been the mentor for my success in all aspects. I am really grateful to be her student and have the chance to be guided by her along my graduate study. Dr. Yuan Liu has successfully supported me to finish dissertation research at Georgia State. Her influence will guide my future life all the time.





**LIST OF ABBREVIATIONS**

ABTS	2, 2'-azino-bis 3-ethylbenzthiazoline-6-sulfonic acid
CB	cytochalasin B
CPZ	chlorpromazine hydrochloride
DAG	diacylglycerol
EGF	epidermal growth factor
fMLF	formyl-methionyl-leucyl-phenylalanine
GAP	GTPase activating protein
GEF	guanine nucleotide exchange factor
GPCR	G-protein-coupled receptor
HBSS	Hank's balanced salt buffer
HBSS (-)	Hank's balanced salt buffer devoid of $\text{Ca}^{2+}$ and $\text{Mg}^{2+}$
HEK293	human embryonic kidney 293 cells
HUVEC	human umbilical vein endothelial cells
ICAM-1	intercellular adhesion molecule 1
ITIM	immunoreceptor tyrosine-based inhibition motif
IP3	inositol trisphosphate
IPTG	isopropyl-beta-D-thiogalactopyranoside
JAM-A	junctional adhesion molecule-A
LTB4	leukotriene B4
LPA	lysophosphatidic acid
MAPK	mitogen-activated protein kinase
MHC	major histocompatibility complex

MMPs	matrix metalloproteinases
MPO	myeloperoxidase
PA	phosphatidic acid
PAF	platelet-activating factor
PBMC	peripheral blood mononuclear cell
PC	phosphatidylcholine
PMN	polymorphonuclear leukocyte
POA	phenylarsine oxide
PI3K	phosphatidylinositol-3 kinase isoform
PIP2	PI 4, 5-bisphosphate
PIP3	PI 3, 4, 5-bisphosphate
PKC	protein kinase C
PLC $\beta$	phosphatidylinositol-specific phospholipase C $\beta$
PLD	phospholipase D
PMA	phorbol myristate acetate
Raf-1 RBD	Ras binding domain of Raf-1
RalBP1	Ral binding protein 1
RalGAP	Ral GTPase activating protein
RalGDS	Ral guanine nucleotide dissociation stimulator
RalGDS-RBD	Ral GDS-Rap Binding Domain
RBC	red blood cell
RBD	GTP-Ral-binding domain
Rgl	ralGDS-like

Rgl3	Ral GEF-like 3
Rlf	RalGDS-like factor
SNAREs	soluble NSF (N-ethylmaleimide-sensitive factor)
TBK1	Tank binding kinase 1
VCAM-1	vascular cell-adhesion molecule 1
WGA	wheat germ agglutinin

## LIST OF TABLES

- |   |         |
|---|---------|
| 1. Damnacanthal treatment induces an upregulation of CD11b/CD18, CD47<br>and SIRP $\alpha$ on PMN surface | Page 67 |
|---|---------|

## LIST OF FIGURES

Figure	Page
1-1 PMN activation and category of chemoattractants	5
1-2 fMLF-mediated activation pathways in PMN	9
1-3 PMN transmigration to the target site	13
1-4 PMN transendothelial migration	14
1-5 Putative structure of integrin CD11b/CD18	15
1-6 PMN transepithelial migration	16
1-7 Putative structure of SIRP $\alpha$ (left) and CD47 (right)	17
1-8 PMN play a pivotal role in inflammation	21
1-9 PMN granules types (A) and degranulation (B) in response to stimulation (e.g. fMLF)	24
1-10 Interchange of GTP-bound form with GDP-bound form of small GTPase	28
1-11 Ral domain structure	41
1-12 Sequence alignment of RalA and RalB	42
1-13 Control of secondary granule release in neutrophils by Ral	44
2-1 GTPase pull down assay	52
2-2 HIV-Tat-Ral expression and purification system	57
3-1 Damnacanthal treatment induces specific release of PMN secondary granules	68
3-2 Damnacanthal inhibits chemoattractant-triggered PMN function	70
3-3 Damnacanthal inhibits chemoattractant-triggered PMN function	71
3-4 Damnacanthal inhibits chemoattractant-triggered PMN function	72
3-5 Lck is not expressed in neutrophils (PMN)	75

3-6	Ral deactivation correlates secondary granule release in PMN	78
3-7	Ral deactivation correlates secondary granule release in PMN	79
3-8	Detecting activity changes of Ral in PMN isolated directly from “buffy coat”	80
3-9	Ral deactivation correlates secondary granule release in PMN	81
3-10	Ral deactivation correlates secondary granule release in PMN	82
3-11	Generation of Tat-tagged wild-type Ral (WT), constitutively active Ral (Ral23V), and dominant negative Ral (28N) protein	87
3-12	Transduction of Tat-tagged Ral proteins including wild-type Ral (WT), constitutively active Ral (Ral23V), and dominant negative Ral (28N) to PMN	88
3-13	Tat-tagged constitutively active Ral sustained endogenous Ral activity in PMN	89
3-14	Constitutively active Ral (Ral23V) inhibits chemoattractant-induced secondary granule release in PMN	90
3-15	Specificity of Tat-tagged Ral proteins in PMN granule release	91
3-16	Constitutively active Ral (Ral23V) inhibits chemoattractant-induced secondary granule release in PMN isolated using lympholyte-poly	92
3-17	Constitutively active Ral (Ral23V) inhibits chemoattractant-induced secondary granule release in PMN isolated directly from “buffy coat”	93
3-18	Constitutively active Ral (Ral23V) inhibits chemoattractant-induced secondary granule release in PMN isolated from “buffy coat”	94
3-19	Detection of RalA and RalB in human leukocytes	95
3-20	Constitutively active RalB (Ral23V) inhibits chemoattractant-induced secondary granule release	96
3-21	Localization of Ral in PMN	100

3-22	In unstimulated PMN, Ral is active in plasma membrane and inactive in secondary granules	101
3-23	Localization of Ral in PMN	102
3-24	Ral translocation from the plasma membrane to secondary granules may follow fMLF-induced endocytic process	103
3-25	Blockage of clathrin-dependent endocytosis inhibits fMLF-induced secondary granule release	104
4-1	Expression of RalGDS in different cell types	112
4-2	A study of chemoattractant stimulation-induced increase of intracellular calcium, secondary granule release and Ral activity changes in PMN	113
4-3	A study of chemoattractant stimulation-induced increase of intracellular calcium, secondary granule release and Ral activity changes in PMN	114
4-4	Mg <sup>2+</sup> inhibits Ral activity in PMN	115
4-5	Effects of damnacanthol alone or in a combination with fMLF on PMN granule release	116
4-6	Subcellular fractionations studying the effects of damnacanthol and endocytosis inhibitors on Ral distribution in PMN	117
4-7	Subcellular fractionations studying the effects of damnacanthol and endocytosis inhibitors on Ral distribution in PMN	118
5-1	RAGE was amplified from human intestinal epithelial cells by RT-PCR	119
5-2	RAGE was detected from epithelial cell lines by western blot	120
5-3	RAGE was detected in intestinal epithelial cells by immunofluorescence staining	121
5-4	Generation of GST-exRAGE fusion protein	122

5-5	RAGE antibody titer test by ELISA	123
5-6	RAGE antibody titer test by western blot	124
5-7	RAGE detection from human PMN	125
5-8	Generation of GST-JAML fusion protein	126
5-9	JAML antibody titer test by ELISA and western blot	127
5-10	JAML was expressed on PMN and monocytes	128
5-11	Ala57, Gln67, and Val57 were key amino acid residues mediating binding interaction of SIRP $\alpha$ to CD47	129



## **CHAPTER I**

### **GENERAL INTRODUCTION**

#### **1. Neutrophils (PMN)**

Neutrophils, also termed PMN, are polymorphonuclear leukocytes characterized by their multi-lobed nuclei [1]. PMN, which are generated from bone marrow, are abundant cells in circulation and account for 40-75% of all leukocytes [2]. Up to  $1-2 \times 10^{11}$  PMN are steadily generated per day in a healthy adult [3]. Constant numbers of PMN in the circulation are very crucial for maintaining host homeostasis [4-6]. Granulocyte colony stimulating factor (G-CSF) has been shown to positively regulate PMN production in bone marrow, but G-CSF is not completely required for PMN generation [7-8]. The release of PMN from bone marrow is largely dependent on CXCR4 [9]. It is likely that CXCR4 functions a gatekeeper for blocking PMN migrating out of bone marrow [10-15]. In CXCR4-deficient chimera mice, myeloid precursors are significantly decreased and peripheral granulocytic cells are increased by about three-fold compared with wild type-litter mates [16-17]. Blocking CXCR4 function with the inhibitory antibody/antagonist, AMD3100, elevates PMN counts in circulation [10, 14-15]. Additionally, AMD3100 dose-dependently increases the release of CD34+ hematopoietic progenitor cells into circulation as demonstrated in healthy human volunteers [10, 14]. Presumably, the negative effect of CXCR4 is through the signaling cascade of CXCL12 (stromal derived factor-1, SDF-1)/ CXCR4 [18]. Under the influence of inflammation, however, PMN production is increased. In circulation, non-activated PMN have 8-16 hours average half-lives [19]. After stimulation, active PMN are recruited to the target tissue where they survive for only 1-4 days [20-21]. PMN are disposed from circulation mainly at the spleen, liver, bone marrow and the site of inflammation [22-24]. Macrophages play a pivotal role in the clearance of both circulating PMN under nonpathologic con-

ditions and inflammatory PMN in the target tissue [4]. In addition to macrophage phagocytosis, PMN apoptosis [21] is also a key factor in preventing excessive PMN infiltration-mediated inflammation, tissue damage and organ dysfunction, thus maintaining cellular homeostasis.

PMN are the first cells recruited to the site of an infection [25]. Recruitment of circulating PMN from blood vessels to the site of inflammation is very important for eliminating invading microorganisms, recovering tissue damage and maintaining homeostasis [26]. Through releasing reactive oxygen species, antimicrobial proteins, proteolytic enzymes and producing cytokines, as well as performing phagocytosis, PMN eliminate microorganisms, and thus are essential for innate immunity [27]. Most notably, PMN infiltration is the hallmark of the early stages of the inflammatory response [28]. On the contrary, dysregulated PMN functions are also closely linked to tissue damage and organ dysfunction.

#### I. Chemoattractants and their receptors in PMN transmigration

Leukocyte chemoattractants include interleukin (IL)-4, IL-8, platelet-activating factor (PAF), and formyl-Methionyl-Leucyl-Phenylalanine (f-Met-Leu-Phe, fMLF), leukotriene B<sub>4</sub> (LTB<sub>4</sub>), C3a and C5a [29]. Leukocyte chemoattractants can be further grouped into several main categories such as chemokines [30], bacterial products, immunoproducts, phospholipids, etc. They are released by numerous types of cells. For example, activated endothelial cells secrete IL-4, LTB<sub>4</sub>, and PAF, while activated stromal cells, including macrophages, epithelial cells, etc. secrete LTB<sub>4</sub> and PAF. In addition, bacteria or dying cells release fMLF [31]. The combination of chemoattractants and their gradient drives PMN chemotactic migration towards an inflammatory site [31] (Figure 1-1).

According to derivation, chemoattractants can be further divided into “regulatory cell-derived chemoattractants” and “end target-derived chemoattractants”. Regulatory cell-derived chemoattractants include IL-8 and LTB<sub>4</sub>, etc. End target-derived chemoattractants are mainly composed of fMLF, derived from bacteria or the mitochondria of dying cells, and complement C3a and C5a [31]. Migrating out of the blood stream, PMN encounter a combination of chemoattractants released from the endothelium and infected tissues. Through integration of those series of chemoattractants, PMN effectively reach the target site. It has been proposed that chemoattractant receptor cross-desensitization is one of the mechanisms regulating PMN chemotaxis [32-34]. Moreover, the combinational and sequential signals of distinct chemoattractants navigate PMN chemotaxis to a great extent [35-37]. When placed in a chemoattractant gradient, PMN vigorously migrate towards the gradient in spite of the original migration pathways. Furthermore, PMN are able to integrate signals from different chemoattractants, and thus migrate toward the target. End target-derived chemoattractants, such as fMLF and C5a, however, are substantially dominant over cell-derived chemoattractants, such as IL-8 and LTB<sub>4</sub> [35-37].

Pre-exposure with fMLF or C5a causes PMN to lose the response to IL-4 and LTB<sub>4</sub>. This phenomenon might be a reasonable explanation for the fact that PMN respond to eliminate existing invading bacteria first compared to tissue damage. It has also been demonstrated that PMN fail to transmigrate towards IL-4 or IL-8 when cells are pre-treated with fMLF or C5a in the presence or absence of an endothelial monolayer. This desensitization of PMN is likely associated with the polymerization of actin filaments [36], because the end target-derived chemoattractants trigger sustained and prolonged actin polymerization. Other studies have shown that PMN are able

to migrate down a concentration gradient towards another chemoattractant. They can also migrate beyond the inhibitory maximum concentration toward another different chemoattractant [35]. In addition to the signals received by PMN upon stimulation with different chemoattractants, chemoattractant receptor cross-desensitization also plays a key role in PMN chemotaxis. Cpd43, an agonist of formyl peptide receptors 1 and 2, not only inhibits the ability of PMN to further respond to IL-8, C5a and LTB<sub>4</sub>, but also results in the loss of the expression of CXCR1, CXCR2, C5a and LTB<sub>4</sub> on cell surface [33]. Treatment of PMN with fMLF or C5a reduces the binding of IL-8R $\beta$  to its antibody [34]. These miscellaneous factors enable PMN efficiently and precisely mobilize to their targets through a complex chemotactic field.

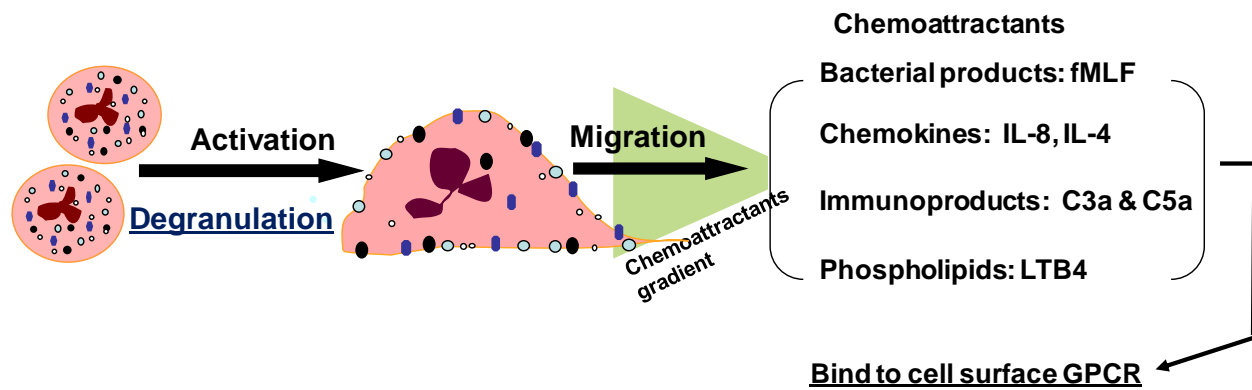


**Figure 1-1.** PMN activation and category of chemoattractants

## II. Chemoattractant, fMLF-mediated signaling transduction cascade in PMN

Various signaling pathways are implicated in PMN migration. One of the well characterized pathways is fMLF-mediated PMN stimulation [38] (Figure 1-2). Upon fMLF binding, its trimeric G-protein-coupled receptor (GPCR), composed of  $\alpha$ ,  $\beta$ , and  $\gamma$  subunits [39], is activated and undergoes a conformational change. Ligand binding induces the switch of GDP-bound inactive form to the GTP-bound active form, resulting in the low affinity of  $G_\alpha$  towards  $G_{\beta\gamma}$ . The dissociation of  $G_\alpha$  with  $G_{\beta\gamma}$  activates its own individual downstream effectors, including phosphatidylinositol-specific phospholipase-C $\beta$  (PLC $\beta$ ), adenylyl cyclase and phosphatidylinositol-3 kinase isoforms (PI3K).

Activated PLC $\beta$  hydrolyzes PI 4, 5-bisphosphate (PIP<sub>2</sub>) into inositol trisphosphate (IP3) and diacylglycerol (DAG). IP3 then diffuses into the cytosol, binds to the IP3 receptor and results in Ca<sup>2+</sup> release from ER storage. Released Ca<sup>2+</sup> involves in activation of PKC and triggers extracellular calcium influx, presumably through the interaction of the IP3 receptor with plasma membrane channels [40-42]. Ca<sup>2+</sup>, a pivotal second messenger, is crucial for the reorganization of actin filaments. Ca<sup>2+</sup> facilitates the binding of myosin, the motor protein, to actin through exposing the myosin binding site on actin, and thus is involved in plasma membrane protrusion, lamellipodia formation, and PMN migration [43]. DAG activates protein kinase C (PKC), thus resulting in a series of protein phosphorylation. Serving as a second messenger, PKC further activates a series of downstream signaling molecules involved in PMN adhesion [44-45]. In PMN, PKC also associates with the respiratory burst [46]. There are five isoforms of PKC expressed in PMN, including PKC- $\alpha$ , PKC- $\beta$ 1, PKC- $\beta$ II, PKC- $\delta$ , and PKC- $\zeta$  [47]. It has been shown that, shortly after fMLF stimulation, PKC- $\alpha$ , PKC- $\beta$ 1, PKC- $\beta$ II and PKC- $\delta$  activate NADPH oxidase, leading

to superoxide anion generation [47]. As demonstrated by in vitro phosphorylation assays, among the different PKC isoforms are PKC- $\alpha$ , PKC- $\beta$ II, PKC- $\delta$  and PKC- $\zeta$  phosphorylate p47<sup>phox</sup> and DADPH oxidase [48]. Inhibition of PKC- $\beta$  with its specific inhibitor results in abolished activity of NADPH oxidase activity induced by PMA [49]. PKC- $\beta$ <sup>-/-</sup> mice, however, show a defect only in NADPH oxidase activity, suggesting that PKC- $\beta$  may not be associated with PMN migration [49-50].

Upon dissociation with G $\alpha$ , the G $\beta\gamma$  subunit also activates PI3K, leading to actin polymerization [51-53]. PMN express four types of PI3K, including PI3K $\alpha$ , PI3K $\beta$ , PI3K $\delta$  and PI3K $\gamma$  [54], which are involved in cytoskeleton organization and respiratory burst. PI3K $\gamma$ <sup>-/-</sup> PMN demonstrate impaired migration in Casein- and Listeria-induced peritonitis mice models [55], and abolished transmigration towards fMLF as illustrated in in vitro transmigration assays [50, 55]. Inhibition of PI3K $\delta$  by a specific inhibitor, IC8711, diminishes PMN spreading in response to fMLF stimulation, and also blocks PMN chemotaxis [56], implicating the important role of PI3K $\delta$  in PMN directional movement. Similar effects are also observed in wortmannin or LY294002 (PI3K inhibitors) -treated HL-60 cells [57]. Treatment of PMN with wortmannin, reverses anti- $\beta$ 3-integrin mAb-mediated inhibited migration in response to fMLF [54], suggesting that the effect of PI3K in PMN migration is likely through targeting  $\beta$ 3-integrin. PI3 $\gamma$ , on the other hand, also contributes to PMN respiratory burst through phosphorylating PIP<sub>2</sub> into PI 3, 4, 5-bisphosphate (PIP<sub>3</sub>), which activates PKC [53].

In contrast to PLC $\beta$  and PI3K, the role of adenylyl cyclase in PMN is not well understood. Studies have shown that fMLF leads to a transient increase of cAMP in PMN through augmenting

the adenylyl cyclase response [58]. Elevated cAMP has been shown to inhibit PMN chemotaxis to fMLF [59]. However, limited studies exploring the role of cAMP in PMN utilizing inhibitors of phosphodiesterase have been performed. Blocking the breakdown pathway of cAMP using inhibitors of phosphodiesterase results in markedly impaired adhesion of PMN to the endothelium and decreased cell surface expression of CD11b/CD18 [60], suggesting adenylyl cyclase is involving in the PMN adhesion step.

Moreover, fMLF activates Rho small GTPase, including Rho, Rac and Cdc42, all of which regulate PMN migration through affecting actin filament formation [39, 52]. The MAPK cascade is also activated after fMLF stimulation, thus leading to chemotaxis activation and superoxide production [38-39]. Considering the complex signaling cascades in stimulated PMN, the fMLF-mediated signaling pathway is very critical to PMN chemotactic migration and superoxide production.



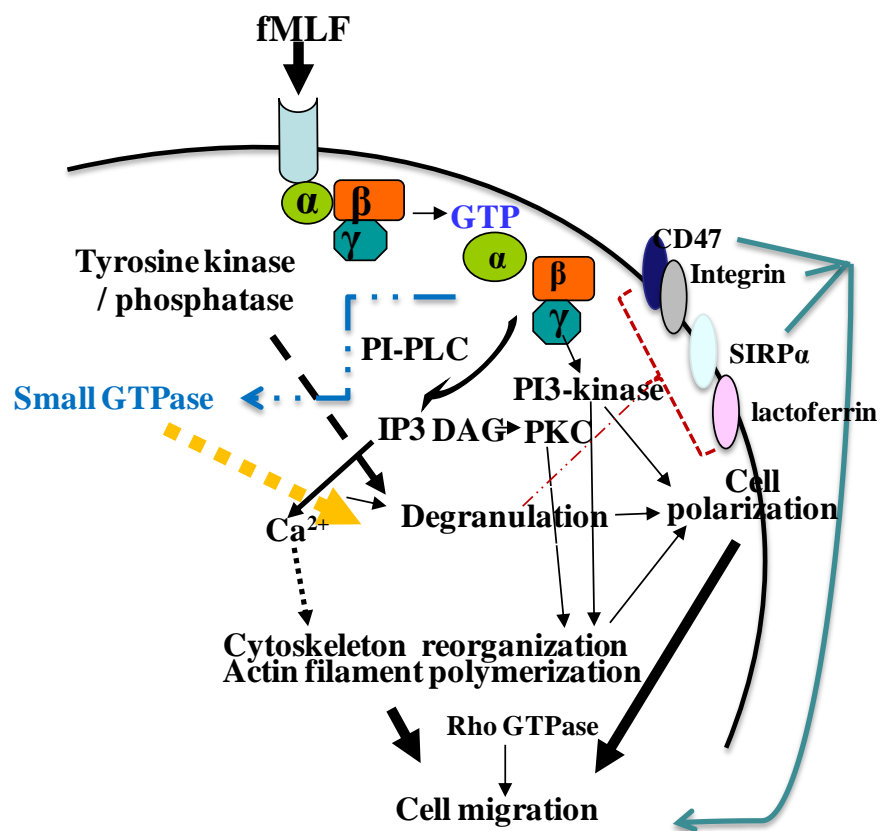


**Figure 1-2.** fMLF-mediated activation pathway in PMN.

### III. Key adhesion molecules involved in PMN transendothelial and transepithelial migration

As a first line of defense, PMN are required to respond quickly to the invading microorganism. They transmigrate toward the sites of injury or inflammation under the influence of the chemoattractant gradient. Depending on the target site, PMN transmigration toward the infectious site is generally composed of transendothelial migration and transepithelial migration (Figure 1-3). Along the process, PMN transform from resting cells into activated cells and directionally migrate toward the target site. A variety of adhesive molecules, cell surface receptors, signaling molecules and adaptor molecules are involved in this transition.

Upon chemoattractant stimulation, adhesion molecules are gradually released from secondary and tertiary granules of PMN to the surface. This vital degranulation process enables PMN to adhere and migrate across the vascular endothelium and tissue layers [26, 61-65].  $\beta_2$  integrin CD11b/CD18, also termed as Mac-1 or  $\alpha_M\beta_2$  [66-67], and Ig superfamily members, including CD47 and SIRP $\alpha$  [68-71], are all required for PMN adhesion and chemotaxis. PMN transendothelial migration (Figure 1-4) is composed of tethering and rolling, adhesion and transmigration [26, 31, 65, 72]. Among those steps, integrin CD11b/CD18 (Figure 1-5) plays a conclusive role in the PMN adhesion step through interacting with its ligand, intercellular adhesion molecule (ICAM)-I [73] located on endothelial cells. It has been shown that CD11b/CD18, mainly localized in the secondary granules of PMN, translocate into the plasma membrane upon stimulation of PMN with fMLF, PMA or ionomycin [74]. The attachment of activated PMN to unstimulated human umbilical vein endothelial cells (HUVEC) is blocked in the presence of anti-CD11b monoclonal antibodies (mAbs) [75-77]. The adherence of unstimulated PMN to stimulated HUVEC

is also inhibited by anti-CD11bAb, LM2/1 [78]. In CD11b/CD18 deficient mice, the attachment of PMN to ICAM-1 is decreased compared with wild-type mice [79].

CD11b/CD18-mediated adhesion not only extensively contributes to transendothelial migration but also transepithelial migration (Figure 1-6). PMN transepithelial migration consists of adhesion, migration and post-migration [67, 80-81]. Adhesion of PMN to epithelial cells is mediated by the interaction of CD11b/CD18 on PMN with its ligands, fucosylated proteoglycan(s), located on epithelial cells. This interaction triggers the opening of apical junction complex mainly through regulation of myosin phosphorylation. As a result, following phosphorylation, junction complexes open and facilitate PMN transmigration. Upon reaching the lumen, CD11b/CD18 interacts with ICAM-1 on the apical epithelial site and further assists PMN transepithelial migration toward the damaged site [65].

In addition to CD11b/CD18, CD47, SIRP $\alpha$  and JAM-A are also actively involved the process of PMN transmigration. CD47 (Figure 1-7) is an important regulator in facilitating PMN transmigration. In PMN, CD47 is kept in the secondary granules and is re-distributed to the cell surface after chemoattractant stimulation, leading to the promotion of PMN migration [69]. It was first discovered that PMN migration was inhibited in the presence of anti-CD47 antibodies [71, 82-83]. Later research further demonstrated PMN transmigration across T84 monolayers and cell-free collagen-coated filters is delayed when cell are treated with inhibitory anti-CD47 antibodies C5D5 and B6H12 [69]. Indeed, functionally inhibitory anti-CD47 mAbs delay, but do not block, the process of PMN transepithelial migration and migration across a collagen-coated transwell toward fMLF [69]. When challenged with *Escherichia coli*, CD47<sup>-/-</sup> mice demonstrated a defect

in the early stages of PMN migration [84]. In addition to its effect in PMN, CD47 has been implicated in the migration in other cell types. Likewise, CD47<sup>-/-</sup>-epidermal dendritic cells (DCs) demonstrate decreased migration toward draining lymph nodes in vivo [29]. Transduction of neuroblastoma cells with CD47 results in neurite and filopodium formation [85]. Additionally, through in vitro experimentation, it is uncovered that CD47 is important for the migratory activity of B cells [86].

SIRP $\alpha$  (Figure 1-7), a counter ligand for CD47 [87], also contributes greatly in PMN migration. Similar to the distribution of CD47 in PMN, SIRP $\alpha$  translocates from secondary granules to the cell surface after fMLF stimulation [68, 70]. PMN transepithelial migration is inhibited using anti-SIRP $\alpha$  mAbs. The SIRP $\alpha$ -CD47 interaction leads to significantly decreased PMN migration [68], suggesting that SIRP $\alpha$  delivers a negative signal to PMN migration through its immunoreceptor tyrosine-based inhibition motif (ITIM).

Junctional adhesion molecule-A (JAM-A) is also engaged in regulating PMN migration, particularly in PMN transendothelial migration [81, 88]. JAM-A redistributes to the cell surface under inflammatory condition [89], thus facilitating PMN migration. Treatment of HUVECs with a blocking antibody against JAM-A [90] impairs PMN transmigration. The effect of JAM-A is likely through the interaction of JAM-A with its ligand,  $\beta_2$  integrin LFA-1, on leukocytes [90].

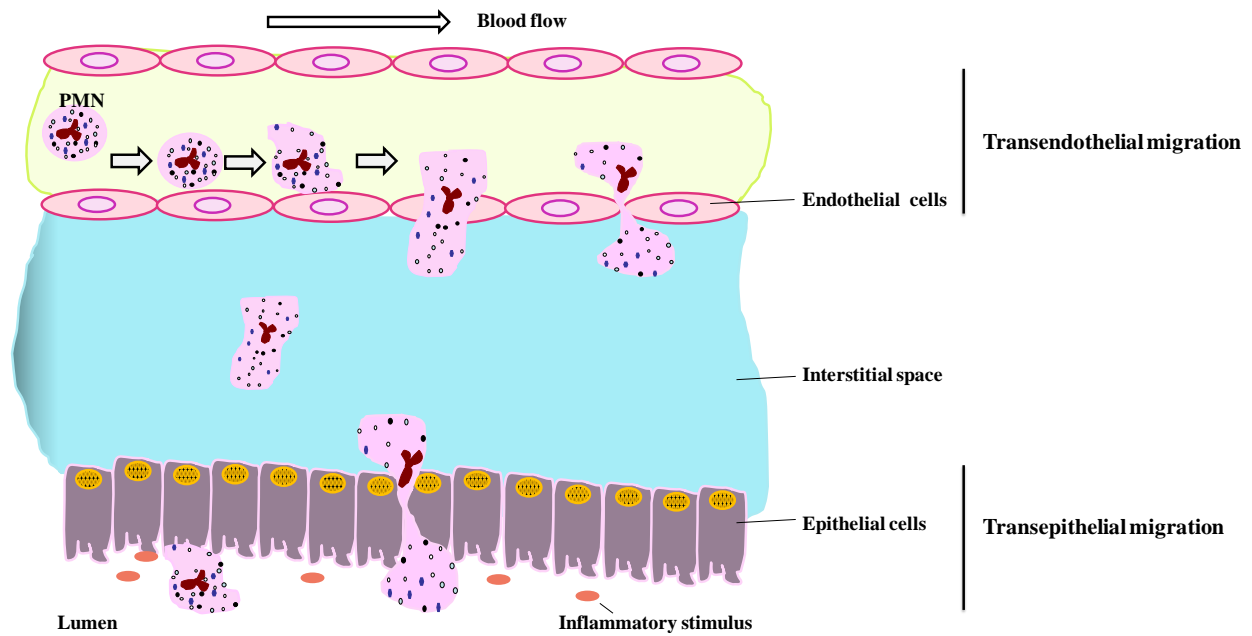


**Figure 1-3.** PMN transmigration to the target site. Depending on the target site, PMN transmigration towards the infectious site is generally composed of transendothelial migration and transepithelial migration.

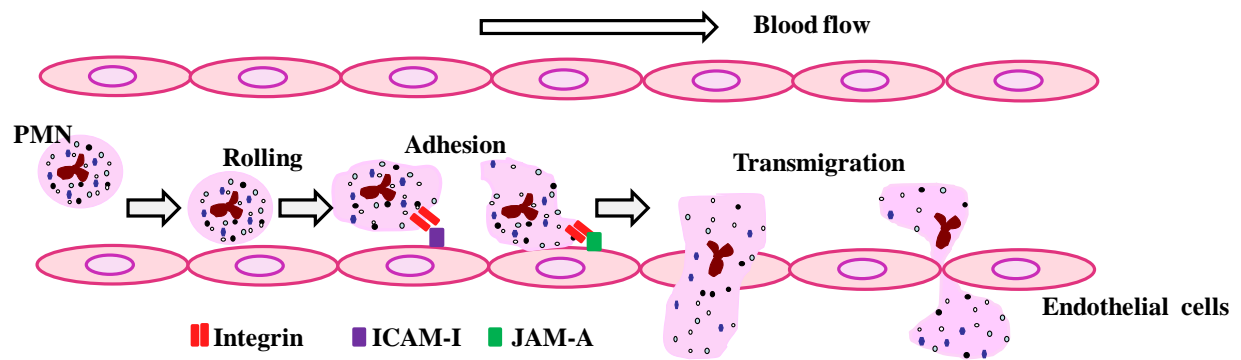


**Figure 1-4.** PMN transendothelial migration.

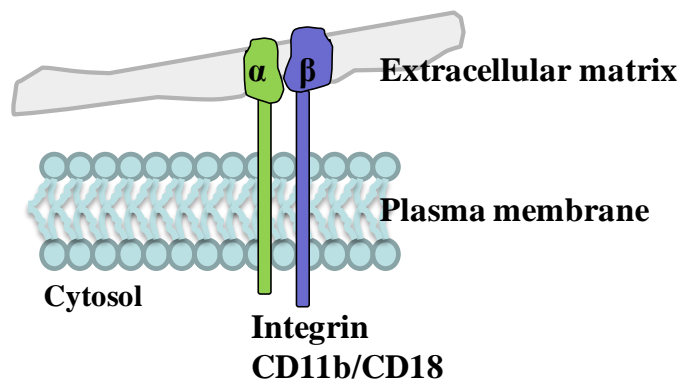


**Figure 1-5.** Putative structure of integrin CD11b/CD18. CD11b/CD18 is composed of  $\alpha$  and  $\beta$  subunits.

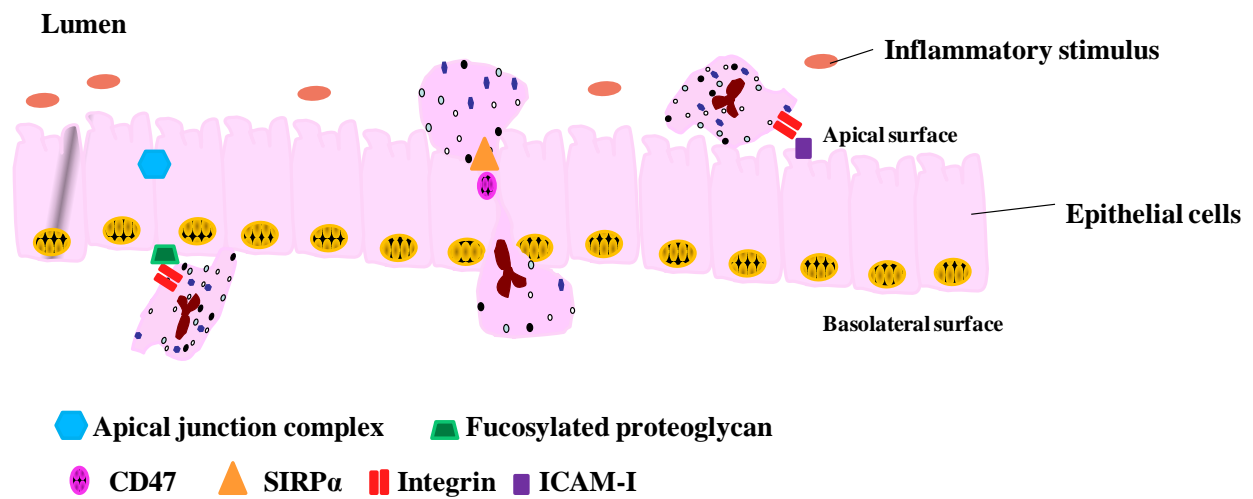


**Figure 1-6.** PMN transepithelial migration.



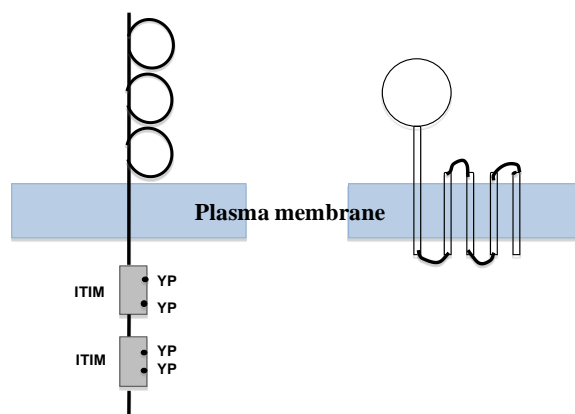


**Figure 1-7.** Putative structure of SIRP $\alpha$  (left) and CD47 (right).

## 2. Inflammation

Throughout evolutionary history, human beings have continued to defend against invasion by microorganisms. We successfully resist to infections most of time because of our complex immune system. The immune system includes both the innate immunity and the adaptive immunity. Innate immune immunity takes place first and occurs within the first 96 hours. PMN and macrophages are the key players for innate immunity. Through phagocytosis, they eliminate invading microorganisms. Incomplete clearance results in the response of the adaptive immune system mainly involving in lymphocytes. Coordination of the innate immunity with the adaptive immunity is crucial to fight efficiently against infection.

Inflammation is an innate immune response to local injury or infection [28] (Figure 1-8). The occurrence of inflammation is due to insufficient removal of invading microorganism. In inflammation, innate immune response takes place first [91]. In the local environment, resident tissue cells sense the presence of pathogens, secrete cytokines acting on other cells and trigger the innate immune response. Under the influence of cytokine networks, vascular dilation occurs and edema takes place, characterized by the leaking of plasma and fluid into connective tissues due to the permeability change of endothelial cells. At the same time, edema leads to a change in the nervous system, thus resulting in a feeling of pain [28]. In addition to vascular events, cellular events also play a primary role in inflammation. In the local environment, high concentrations of chemoattractants secreted by activated stromal cells, including activated endothelial cells and macrophages, etc. [31], and increased surface expression of adhesion molecules on the endothelium lead PMN to undergo rolling, activation, adhesion and transmigration across the endothelial mo-

nolayer to the targeted tissue to release anti-microbial substances and phagocytize pathogens [92].

PMN are vital for the beginning stage of inflammation [25]. PMN infiltration is the hallmark of the early-stage of inflammatory response [28]. After they arrive at the target site, PMN execute their function by releasing reactive oxygen species, antimicrobial proteins and proteolytic enzymes, as well as by producing cytokines and performing phagocytosis [27]. Thus, sufficient recruitment of PMN is very important for eliminating invading microorganisms, recovering tissue damage and maintaining homeostasis [26]. In particular, during acute infection and inflammation, PMN sense chemoattractant signals and swiftly migrate across the microvasculature and underlying tissues to accumulate at inflammatory foci. Here, these cells execute forceful antimicrobial and tissue damaging functions. Therefore, the timely and precise response of PMN is critical for innate immune response.

In spite of the critical role of PMN in acute inflammation, efficient removal of PMN in the late stage of inflammation is substantial [93-94]. PMN apoptosis [95] and removal by macrophages control the extent of inflammation. The prolonged existence of PMN in the targeted tissue also frequently results in host-tissue damage. PMN-mediated inflammation is one of the central components of many pathophysiological processes; thus, diseases in which dysregulated PMN transmigration and activation occur often result in severe tissue injuries and organ dysfunction [25, 96]. Many active stage of human diseases are characterized by excessive PMN infiltration, including bacterial infection, inflammatory bowel disease, ischemia-reperfusion injury, rheumatoid arthritis, etc. [31].

Furthermore, resident tissue cells such as macrophages and dendritic cells contribute largely to inflammation [93-94, 97-98]. After engulfing pathogens, macrophages secrete cytokines to further recruit other cells for assistance. After engulfing pathogens, dendritic cells migrate toward secondary lymphoid organs to induce adaptive immune responses. Upon dendritic cell migration into the secondary lymphoid organs, degraded pathogens are presented by major histocompatibility complex (MHC) on the surface and recognized by naive T lymphocytes. Activation through recognition of the MHC-antigen complex with T cell receptors and co-stimulatory signals causes pathogen-specific T lymphocytes to differentiate to T helper cells or cytotoxic T cells. T helper cells are able to activate B cells leading to the generation of plasma cells and secrete antibodies. Some plasma cells and antibodies leave lymphoid organs and enter infectious tissues for eliminating pathogens. Through releasing cytokines, T helper cells also further activate macrophages in the tissue to increase their abilities to phagocytize pathogens. Compared with T helper cells, cytotoxic T cells migrate to the target tissue and directly remove pathogens through releasing cytotoxins or inducing apoptosis through a Fas ligand-Fas interaction. In conclusion, inflammation is a complex process whereby innate immunity coordinates with adaptive immunity to fight against pathogens.

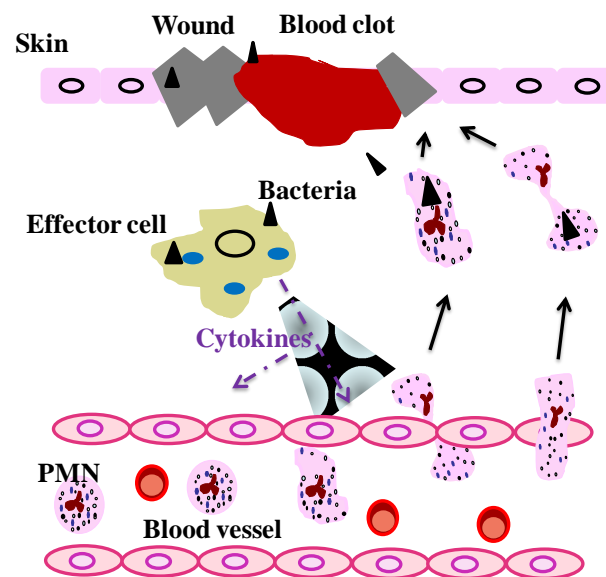


**Figure 1-8.** PMN play a pivotal role in inflammation. PMN infiltration is the hallmark of the early stage of the inflammatory response.

### 3. PMN granules

Different from other cells types, circulating PMN only express a few cell surface proteins [62]. Instead, they keep most of those proteins in special membrane bound storages called granules [61] (Figure 1-9). According to size and morphology, PMN granules are composed of four categories, primary granules (azurophil granules), secondary granules (specific granules), tertiary granules (gelatinase granules) and secretory vesicles [63]. Each granule contains different protein components and possesses distinct functions.

Primary granules, regarded as lysosomes, undergo limited degranulation in response to outside stimuli [99]. Primary granules are important storage for antimicrobial proteins, serine proteases [100-101] including elastase and cathepsin G [102], and proteinase 3 [63]. Myeloperoxidase (MPO) is a marker for primary granules [103]. It plays a key role in PMN phagocytic function, due to its strong antimicrobial activity [104], through interaction with  $H_2O_2$  formed by superoxide anions in the respiratory burst system. During the process of phagocytosis, serine proteases, localized inside phagolysosome, work together with hypochloric acid, a final product generated in a series of reactions catalyzed by MPO, to execute antimicrobial activities. In addition to killing microorganisms in phagolysosomes, elastase are also released during PMN activation in response to various chemoattractants stimulation [105]. Upon release, serine proteases play a very important role in chemokine modification that leads to an increased binding affinity towards the chemokine receptor. Chemokines modified by serine proteases gain increased chemotactic activity for PMN ,and thus, are essential for PMN migration [100]. Serine proteases are also capable of cleaving intercellular adhesion molecules, ICAM-1 [106], vascular cell-adhesion molecule

1 (VCAM-1) [107] and epithelial (E)-cadherin [108], thus facilitating PMN transmigration across the endothelium and epithelial cells. As a result, certain primary granules not only function as lysosomes during PMN phagocytosis, but also contribute to the interaction between PMN and the extracellular matrix during PMN migration.

Secondary granules are important stores of adhesion molecules, membrane receptors and other critical proteins, such as lactoferrin, fMLF receptors, CD47, SIRP $\alpha$ , and CD11b/CD18, facilitating PMN migration [63, 68-69]. Lactoferrin is a marker of secondary granules [103], and its antimicrobial activity comes from competing with microorganisms for iron [109]. PMN from patients with neutrophil-specific granule deficiency [110] are defect in chemotaxis in response to stimuli, decreased binding capability to fMLF, decreased antibacterial activity and less activity in response to fMLF stimulation. Other cases of PMN secondary granule deficiency also illustrated decreased chemotaxis and impaired killing of microorganisms [111]. These characteristics further suggest that secondary granules, enriched in receptors and adhesion molecules, are indispensable for PMN to execute anti-infection functions.

Tertiary granules serve as reservoirs of matrix-degrading enzymes [63]. The key component in tertiary granules is gelatinase. Gelatinase, also termed matrix metalloproteinases (MMPs), enzymatically digest extracellular matrix proteins during PMN transmigration. In human PMN, two MMPs have been identified. They are MMP-9 (92KDa) and leukolysin (MT6-MMP/MMP-25) (56KDa) [63, 112]. Compared with secondary granules, tertiary granules are more mobilized and easily exocytosed upon stimuli activation [99].

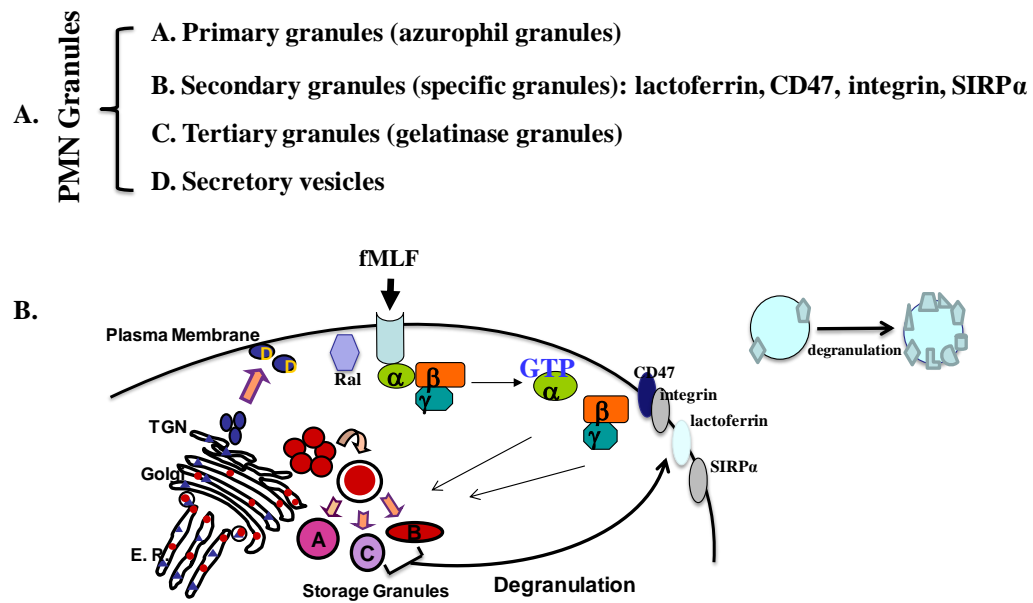


**Figure 1-9.** PMN granules types (A) and degranulation (B) in response to stimulation (e.g. fMLF).



Secretory vesicles are highly mobilized [99], and they contain membrane-associated receptors and are able to furnish PMN with the first batch of proteins for sensing and triggering activation during PMN-mediated immune responses [61]. Secretory vesicles contain the marker protein albumin [113]. It has been demonstrated that albumin is originally from PMN plasma membranes, not from new synthesis, suggesting that albumin comes from endocytosis pathway. The quick interchange of albumin between the plasma membrane and secretory vesicles further implies that secretory vesicles are very sensitive to exocytosis. Furthermore, PMN are able to mobilize secretory vesicles even in the absence of stimulation [114].

The classification of granules does not only rely on the size and morphology of granules. The components in each granule depends on the time that those proteins are synthesized (targeting-by-timing hypothesis) and the characteristics of each protein, i.e. whether it is able to co-exist to avoid degradation [99]. In addition to the presence or absence of MPO, the major difference between the secondary and primary granules lies in the fact that proteases stored in primary granules are in activated forms; proteases in secondary granules exist as latent forms and need to be activated after release from PMN. However, the detailed mechanisms underlying processing and targeting of granule proteins in PMN are unclear. It has been implied that the Golgi network is likely to function as a sorting apparatus in PMN [61]. Studies of serine proteases stored in primary granules have shown that glycosylation, a major function of the Golgi network, is not required for granule protein targeting [99]. Specifically, Cathepsin G does not require glycosylation for granule targeting [115]. Through site-directed mutagenesis, Cathepsin G lacking an N-linked glycosylation site was still shown to be transported to lysosomes. In addition to protein confor-

mation and modification, such as glycosylation, protein-protein interaction is also crucial for correct granule targeting, particularly for lactoferrin, which is a key component for secondary granules [103]. A study on transport of newly synthesized lactoferrin demonstrated that the transport of lactoferrin was blocked by interfering ionic interaction at the plasma membrane and acidification environment inside the cell [103].

To date, the most sufficient experimental approach to investigate the localization of proteins of interest in PMN is subcellular fractionation, which has been previously demonstrated to successfully separate neutrophil plasma membranes from intracellular granules [70, 116]. Thus, in this study, a series of these experiments were performed to identify the localization of Ral in PMN.

#### **4. Mechanisms underlying granule release**

Mobilization of intracellular granules and vesicles also contributes, to an extraordinary degree, to PMN migration. As we know, cytoplasmic granules and vesicles of PMN are composed of not only antimicrobial proteins and proteolytic enzymes for eliminating foreign microorganisms but also a variety of cell surface receptors, functional proteins and granule matrix proteins involved in PMN extravasation. During degranulation, the PMN cell surface is incorporated with granule proteins and receptors. Subsequently, those fused proteins facilitate the activation of resting PMN to engage in cell-cell interactions and cell-extracellular matrix interactions in the process of transmigration. CD47, as an example, has been illustrated to facilitate PMN migration only after re-distribution from secondary granules to the cell surface upon chemoattractant stimulation [69]. As a result, controlled and effective degranulation of PMN is very important in inflammation and preventing overwhelming PMN-mediated tissue damage, thus maintaining homeostasis.

However, the molecular mechanism(s) by which PMN regulate individual intracellular granule release is still unclear. The signaling events elicited by chemoattractant stimulation (e.g. fMLF) leading to the release of each type of granule are still unclear. In other cell types, Ral, a Ras family small GTPase, involves in intracellular vesicle transportation, including both endocytosis and exocytosis [117-121]. Small GTPases are monomeric G proteins that are actively involved in many cellular functions [122]. They are further divided into five families based on sequence: Ras, Rho, Rab, Ran and Sar1/Arf [123]. According to structure, there are two interconvertible forms of small GTPases: GTP-bound active form and GDP-bound inactive form (Figure 1-10). Upon upstream activator binding, GDP is dissociated from the small GDP-bound form because of the conformation change, and is replaced with GTP. The GTP-bound form relays the signal from upstream to downstream through binding downstream effectors [122]. As a result, small GTPases serve as a molecular switch in signaling cascades. The interexchange of the GTP-bound form with the GDP-bound form is controlled by guanine nucleotide exchange factor (GEF) and GTPase activating protein (GAP). GEF triggers the formation of GTP-bound active form. GAP, increases the conversion of GTP to GDP, thus resulting in the formation of GDP-bound inactive form [122].

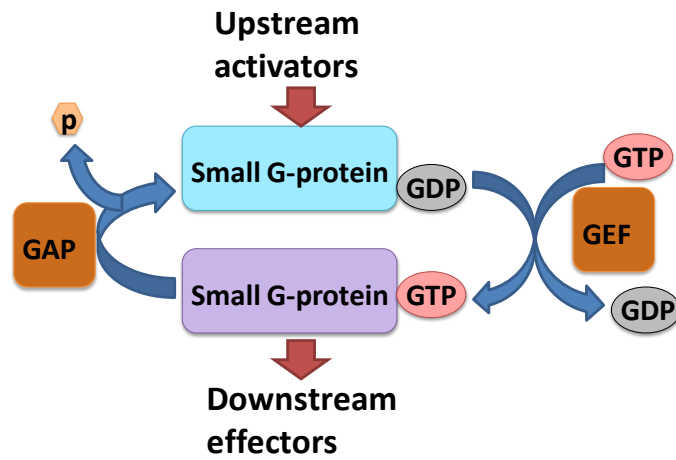


**Figure 1-10.** Interchange of the GTP-bound form with the GDP-bound form of small GTPase. GEF: guanine nucleotide exchange factor; GAP: GTPase activating protein.

Given the importance of Ral in other cell types, in this study, the potential role of Ral in regulating PMN granule mobilization and chemotactic function was investigated.

To date, the dynamics of actin cytoskeleton,  $\text{Ca}^{2+}$  signaling, src family kinases,  $\beta$ -arrestin, small GTPases and SNARE molecules have been reported to be involved in PMN degranulation.

Small GTPases play important roles in regulating PMN granule release. Rac2, a Rho family GTPases family member, is pivotal for neutrophil primary granule release [124-127]. Rac2<sup>-/-</sup> mice have shown defects in PMN primary granule release but not secondary or tertiary granule release. Rac2<sup>-/-</sup> mice also demonstrated defects in the translocation of primary granules [124]. Bone marrow PMN isolated from Rac2<sup>-/-</sup> mice fail to release primary and tertiary granules upon fMLP, LTB<sub>4</sub>, and CB-LTB<sub>4</sub> [125] stimulation. In addition, Rac2 is also associated with superoxide anion ( $\text{O}_2^{\cdot-}$ ) production [125]. In animal models and patients, the Rac mutation D57N, characterized by the loss of binding capability to GTP, has been [110, 127] found to prevent the MPO release and superoxide anions production in response to fMLF and phorbol myristate acetate (PMA), but not the release of secondary granules [126].

Rab, a family protein of small GTP, have been widely studied in targeting vesicles to particular compartments through tethering. In PMN, Rab27a has been implicated in regulating primary granule release through interacting with its effector protein JFC1/Slp1 [128-129]. Rab27<sup>-/-</sup> mice fail to release MPO upon LPS challenge. Subcellular distribution of Rab27a by fractionation and immunofluorescence staining further supports the fact that Rab27 is a constituent of exocytotic

machinery of primary granules in PMN. Rab27b has also been demonstrated to be the key component in regulating PMN primary granule release [130].

Rap1 and Rap2 are associated with PMN secondary granules but not primary granules or cytosol, as demonstrated by PMN subcellular fractionation and immunostaining. Accompanied with degranulation, Raps translocate to the plasma membrane from secondary granules, further suggesting their roles in controlling PMN secondary granule release [131].

Studies have also found that Rho family small GTPases regulate granule release. Pretreatment of PMN with MAPK phosphorylation inhibitors diminishes phagocytosis of *C albicans* and granule mobilization. Similarly, overexpression of the dominant-negative Rac and Cdc42 in PMN, through viral delivery, leads to abolished phagocytosis and granule release, implicating Rac and Cdc42 in regulating PMN granule release through the MAPK signaling pathway [132].

As a key component of the cytoskeleton, actin filaments not only contribute to cell motility, but also intracellular trafficking [133]. They are also involved in endocytosis and exocytosis [134]. Dynamic actin assembly and disassembly are associated with PMN primary granule release. In particular, actin polymerization is likely to initiate the release of primary granules. Primary granules are released from PMN treated with fMLF and cytochalasin B (CB) [135]. However, stabilization of actin results in inhibition of primary granule release. Inhibition of Rac also leads to reduced primary granule release through jeopardizing F-actin formation. Another study has suggested that the actin cytoskeleton might regulate the release of all types of granules in the PMN in response to stimulation [136]. With the exception of secretory vesicles, CB significantly in-

creases fMLF-simulated secondary and tertiary granule release. Additionally, CB triggers primary granule release that is failed to be released by fMLF alone. All of the above suggest that the actin cytoskeleton restricts the release of granules and maintains PMN in the resting condition. In addition to actin filaments, microtubules have been demonstrated to be associated with PMN granules [137]. Granule-microtubules, including primary granule-microtubule complexes and secondary granule-microtubule complexes, have been isolated from PMN, suggesting the critical role of microtubules in regulating PMN granule release.

During granule release, tethering and fusion of vesicles toward the target compartment involves a complex process that is not well understood. SNAREs, (soluble NSF (N-ethylmaleimide-sensitive factor), are key proteins involving in the docking and fusing of vesicles to the target compartment [138-140]. In human PMN, (t-) SNARE isoform syntaxin 6 has been cloned and shown to be localized only in the plasma membranes of resting and activated PMN [141]. In contrast to syntaxin 6, SNAP-23, another isoform of (t-) SNARE, localizes in tertiary and secondary granules in PMN and translocates to the plasma membrane upon stimulation. Antibodies against SNAP-23 block secondary granule release, whereas, anti-syntaxin 6 antibodies, block primary and secondary granule release from PMN. The above suggest that SNAP-23 and syntaxin 6 particularly regulate secondary and primary granule release. Vesicle-associated membrane protein (VAMP)-7, a (v-) SNARE in PMN [142], has been detected in primary granules in PMN. Treatment of PMN with antibodies against VAMP-7 dose-dependently abrogates primary granule, secondary granule and tertiary granule release. VAMP-2 and syntaxin 4 are associated with secretion of secondary and tertiary granules from PMN [143]. VAMP-2 is identified in PMN. Application of specific antibodies against 2-17aa in the N terminal of VAMP-2 to electroporabi-

lized PMN leads to the inhibition of secondary and tertiary granule release, but not primary granule release from PMN. This suggests an important role for VAMP-2 in release of those two granules PMN. Furthermore, VAMP-2 has also been suggested to control granule release in PMN after stimulation through interaction with syntaxin 4, which was demonstrated by the co-immunoprecipitation assay. Regarding the different types of granules in PMN, distinct SNAREs are likely to associate with each individual granule, and thus regulate PMN granule release.

Although signaling pathways regulating PMN granule release are not well understood, GPCR-mediated signaling cascades in PMN activation have been well established. As a scaffold protein,  $\beta$ -arrestin has been shown to be involved in PMN granule release. Upon IL-8 binding to CXCR1 on PMN [144],  $\beta$ -arrestin binds to phosphorylated receptors and forms more  $\beta$ -arrestin-Hck complexes. It has been demonstrated that  $\beta$ -arrestin translocates from the plasma membrane to secondary granules in PMN upon stimulation, suggesting its potential role in regulating PMN secondary granule release.

The effect of Src family kinases has also been demonstrated. P59<sup>Hck</sup> was first found to be mainly localized on granules, in contrast to plasma membranes and cytosol, in PMN [145]. Subsequently, it is found to be localized only on primary granules in PMN and is translocated to phagosomal membranes in HL60 cells during phagocytosis, indicating its role in regulating fusion of primary granules with lysosome. P55<sup>c-fgr</sup> has also been detected in human PMN and it is present in PMN membrane portions mainly on the plasma membrane of secondary and tertiary granules. P55<sup>c-fgr</sup> partially translocates to the plasma membrane in PMN stimulated with fMLF together with CB[146], suggesting its role in granule release.  $hck^{-/-}fgr^{-/-}$  PMN demonstrate the diminished re-



lease of lactoferrin in response to TNF stimulation when cells are placed in tissue culture plates or on collagen coated surfaces, suggesting that hck and fgr are involved in PMN adhesion-dependent granule release [147].

Calcium signaling also plays an essential role in PMN degranulation. It has been shown that increased intracellular calcium levels leads to release each type of granules in a hierarchical order [148]. Raised intracellular calcium is not only led by extracellular calcium influx, but also by other factors. It has been demonstrated that intracellular calcium in PMN is increased by ligation of L-selectin with its ligand, sulfatides [149], fMLF stimulation [149] and cross-linking of CD11b/CD18 on the PMN surface using its mAb [150]. Particularly, ligation of CD11b/CD18 induces the activation of cytoplasmic protein tyrosine kinases, such as  $p58^{\text{fgr}}$ , resulting in CD11b/CD18 dependent tyrosine phosphorylation. Patients with loss of  $\beta 2$  integrins fail to response to TNF-mediated tyrosine phosphorylation in PMN [151-152]. Furthermore, activation of CD11b/CD18 phosphorylates and activates a series of proteins. The effect of CD11b/CD18 might be  $\text{Ca}^{2+}$  dependent [153-154].

In PMN, several annexins have been identified [155]. Among them, annexin I is associated with secondary granules, the plasma membrane and secretory vesicles, but not primary granules. The effect of Annexin I likely depends on high concentrations of  $\text{Ca}^{2+}$  [156]. Annexin II, IV and VI are associated with all of the granule populations. The above suggests that different isoforms of annexin convey distinct effects on the release of different categories of granules from PMN.

## 5. Ral

The molecular mechanisms underlying PMN degranulation are still poorly understood. Considering the complex signal cascades involved in each type of granule release, it still remains unclear how PMN control the orderly release of individual granule subsets in response to different stimuli.

Ral is a member of Ras small GTPases. Like other small GTPases, Ral activity is regulated by GAP and GEF. To date, six GEFs have been identified. Based on structural similarity, they are further divided into two subfamilies. The first family of Ral GEFs is composed of RalGDS, ralGDS-like (Rgl), RalGDS-like factor (Rlf), and Ral GEF-like 3 (Rgl3). They contain Ras-GTP-binding domains, suggesting that Ral is activated through a Ras-dependent pathway. The other family consists of RalGPS2/RalGEF2 and RalGPS2, without a Ras-GTP-binding domain, suggesting the Ras-independent pathway for Ral activation [157]. Compared to GEFs, only two GAPs, GAP1 and GAP2 [157], have been identified by in vitro experiments. Ral activation involves complex signal cascades including both Ras-dependent [158-161] and Ras-independent pathways [162-163]. Studies by Rob M.F. Wolthuis demonstrate that Ral activation requires Ras activation [158]. Most importantly, Ral activation correlates with Ras activation. In contrast, other studies have also illustrated that the Ras-independent activation mechanism also extensively contributed to Ral activation [162-163]. In Rat-2 cells [162], not only does Ral activation require Ras activation, but is also triggered by increasing intracellular  $\text{Ca}^{2+}$  using ionomycin. Meanwhile, PLC is also required for Ral activation induced by LPA or EGF.  $\text{Ca}^{2+}$ -mediated Ral activation is observed in platelets as well. Increased intracellular calcium levels and/or increased calcium influx lead to Ral activation in platelets [163]. Bhattacharya M et al., using human embryonic kidney 293 cells (HEK293), discovers that RalGDS dissociation from beta-arrestin and

translocation to the plasma membrane leads to Ral activation [164]. This result implies an essential function for Ral in cytoskeletal reorganization and granule release.

The detailed mechanism that inactivates Ral, however, is still unknown. Thus, it is critical that more studies exploring this mechanism be performed. In particular, Ral deactivation is critical for PMN. Results from my study suggest that the loss of Ral activity results in secondary granule release; through secondary granule release, adhesion molecules incorporate into the PMN surface, and thus facilitate PMN migration, interaction with extracellular matrix and communication with other cells in inflammation.

There are two Ral genes in mammalian cells. The Genebank IDs for RalA and RalB of *Homo sapiens* are AF493910.1 and X15015.1, respectively. RalA and RalB are highly homologous, with about 85% identical amino acids [165] (Figure 1-12). The distinct sequences are mainly located at the carboxyl-terminus, in amino acids 192-204 [166]. RalA and RalB contain the same amino acid sequences within two effector binding regions, shown in Figure 1-12, suggesting that they are likely to harbor overlaid functions. As a typical family member of Ras small GTPase, in the C-terminus, Ral contains an atypical CAAX motif (where C stands for cysteine, A stands for aliphatic amino acid, X stands for methionine or serine); CAAX is a lipid modification motif [167] and suggests that Ral is likely to be associated with the membrane.

As shown in Figure 1-11, Ral contains two effector binding regions that are also termed “switch regions”, which mediate the recognition of effectors. Ral performs distinct and important biological functions through interacting with different downstream binding partner proteins. Five

binding partners have been identified to date. They include RalBP1, Sec5/Exo84 (subunit of exocyst), PLC- $\delta$ 1, and ZONAB, and phospholipase D 1 (PLD1) [168]. Except for PLD1 binding to the first 11 amino acids of Ral, others all bind to the switch regions. Through interaction with diverse effectors, Ral executes different biological functions. Particularly, Ral employs primary functions in vesicle trafficking through downstream effectors, RalBP1, Sec5/Exo84 and PLD1.

Although Ral engages in many aspects of cellular processes, it executes its major function in exocytosis and endocytosis, mainly by regulating exocyst, which is seen in a variety cell types [169]. Exocyst is a protein complex composed of Sec3, Sec5, Sec6, Sec8, Sec10, Sec15, Exo70 and Exo84 subunits, and is implicated in the fusion of vesicles to the plasma membrane [170]. The regulation of the exocyst is largely dependent on small GTPases. Ral small GTPases are key players in this process. A number of publications have demonstrated that Ral promotes exocyst assembly [171-172]. Using the double-mutant protein Ral23V49N as a probe in the yeast two-hybrid system, active Ral was found to directly associate with Sec5, a subunit of exocyst and the association was confirmed by the decreased formation of exocyst in the absence of Ral [173].

The functions of RalA and RalB are not completely understood. They play a collaborative role in regulating cytokinesis through exocyst [174], suggesting that RalA and RalB have compensatory roles in exocytosis. It has been postulated that dense granule releases from permeabilized platelets stimulated with GppNHp, a non-hydrolyzable analog of GTP are triggered by active RalA/RalB [175]. The release of dense granules is abrogated by overexpression of Sec5- GTP-Ral-binding domain (RBD), which suggests the secretion of dense granules from platelets is regulated by the Ral-Exocyst pathway.

The influence of Ral on vesicle release has also been demonstrated in the neuron signaling system. The expression of a dominant-inhibitory mutant of Ral results in dramatically inhibited release of vesicles in the presynaptic nerve terminal in response to  $\text{Ca}^{2+}$ . The regulation is likely through active Ral-exocyst interaction [118]. In addition, active RalA interacts with the mammalian brain exocyst complex [119]. In neuronal cells, chromaffin and PC12 cells, Ral associates with the plasma membrane in resting cells; however, after stimulation, it is thought to interact with effector protein(s) and form a complex. Activation of Ral in stimulated PC12 cells by  $\text{K}^+$  triggers the release of large, dense core secretory granules. Furthermore, overexpression of a constitutively active form of Ral increases the exocytosis of those granules from PC12 cells [117].

In polarized epithelial cells, Ral directs vesicle transportation. Protein transportation that was originally directed only towards the basolateral membrane was changed to the basolateral and apical membranes in the presence of active Ral [173]. Overexpression of the constitutively active form of Ral, Ral23V, or the inhibitory construct containing the Ral-binding domain leads to the inhibition of granule exocytosis in PC12 cells [173]. RalB is required for exocyst complex formation in rat kidney epithelial cells [176]. Active RalA binds exocyst and increases the translocation of E-cadherin in epithelial cells [177]. Adhesion-mediated RalA activation is also required for integrin-mediated membrane raft endocytosis and recycling during regulation of growth signaling [120].

In addition to exocytosis, it is reasonable to predict that Ral is also associated with endocytosis, based on studies demonstrating the function of RalBP1. RalBP1/RLIP76, another important downstream effector of Ral, is a member of the machinery regulating receptor-mediated endocytosis [121, 178-179]. Using a two-hybrid assay, RalBP1 is found to associate with  $\mu 2$ , the medium chain of AP2 adaptor protein complex [121] that is requisite for clathrin-mediated endocytosis by recruiting clathrin to plasma membrane [180]. Overexpression of constitutently active Ral also blocked endocytosis of transferrin in HeLa cells [121], A431 cells [178], and CHO-IR cells [178].

Not only does Ral play a crucial role in regulating vesicle trafficking, its functions have also been explored in tumorigenicity [181]. In human bladder cancer [181], RalA mRNA is significantly upregulated and is associated with invasive tumors. The RalA mRNA level is also highly associated with cancer protein expression [181]. RalA is required for the growth of human pancreatic carcinoma cells [182]. Also, inhibition of RalB by siRNA resulted in remarkably decreased cell migration in bladder carcinoma and prostate carcinoma cells [183]. RalB is involved in host defense signaling through suppressing tumor apoptosis, thus leading to cancer cell survival [184-185]. It has been shown that RalB activation promotes the complex formed between Sec5 and the exocyst subunit, along with TBK1 (Tank binding kinase 1), an atypical I $\kappa$ B kinase member, resulting in cancer survival.

The effect of Ral in vesicle trafficking has also been elucidated through investigating the function of PLD. PLD1 and its product PA are actively involved in vesicle trafficking, exocytosis and endocytosis [186-187]. The role of PLD1 is likely to be regulated by ARF6, a small GTPase, due

to the fact that 1) the activity of PLD1 depends on ARF6, and 2) the inhibition of PLD1 activity by myr-Arf6 (N-terminal-myristoylated Arf6) [188] peptide leads to impaired exocytosis induced by calcium in chromaffin cells [189]. PLD1 functions coupled with active Ral are required for exocytosis. Furthermore, Ral, PLD1 and ARF6 physically associate with each other and form a complex, mediating exocytosis upon stimulation. The expression of a vector bearing the coding sequence for active Ral, but lacking in binding sequence for PLD1, fails to elicit granule release, indicating that Ral functions in concert with PLD1 to modulate exocytosis [117].

The effect of RalA and RalB in PMN is still inconclusive. Using RT-PCR (Figure 3-19), in this study it was demonstrated that RalA and RalB are both present in human PMN, and RalB is more dominant than RalA. In my experimental approaches, I utilized a Ral pull-down assay to investigate the activity switch of Ral. Pull-down assays are widely accepted and used to address the activity of a variety of small GTPases including Ras, Rac1, Cdc42, Rho, Rap, Arf and Ral. The assay takes advantage of the specific interaction between RalBP1 and active Ral. It has been illustrated that amino acids 375-626 of RalBP1 comprise the putative binding domain that mediates the interaction with amino acids 37-56 of RalA [190]. As shown in Figure 1-11 and Figure 1-12, RalA and RalB bear identical amino acid sequences in the binding domain of RalBP1. Although, the Ral pull-down assay was designed originally for the detection of RalA activity, it is expected that RalBP1 will be able to pull-down the active form of RalB, which has been illustrated in another study [183].

Taken together, the current research is not focused on differentiating the role of RalA and RalB in regulating secondary granule release in PMN. As shown in Figure 1-11 and Figure 1-12, RalA

and RalB are highly homologous proteins and share most (if not all) of the functional domains identified to date. The possible Ral downstream effector proteins relevant to our study involving in receptor endocytosis, such as RalBP1/RLIP76 [121, 178-179], were found to bind to RalA and RalB at sites with an identical amino acid sequence (aa 37-56). Given the overlapping functions of RalA and RalB, and the fact that both of these forms are expressed in PMN, we decided to use Ral in my study.

In this dissertation, Ral, another family member of small GTPases, is demonstrated to play a vital role for PMN secondary granule release.



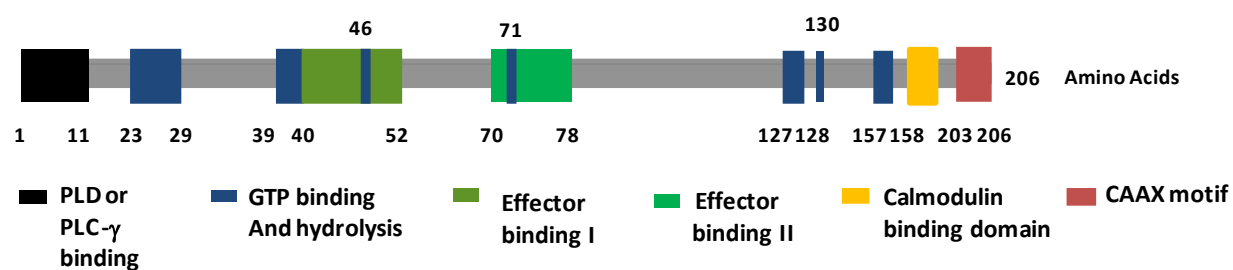


**Figure 1-11.** Ral domain structure. The Ral domain structure was adopted from VanDam and Robinson [168] with modifications using NCBI's conserved domains software.

82.1% identity in 206 residues overlap; Score: 855.0; Gap frequency: 1.0%

```

Rala,      1 MAANKP KGQNSLALHKVIMVGSGGVGKSALT LQFM YDEFVEDYEPTKADSYRKKVVL DGE
RalB,      1 MAANKS KGQSSLALHKVIMVGSGGVGKSALT LQFM YDEFVEDYEPTKADSYRKKVVL DGE
          *****

Rala,     61 EVQIDILDTAGQEDYAAIRDNYFRSGEGFL CVFSITE MESFA ATADFREQILRVK-EDEN
RalB,     61 EVQIDILDTAGQEDYAAIRDNYFRSGEGFL LVFSITE HESFT ATAEFREQILRVKAEEDK
          *****

Rala,    120 VPFLLVGNKSDLEDKRQVSVEEAKNRAEQ WNVNYVETSAKTRANVDKVFFDL MREIRARK
RalB,    121 IPLLVGNKSDLEERRQVPVEEARSKAEEWG VQYVETSAKTRANVDKVFFDL MREIRTKK
          + + + + +

Rala,    180 MEDSKEKNGKKK RSLAKRIRERCCIL
RalB,    181 MS ENKDKNGKKSSKN-KK SFKERCCLL
          * + + + +

```

**Figure 1-12.** Sequence alignment of RalA and RalB. Protein sequence alignment and domain structures of human RalA and RalB. Alignment of the primary structures of RalA and RalB reveals a high similarity between these proteins. The identical amino acids are indicated by “\*” and the homologous amino acids are indicated by “+”. The different amino acids are highlighted in purple.

**Summary**

This dissertation describes the regulatory function of Ral, a small GTPase, in vesicle trafficking in the aspect of exocytosis. In particular, my dissertation work investigates the Ral-mediated complex signaling pathway in the regulation of granule release from a very unique cell type, PMN. My work, for the first time, reports the novel finding that Ral controls secondary granule release from PMN (Figure 1-13). Active Ral prevents degranulation of secondary granules from PMN. The function of Ral as a gate-keeper for secondary granules is further illustrated by over-expression of a constitutively active Ral during PMN chemoattractant stimulation. Inhibition of Ral activity is intimately related with PMN dysfunction. Thus, my work suggests that Ral is vital for PMN secondary granule mobilization and is intimately linked to chemotactic function. Regarding the pivotal role of PMN in innate immune response and inflammation, my work will shed new light on drug design through targeting Ral in PMN in order to defend against a variety of inflammatory conditions.

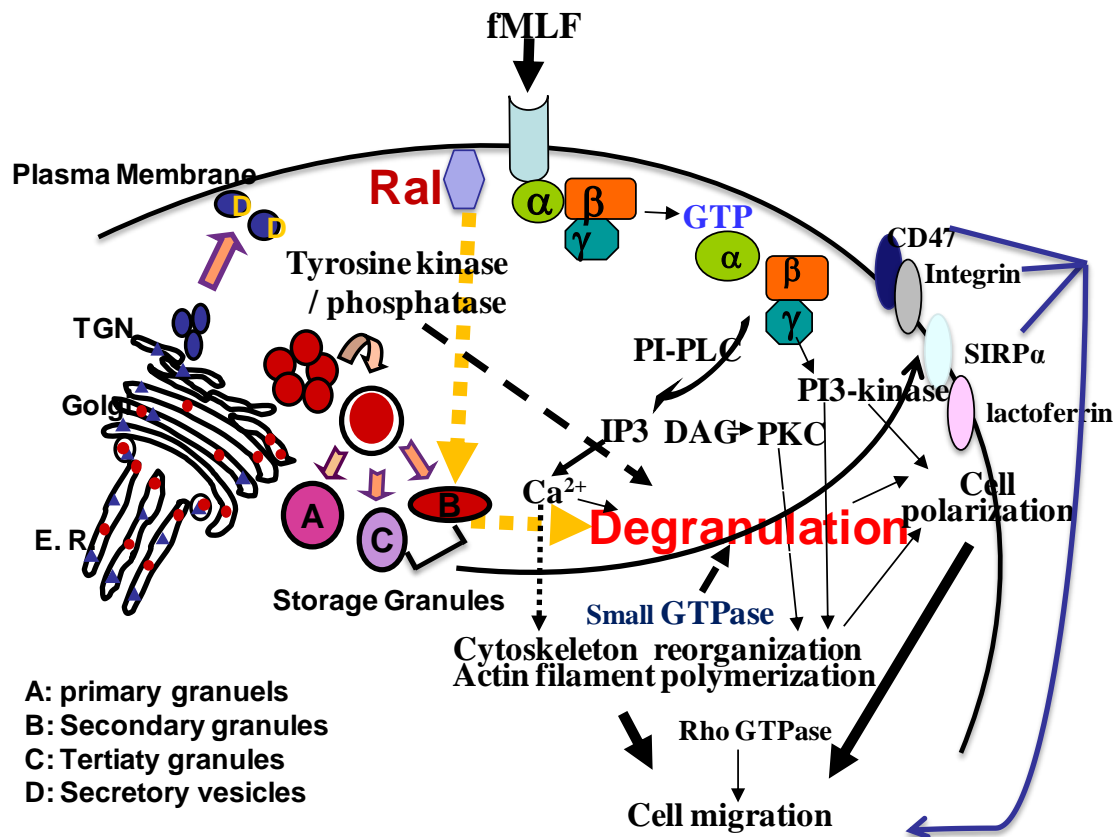


**Figure 1-13.** Control of secondary granule release in neutrophils by Ral

## **CHAPTER II:**

### **MATERIAL AND METHODS**

#### **2.1 PMN isolation**

##### **2.1.1 PMN isolation by dextran-ficoll (DEAE-Ficoll)**

Human whole blood was drawn from volunteers followed by centrifugation at 200×g for 10 min and stopped, without breaking, to separate the platelet-rich plasma and blood cells. After decanting plasma, 2% dissolved in 0.9% NaCl was utilized to separate red blood cells (RBC) from leukocytes (35min, 4 °C). The upper layer containing leukocytes were collected into a new tube followed by centrifugation (10min, 4 °C). The 10ml resuspended pellet in 0.9% NaCl was placed onto 3ml ficoll followed by centrifugation (40min, 4 °C). Pellet on the bottom of the tube was composed of PMN and RBCs, while peripheral blood mononuclear cells (PBMCs) including lymphocytes, monocytes and macrophages formed a layer approximately 1ml above the pellet. After discarding the top solution and the PBMC layer, the pellet containing PMN and RBCs was resuspended in cold RBC lysis buffer composed of 155 mM NH<sub>4</sub>Cl, 2 mM NaHCO<sub>3</sub> and 0.1 mM EDTA. After centrifugation, PMN were resuspended in cold HBSS (-) after washing once. PMN were used within 4 hours of isolation. The purity of PMN isolated using DEAE-Ficoll method was greater than 95%.

##### **2.1.2 PMN isolation from “buffy coat”**

Human whole blood was centrifuged at 1300 rpm for 10 min at 4 °C. After removing the plasma and top “buffy coat”, a thin layer containing PMN was collected and kept in a new conical tube. In order to maximally retract PMN from the buffy coat, a thin layer of RBCs underneath the PMN were also collected and transferred to the same tube. To remove RBCs, two rounds of lysis

using hypotonic buffer containing 155 mM  $\text{NH}_4\text{Cl}$ , 2 mM  $\text{NaHCO}_3$ , 0.1 mM EDTA were applied. After centrifugation, PMN were resuspended in cold HBSS (-) after washing once. The purity of PMN isolated using this method was about 70% to 80%.

### 2.1.3. PMN isolation using lympholyte-poly

Human whole blood drawn from healthy donors was added on top of an equal volume of lympholyte-poly (Cedarlane Laboratories Limited) in a 15ml centrifuge tube followed by centrifugation at 500g for 40 min at 25°C. After centrifugation, the RBCs were in the pellet on the bottom of the tube, while two visible leukocyte bands were formed at 1/3 the length of the tube. The PBMCs remained at the sample/medium interface (upper band) and the PMN formed a band (lower band). After removing the upper band containing PBMCs, PMN in the lower band were harvested into a new conical tube. PMN were washed twice with HBSS (-) without  $\text{Ca}^{2+}$  and  $\text{Mg}^{2+}$  followed by centrifugation at 400g for 10 min at 25°C. The PMN pellet was then lysed once with lysis buffer (Roche, Inc) to remove excessive RBCs followed by centrifugation at 400g for 10 min at 25°C. After centrifugation, PMN were resuspended in cold HBSS (-) after washing once

## **2.2 Platelet isolation**

Human whole blood was centrifuged at 1000 rpm for 10 min at 4 °C, without breaking, to separate the platelet-rich plasma and blood cells. The top layer containing the platelet-rich plasma was placed into a new tube. To isolate platelets and prevent activation during the isolation process, the collected plasma was supplemented with 0.1 volume ACD (2.5% trisodium citrate, 1.5% citric acid, 2% D-glucose) followed by centrifugation at 3000rpm for 15 min. The pelleted

platelets were washed with a citrate buffer (120mM NaCl, 4.26mM NaH<sub>2</sub>PO<sub>4</sub>, 5.5mM glucose, 4.77mM sodium citrate and 2.35mM citric acid, pH 6.5), and finally resuspended in HBSS (-) at 4 °C.

### **2.3 Treatment of PMN with inhibitors and agents**

For treating PMN, damnacanthol (Calbiochem) was freshly dissolved in DMSO, followed by further dilution in HBSS(-) at concentrations ranging from 0.1μM to 18μM before incubation with PMN ( $5 \times 10^6$  cells) at 25°C for 15 min. Other inhibitors, such as Bruton tyrosine kinase inhibitor LMF-A13, Src family inhibitors PP1 and genistein, Syk inhibitor piceatannol, mitogen-activated protein kinase (MAPK) inhibitor SB203580 and MEK inhibitor PD98059 (all from Biomol), PI3 kinases inhibitor LY294002 (both from Calbiochem) and others, were used as described previously [191-192]. To block the clathrin-mediated endocytosis, dynamin inhibitor dynasore [193] and an AP-2 binding peptide fragment of the EGFR protein tyrosine kinase substrate #15 (Eps15-DIII) [194-195] were used as previously described. Eps15-DIII was delivered into PMN by tagging with HIV Tat. PMN were pre-treated with these reagents for 5-15 minutes before stimulation with 1μM fMLF at 37°C.

The endocytosis inhibitors phenylarsine oxide (POA) and chlorpromazine hydrochloride (CPZ) [196] were purchased from Sigma and freshly prepared prior to the study. POA was dissolved in DMSO followed by dissolving in HBSS (+) at the final concentration of 20μM, followed by incubation with PMN ( $1.5 \times 10^7$ ) at 37°C for 5 min before fMLP stimulation. DMSO, at a final concentration of 0.06%, was used as the vehicle control for POA. CPZ, sucrose (Thermo Fisher Scientific, Inc), NaCl (Thermo Fisher Scientific, Inc), and succinic acid pH 5.5 (Thermo Fisher

Scientific, Inc) [197-198] were dissolved in HBSS (+) at a final concentration of 50 $\mu$ M, 500mM, 760mM and 20mM, respectively, followed by incubation with PMN ( $1.5 \times 10^7$ ) at 37°C for 5 min.

## 2.4 PMN degranulation assays

To test the effect of inhibitors on resting PMN, PMN ( $5 \times 10^6$ ) were incubated in 400 $\mu$ l of HBSS (-) with different inhibitors or the same dilution of DMSO at 25°C for 15 min followed by centrifugation. Clear supernatants without cell debris were collected and assayed for specific granular markers including myeloperoxidase (MPO), lactoferrin and gelatinase correlating to the release of primary, secondary and tertiary granules, respectively [69, 191]. MPO activity was assayed using 2, 2'-azino-bis (3-ethylbenzthiazoline-6-sulfonic acid (ABTS). Lactoferrin was assayed by ELISA using anti-lactoferrin antibody (Jackson ImmunoResearch Laboratories). Gelatinase was assayed by zymogram using gelatin-embedded gels (BioRad).

To assay degranulation after chemoattractant stimulation, PMN, untreated or treated with Tat-tagged peptides, PMN ( $2.5 \times 10^6$ ) were incubated with purified Tat-tagged wild-type Ral (Ral), the constitutive active form (RalG23V) and dominant negative form (RalS28N) of RalA at concentrations of 10nM and 40nM for 15 min at 15°C followed by stimulation in 250 $\mu$ l HBSS (+) with fMLP (1 $\mu$ M) for 20 min at 37°C. Following a similar procedure, supernatants without cell debris were collected and assayed for the release of granular markers. To assay PMN degranulation after treatment with endocytosis inhibitors, PMN ( $1.5 \times 10^7$ ) were incubated in 1.2ml HBSS (+) with different inhibitors at 37°C for 5 min followed by fMLP (1 $\mu$ M) stimulation at 37°C for



10 min followed by assaying for the release of granular markers. Positive degranulation controls were performed by stimulating the same amount of PMN with fMLF plus 10 $\mu$ M CB [135].

## **2.5 PMN transmigration assay**

PMN migration across collagen-coated transfilters was performed as described previously [69, 191]. Briefly, freshly isolated PMN ( $1 \times 10^6$ ), non-treated or treated with inhibitors (15 min, 25°C) or Tat-tagged Ral peptides (30 min, 4°C) at final concentration of 10nM and 40nM were loaded into the upper chambers of the transmigration setups in 150 $\mu$ l HBSS (+). Transmigration was initiated by adding 0.1 $\mu$ M fMLF in the lower chambers containing 500 $\mu$ l HBSS (+) and incubation at 37°C. PMN that migrated into the lower chambers were quantified by measuring the activity of myeloperoxidase (MPO), a marker for primary granules. MPO was released by lysing plasma membrane using Triton X-100. 25 $\mu$ l 10% Triton X-100 was added to the lower chamber containing migrated PMN at a final concentration of 5%. 25 $\mu$ l 1M citrate buffer pH 4.2 was also added to the lower chamber to adjust the pH to 4.2. Equal amounts of sample were mixed with the solution containing 1 mM ABTS, 10 mM H<sub>2</sub>O<sub>2</sub>, and 100 mM citrate buffer pH 4.2. Color matrix was developed at 405nm on a plate reader. In order to quantify the number of the migrated cells in the lower chamber, a standard curve was also generated using known concentrations of PMN.

## **2.6 Ras family GTPase activation assay**

### Ras GTPases activation assay in PMN

The GTPase activities of Ras, Rap and Ral in PMN were assayed using Ras, Rap and Ral activation assay kits (Millipore) with modifications. Briefly, PMN ( $2 \times 10^7$  cells/per condition) or plate-

lets ( $3 \times 10^8$  cells/per condition), with or without different treatment, were lysed with a buffer containing 25mM Hepes, pH7.5, 150mM NaCl, 2mM  $MgCl_2$ , 1% NP-40, 0.5% Na deoxycholate, 1% Triton X-100, 2% glycerol and protease inhibitors (cocktail (Sigma) and 10mM PMSF) followed by incubation with Raf-1 RBD, RalGDS-RBD or RalBP1 (residues 397-519 of rat RalBP1)-conjugated agarose for 45 min at 4°C. After washing the agarose, the pulled-down active Ras, Rap and Ral were detected by Western blot. Positive and negative controls were performed by addition of GTP $\gamma$ S or GDP $\gamma$ S to the cell lysates before pull-down. In addition, whole lysates from both control and treated cells were saved and run in parallel, serving as an internal loading control to determine the total amount of Ras, Rap and Ral proteins.

Alternatively, active Ral in PMN was also pulled down using a RalBP1 of human origin (amino acids 397-518 of human RalBP1) and GST fusion protein, a gift from Dr. Johannes Bos (Utrecht University, Netherlands) [163]. Our results indicated that RalBP1 of either human or rat origin worked equally well to pull down active human Ral.

#### Ral GTPases activation assay in platelets

Fresh isolated human platelets ( $3 \times 10^8$  cells/per condition) with or without thrombin stimulation were subjected to the Ral activation assay. Isolated platelets were stimulated with human recombinant thrombin (Sigma, Saint Louis) at a final concentration of 0.1UN/ml in tissue culture-treated 6-well plates (Costar, Corning Incorporated) at 37°C for 20 min. Cells were lysed in the buffer containing 25mM Hepes, pH 7.5, 150mM NaCl, 1% NP-40, 1% Triton, 2% glycerol, 0.5% Na-deoxycholate, 10  $\mu$ g/ml leupeptin, 10  $\mu$ g/ml aprotinin, and 1 mM PMSF. After centrifugation, the cleared supernatant was incubated with 30  $\mu$ g GST-RalBP1 (human sequence) fu-

sion protein-coupled glutathione-sepharose with gentle agitation for 1 hour at 4°C to pull down the active form of Ral. The sepharose mixture was pelleted down, washed with lysis buffer. Active Ral was detected by western blot using an anti-Ral antibody. In addition, whole cell lysates from unstimulated and stimulated platelets were saved and applied to western blots to assay the total Ral proteins.

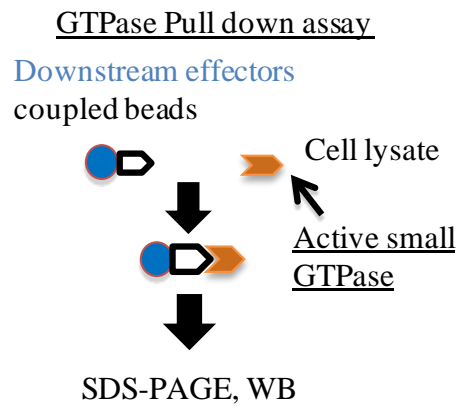


**Figure 2-1.** GTPase pull down assay

## 2.7 Generation of HIV Tat-tagged recombinant proteins

A GST gene fusion system was used to express and purify Ral and Eps 15-DIII fusion proteins in *Escherichia coli*. Three pGEX-5X1 vectors expressing the full length (wild-type), the constitutive active form (G23V) and dominant negative form (S28N) of Ral protein were constructed (Figure 2-2). For Eps15, two constructs expressing Eps15-DIII with the binding ability to AP-2 and Eps15-Δ without the binding ability to AP-2 were obtained.

### 2.7.1 Generation of HIV Tat-tagged Ral recombinant proteins under soluble conditions

Briefly, to generate Tat-tagged Ral proteins, the entire cDNA of wild-type Ral was RT-PCR amplified from leukocytes (Marathon Ready cDNAs, Clontech) using a sense primer, 5'- atatg-gatccccctacggccgcaagaaacgccgccagcgccgccgcatggctgcaaataagcccaagggt, (underlined) coding for the 11 residues of HIV Tat (YGRKKRRQRRR) [199-201], and an antisense primer, 5'- atatctcgagttataaaatgcagcatctttc, followed by cloning into pGEX-5X1 vector through BamHI and XhoI site, respectively. To produce the constitutively active (Ral23V) and dominant-negative (Ral28N) mutants [117, 167, 202], Gly23 and Ser28 in wild-type Tat-Ral were mutated to Val and Asn, respectively, using GeneTailor™ Site-Directed Mutagenesis kit (Invitrogen, USA). After production of the recombinant proteins, GST within the fusion was removed by Factor Xa (New England Biolabs) and the obtained Tat-tagged Ral and Eps15 proteins were obtained followed by filtering through 0.22μm filters. To label peptides with fluorescein (FITC), an EZ-Label FITC protein labeling kit (PIERCE) was used. For transduction into PMN, Tat-tagged pro-

teins (10-100nM) were directly incubated with freshly isolated PMN in HBSS (-) for 10-30 min at 4°C.

Considering the high possibility of protein precipitation due to the positive charge of HIV-Tat, the HIV-Tat-tagged protein is commonly purified under denatured conditions. Given that PMN are very prone to be activated, the common procedure for protein expression and purification of HIV-Tat-tagged protein was modified in this research.

#### 2.7.1.1 Induction and purification of GST-Tat-Ral fusion protein

Followed by transformation to *E. coli* BL21 cells, GST fusion protein expression was induced by IPTG (isopropyl-beta-D-thiogalactopyranoside). In order to obtain high level of protein expression and prevent protein formation into inclusion body, the induction environment was modified before large-scale protein induction. Bacteria growth to the saturate status was required, and OD600 was measured to be 0.8 before IPTG induction.

Wild-type Ral protein was induced by IPTG at a final concentration of 0.5mM at 20°C with constant shaking overnight. While, the final concentration of IPTG for inducing mutant forms of Ral was decreased to 0.1mM due to the fact that under the same induction condition, protein expression levels of the constitutively active form (G23V) and dominant negative form (S28N) of Ral were very low compared with that of wild-type protein. In order to increase protein expression level, the final concentration of IPTG was decreased to 0.1mM to prevent protein aggregation in the inclusion body.

After IPTG induction and centrifugation, cell pellet was resuspended in 1× ice cold PBS, followed by sonication. A clear cell lysate was obtained after centrifugation at 15000rpm for 10 min at 4°C. GST fusion proteins were purified by affinity purification using glutathione-sepharose 4B (Amersham Biosciences). Glutathione-sepharose was incubated with the clear lysate with gentle agitation for 2 hours at 4°C. According to the binding capacity that 1 ml drained glutathione-sepharose is able to bind 8 mg fusion protein, a sufficient amount of glutathione-sepharose was added to the lysate. Medium mixed with cell lysate and sepharose was then packed into column (Pierce) followed by washing with 500 ml 1× ice cold PBS and eluted with 10mM reduced glutathione in 50mM Tris pH 8. The eluted protein was then concentrated using Millipore Amicon Ultra-4 10,000 mwco to the final concentration of approximately 0.6 mg/ml, followed by dialysis against 1×PBS by using dialysis tubing (Spectrum Spectra, 12-14,000 mwco). In order to prevent activation of the protein precipitation cascade, protein concentration was modified below 1 mg/ml, and several rounds of high speed centrifugation were required to remove any small precipitants before dialysis. After dialysis and sterilization through 0.2µm filter, protein purity was analyzed by coomassie blue staining and western blot.

#### 2.7.1.2 Cleavage of GST-Tat-Ral fusion protein

In order to obtain Tat-Ral proteins, GST-tag was cleaved from GST fusion protein by Factor Xa (NEB). Briefly, GST fusion proteins were incubated with Factor Xa at 0.3µg Factor Xa to 25 µg GST fusion protein at 25°C for 2.5 hours followed by incubation with glutathione-agarose with agitation at 4°C for 4 hours. The Tat-Ral protein in the run-through was obtained after passing protein mixture through the column (Pierce). Purity was then analyzed by coomassie blue staining. In particular, before cleavage, GST fusion protein concentration was adjusted below 1mg/ml

to prevent Tat-Ral protein precipitation during cleavage, likely due to the exposure of highly charged amino acids.

### 2.7.2 Generation of HIV Tat-tagged Eps15 recombinant proteins under soluble conditions

The same approach of generation and purification of HIV Tat-tagged Eps 15 protein as HIV Tat-tagged Ral protein was applied. Two Tat-tagged Eps15 C-terminal peptides were produced, the AP-2 -binding peptide (amino acids 563-885, designated as Eps15-DIII) and non-binding peptide (amino acids 740-885, designated as Eps15- $\Delta$ ) [194-195]. To construct these proteins, RT-PCR were performed using an antisense primer, 5'-tagccagttctaagtcttc, and Tat sequence-containing sense primers, 5'-atatggatcccctacggccgcaagaaacgccgccagcgccgccgcctgaactactgccttctggtgtga and 5'-atatggatcccctacggccgcaagaaacgccgccagcgccgccgctcagccacatcgagctctgtcagcaac, respectively. HIV Tat-tagged Eps15 protein was expressed and purified in the same way describe in 2.7.1.



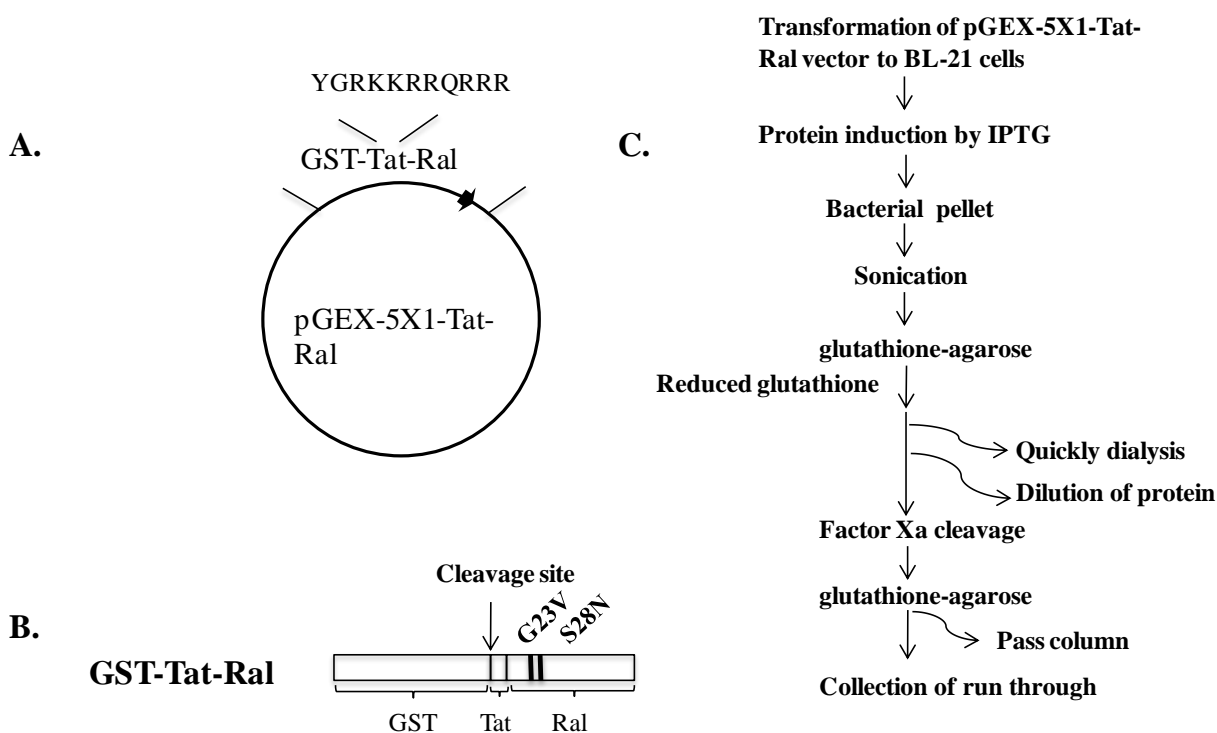


**Figure 2-2.** HIV-Tat-Ral expression and purification system. A) pGEX-5X1-Tat-Ral expression vector. B) Structure of GST-Tat-Ral protein. There were three pGEX-5X1 vectors expressing the full length (wild-type), the constitutive active form (G23V) and dominant negative form (S28N) of Ral protein. After Factor Xa cleavage, GST-tag was removed from Tat-Ral peptide. C) Detailed Tat-Ral protein expression and purification workflow

## 2.8 Zymogram assay

Gelatinase activity was assayed by gelatin zymography (Bio-Rad, Inc). Briefly, the clear supernatant was mixed with non-reducing SDS gel sample buffer and subjected to a gelatin gel with 10 µg protein per lane. The gel was then washed twice in 2.5% TritonX-100 in 50 mM Tris pH 7.4, 5 mM CaCl<sub>2</sub>, 1 microM ZnCl<sub>2</sub> at 25°C followed by incubation in the same buffer without Triton X-100 at 37°C for 20 h. The polyacrylamide gel was then stained with coomassie blue R-250 for 1 hour at 25°C followed by destaining for 30 min at 25°C. Gelatinase activity was shown by the white areas of loss of coomassie blue staining.

## 2.9 Subcellular fractionation of PMN

Freshly isolated PMN (10<sup>8</sup>/per condition), with or without fMLF stimulation or inhibitor treatment, were lysed in a buffer containing 25mM Hepes pH7.5, 150mM NaCl, 10% sucrose, 2mM MgCl<sub>2</sub> and protease inhibitors using a dounce homogenizer followed by centrifugation at 200×g for 5min. Meanwhile, discontinuous sucrose density gradients were prepared by layering 5 layers of successive decreasing sucrose density solutions (5ml/layer) upon one another (60%, 50%, 40%, 30% and 20%). PMN lysates (10ml) were then layered on top of the gradients. After centrifugation with a Beckman SW28 swinging bucket ultracentrifuge rotor for 3h at 28, 000rpm (141,000×g) (4°C), the gradients were fractionated (1ml/fraction) followed by analysis for plasma membrane (alkaline phosphatase), primary granule (myeloperoxidase), secondary granule (lactoferrin) and tertiary granule (gelatinase) [69-70].

## 2.10 FITC Protein Labeling

Tat-tagged Ral protein was fluorescently labeled using EZ-Label™ FITC Protein Labeling Kit (PIERCE). Briefly, Tat-tagged Ral proteins were dialyzed against BupH Borate buffer containing 50 mM borate, pH 8, using Slide-A-Lyzer MINI Dialysis Unit with 3500 MWCO (PIERCE) for 1 hour at room temperature to exchange protein buffer for optimizing protein labeling. After buffer exchange, FITC was added into protein according to the formula\* and incubated at room temperature for 1 hour. FITC-protein mixture was then dialyzed against 1×PBS at 25°C for 1 hour in the same dialysis unit to remove excess fluorescent dye followed by transduction to PMN.

microliters of FITC solution to add to labeling reaction=

Simplified formula\*:

$$\text{ml protein} \times \text{protein concentration} \times \frac{\text{mmol}}{\text{Xmg}} \times \frac{24\text{mmol}}{\text{Xmg}} \times \frac{389}{\text{mmol}} \times \frac{100\mu\text{l}}{1\text{mg}}$$

X=Molecular Weight of the protein

## 2.11. Immunofluorescence labeling and flow cytometry

Fresh isolated PMN ( $5 \times 10^6$ ) were pretreated with tyrosine kinases and other pharmacological inhibitors in HBSS (-) for 10 min (20°C). After centrifugation at 1300rpm for 5 min at 4°C, the

cell pellet was resuspended with blocking buffer containing 0.5% BSA. Cell surface expression of CD11b, CD47 and SIRP $\alpha$  was assessed by labeling non-permeabilized PMN with anti-CD11b mAb LM2/1, anti-CD47 mAb B2H6 and anti-SIRP antibodies (10 $\mu$ g/ml each, 1h, 4°C), respectively. After washing, PMN were briefly fixed with 3% paraformaldehyde (PF) for 5 min at 25°C followed by incubation with fluorescence conjugated secondary antibodies (1:1000 dilution in blocking solution) for 30 min. Cells were observed under confocal microscope (Zeiss) or analyzed by flow cytometry (BD). Cell surface labeling by various antibodies was compared with that obtained with isotype-matched control IgG. For intracellular localization staining, cells were fixed with 3% PF and then permeabilized by 0.03% Triton X-100 for 10 min at 4°C before antibody labeling. For plasma membrane labeling, cells were incubated with wheat germ agglutinin (WGA) at the final concentration of 5  $\mu$ g/mL for 1 min at 25 °C followed by washing with HBSS (-).

## 2.12. Other reagents

Hybridoma cell line that produces anti-CD11b antibody LM2/1 was obtained from the American Type Culture Collection (ATCC). Monoclonal antibody against the extracellular domain of CD47 (PF3.1) was generated previously [69]. Rabbit polyclonal antibodies against the extracellular domains of SIRP $\alpha$  (anti-SIRP $\alpha$ .ex) and JAM-A (anti-JAM-A.ex) were raised by immunizing rabbits with purified fusion proteins comprised of rabbit Fc and the entire extracellular domains of SIRP $\alpha$  or JAM-A[87, 203]. Antibodies against Ral, Ras and Rap1 were purchased from Millipore. Anti- $\beta$  actin mAb was purchased from Sigma. Rabbit anti- $\alpha$ -adaptin was purchased from Santa Cruz Biotechnology. Rabbit anti-RalGDS was purchased from EMD Millipore. Alexa Fluor 594 conjugated WGA was purchased from Invitrogen.

### **2.13 Statistical analyses**

All the data was analyzed using Prism software. P value for statistical significance was below 0.05.

**CHAPTER III:**  
**CONTROL OF SECONDARY GRANULE RELEASE IN**  
**NEUTROPHILS BY RAL GTPASE**

**PUBLICATION: CHEN CX, SOTO I, GUO YL, LIU Y. CONTROL OF SECONDARY GRANULE RELEASE IN NEUTROPHILS BY RAL GTPASE. J BIOL CHEM, 2011 APR 1; 286(13): 11724-33.**

NOTE:

I PERFORMED ALL OF THE EXPERIMENTS IN THIS CHAPTER, EXCEPT FOR TABLE

1.

DR. YUAN LIU AND I PERFORMED THE EXPERIMENTS SHOWN IN FIGURE 3-1.

DR. YAUN LIU AND I PERFORMED THE EXPERIMENTS SHOWN IN FIGURE 3-2.

YAN-LAN GUO AND I PERFORMED THE EXPERIMENT SHOWN IN FIGURE 3-3 and 3-

4.

DR. YUAN LIU PERFORMED THE EXPERIMENTS FOR FIGURE 4-2A.

## **Introduction**

Neutrophils, or polymorphonuclear leukocytes (PMN), occupy the largest population in peripheral leukocytes and play a crucial role in innate immunity. During acute infection and inflammation, PMN sense chemoattractant signals and swiftly migrate across the microvasculature and underlying tissues to accumulate at inflammatory foci, where these cells execute forceful antimicrobial and tissue damaging functions. Therefore, the timely and precise response of PMN constitutes an essential first-line defense against invading microbial. On the other hand, PMN-mediated inflammation is also a central component of many pathophysiological processes and diseases in which dysregulated PMN transmigration and activation often result in severe tissue injuries and organ dysfunction [25, 96]

Different from most of other cell types, PMN contain a highly granular cytoplasm. At least four types of granules and vesicles have been classified in PMN including peroxidase-positive primary granules (also termed azurophil granules), peroxidase-negative secondary and tertiary granules (also termed as specific and gelatinase granules, respectively), and a group of highly mobilizable secretory vesicles [61-62]. These various granules and vesicles in PMN constitute an important reservoir of antimicrobial peptides, proteases, respiratory burst oxidases, as well as many membrane-bound receptors and adhesion molecules. PMN functions in response to inflammatory stimuli are largely dependent on the mobilization and release (degranulation) of these cytoplasmic granules and vesicles. In general, the secretory vesicles are highly mobilized for extracellular release. These vesicles provide the PMN cell surface with essential, but low levels of receptors and molecules that are important in PMN sensing and triggering activation [61-63]. Upon chemoattractant stimulation, secondary and tertiary granules are released, and this

vital degranulation process enables PMN to adhere to and migrate across vascular endothelium and tissue layers [26, 61-64]. PMN secondary granules contain a large number of key cell adhesion molecules, such as the  $\beta_2$  integrin CD11b/CD18 [66-67] and the Ig superfamily members CD47 and SIRP $\alpha$  [68-70], all of which are required for PMN adhesion and chemotaxis. Degranulation of secondary granules also releases the anti-pathogen protein lactoferrin. Tertiary granules have a high content of gelatinases; release of these collagenolytic metalloproteases plays a critical role in degradation of the extracellular matrix during PMN extravasation. In addition to these granules / vesicles, studies have also found that certain primary granules are also released during PMN activation and that some of the primary granule components, such as elastase, are indispensable for PMN migration in the tissues.

The molecular mechanisms that control PMN degranulation are, however, still unclear. The signaling events elicited by chemoattractant stimulation leading to PMN degranulation of each type of granule are complex, and only inadequately understood. In other cell types, Ras family small GTPase Ral has been shown to be required in intracellular vesicle transportation, including both endocytosis and exocytosis [117-121]. Here, we report our experimental findings which reveal for the first time that Ral controls PMN release of secondary granules. In particular, our studies suggest that active Ral serves as an essential gatekeeper which prevents secondary granule release. Disruption of Ral regulation, either by inhibition of Ral activity in resting PMN or overexpression of a constitutively active Ral during chemoattractant stimulation, results in dysregulation of secondary granule mobilization and impairment of PMN chemotactic function.

## **Results**



### **Ras family inhibitor damnacanthal triggeres release of PMN secondary granules.**

PMN surface adhesive proteins, such as CD47 [69, 71], CD11b/CD18 [66-67] and SIRP $\alpha$  [68, 204], play important roles in PMN adhesion, transmigration and phagocytosis. Instead of being constitutively expressed on the cell surface, these essential proteins are mainly stored in intracellular granules under resting conditions, but are rapidly upregulated onto the cell surface in response to inflammatory chemoattractants following the process of PMN degranulation [69-70]. To reveal the mechanisms involved in control of PMN storage of these important cell surface proteins and PMN degranulation, a panel of pharmacological probes / inhibitors targeted different signaling molecules and pathways were tested for their effects on the cell surface protein expression. Treatment of PMN with damnacanthal, a membrane-permeable inhibitor of the Ras family GTPases and the Src family tyrosine kinase Lck [205-207], was found to result in a dramatic increase of CD11b/CD18, CD47 and SIRP $\alpha$  on the PMN cell surface despite the lack of chemoattractant stimulation. As shown in Table 1, after damnacanthal treatment, FACS analysis showed increases of the mean fluorescence intensities (MFI) of cell surface CD11b/CD18, CD47 and SIRP $\alpha$  labeling from the basal level of 90.7, 35.2 and 14.2 up to 203.8, 112.8 and 67.8, respectively. In contrast, treating PMN with the vehicle control or other inhibitors, such as genistein, piceatannol, LFM-A13, PP1, PD98059, LY294002 and others, did not change the levels of these proteins on PMN cell surface. Analysis of the cell shape and/or sizes by FSC and SSC parameters also indicated a visible shift of the PMN population towards lower FSC/SSC after damnacanthal treatment (data not shown), suggesting a potential of PMN degranulation.

Since PMN contain multiple types of intracellular granules, and CD47, CD11b/CD18 and SIRP $\alpha$  are mainly stored in secondary granules [69-70], it was thus highly possible that increase of these

proteins on the cell surface by damnacanthal treatment was through PMN degranulation. Therefore, the release of primary, secondary and tertiary granules after damnacanthal treatment was analyzed. As shown in Figure 3-1, compared to other inhibitors that did not cause PMN degranulation, damnacanthal dose-dependently induced PMN release of secondary granules. In contrast, no apparent release of primary or tertiary granules was observed by treating PMN with damnacanthal. In the experiments, PMN were also treated with chemoattractant fMLF and a combination of fMLF and actin filament disruption reagent cytochalasin B (CB) to serve as positive degranulation controls [135]. As shown in Figure 3-1, as predicted, treating PMN with only fMLF resulted in significant degranulation of secondary and tertiary granules, but not primary granules, while treatment with fMLF-CB combination induced a robust and complete degranulation of all the granules. At a concentration of 18 $\mu$ M, damnacanthal treatment could generate amounts of lactoferrin release comparable to the combined fMLF and CB treatment, indicating a nearly complete degranulation of secondary granules (Figure 3-1). In conclusion, these studies found that treatment of PMN with damnacanthal selectively induced the degranulation of secondary granules.

**Table 1.** Damnacanthal treatment induces an upregulation of CD11b/CD18, CD47 and SIRP $\alpha$  on PMN surface.

**Effects of pharmacological inhibitors on PMN cell surface protein expression**

<b>Inhibitors</b>	<b><u>PMN surface mean fluorescence intensity (MFI)</u></b>			
	<b><i>Ctl IgG</i></b>	<b><i>CD11b/CD18</i></b>	<b><i>CD47</i></b>	<b><i>SIRP<math>\alpha</math></i></b>
Vehicle ctl (DMSO)	3.2 $\pm$ 0.08	90.7 $\pm$ 0.11	35.2 $\pm$ 0.038	14.2 $\pm$ 0.09
<b>Damnacanthal (10<math>\mu</math>M)</b>	<b>2.5<math>\pm</math>0.18</b>	<b>203.8<math>\pm</math>0.22</b>	<b>112.8<math>\pm</math>0.19</b>	<b>67.8<math>\pm</math>0.16</b>
Genistein (100 $\mu$ g/ml)	4.3 $\pm$ 0.13	76.6 $\pm$ 0.28	30.0 $\pm$ 0.13	19.6 $\pm$ 0.14
Piceatannol (40 $\mu$ M)	5.5 $\pm$ 0.26	94.0 $\pm$ 0.17	28.2 $\pm$ 0.14	13.5 $\pm$ 0.16
PP1 (18 $\mu$ M)	2.7 $\pm$ 0.33	85.2 $\pm$ 0.43	29.3 $\pm$ 0.46	11.6 $\pm$ 0.31
LFM-A13 (140 $\mu$ M)	4.4 $\pm$ 0.51	89.3 $\pm$ 0.44	28.5 $\pm$ 0.69	9.7 $\pm$ 0.42
Herbimycin A (2 $\mu$ M)	5.2 $\pm$ 0.26	95.7 $\pm$ 0.25	30.3 $\pm$ 0.15	16.3 $\pm$ 0.45
Lavendustin A (10 $\mu$ M)	5.5 $\pm$ 0.16	91.4 $\pm$ 0.32	32.2 $\pm$ 0.21	20.1 $\pm$ 0.25
Erbstatin analog (25 $\mu$ M)	4.8 $\pm$ 0.17	81.6 $\pm$ 0.20	29.8 $\pm$ 0.19	18.3 $\pm$ 0.23
SB203580 (1 $\mu$ M)	6.1 $\pm$ 0.30	83.8 $\pm$ 0.40	28.8 $\pm$ 0.15	15.2 $\pm$ 0.23
PD98059 (80nM)	3.7 $\pm$ 0.16	89.9 $\pm$ 0.24	26.7 $\pm$ 0.18	12.5 $\pm$ 0.25
LY294002 (100nM)	3.0 $\pm$ 0.14	79.6 $\pm$ 0.13	31.9 $\pm$ 0.30	19.1 $\pm$ 0.15
AG126 (150 $\mu$ M)	4.3 $\pm$ 0.17	97. $\pm$ 0.19	30.7 $\pm$ 0.14	14.6 $\pm$ 0.24

**Table 1.** In these experiments, freshly isolated PMN ( $5 \times 10^6$ ) were incubated with damnacanthal or other inhibitors in their working concentrations for 15min at 25°C. After blocking with 5% normal goat serum, PMN cell surface CD11b, CD47 and SIRP $\alpha$  were labeled with LM2/1, PF3.1 (10 $\mu$ g/ml each) and anti-SIRP $\alpha$ .ex (1:2000 dilution), respectively, for 1h (4°C). After washing and fixation with 3% paraformaldehyde (5min, 20°C), cells were incubated with Alexa Fluor-conjugated secondary antibodies followed by washing and analysis by flow cytometry. PMN labeled with normal mouse IgG served as baseline. The table shows the mean fluorescence intensity  $\pm$ SEM. SEM: SD divided by the square root of the sample size.

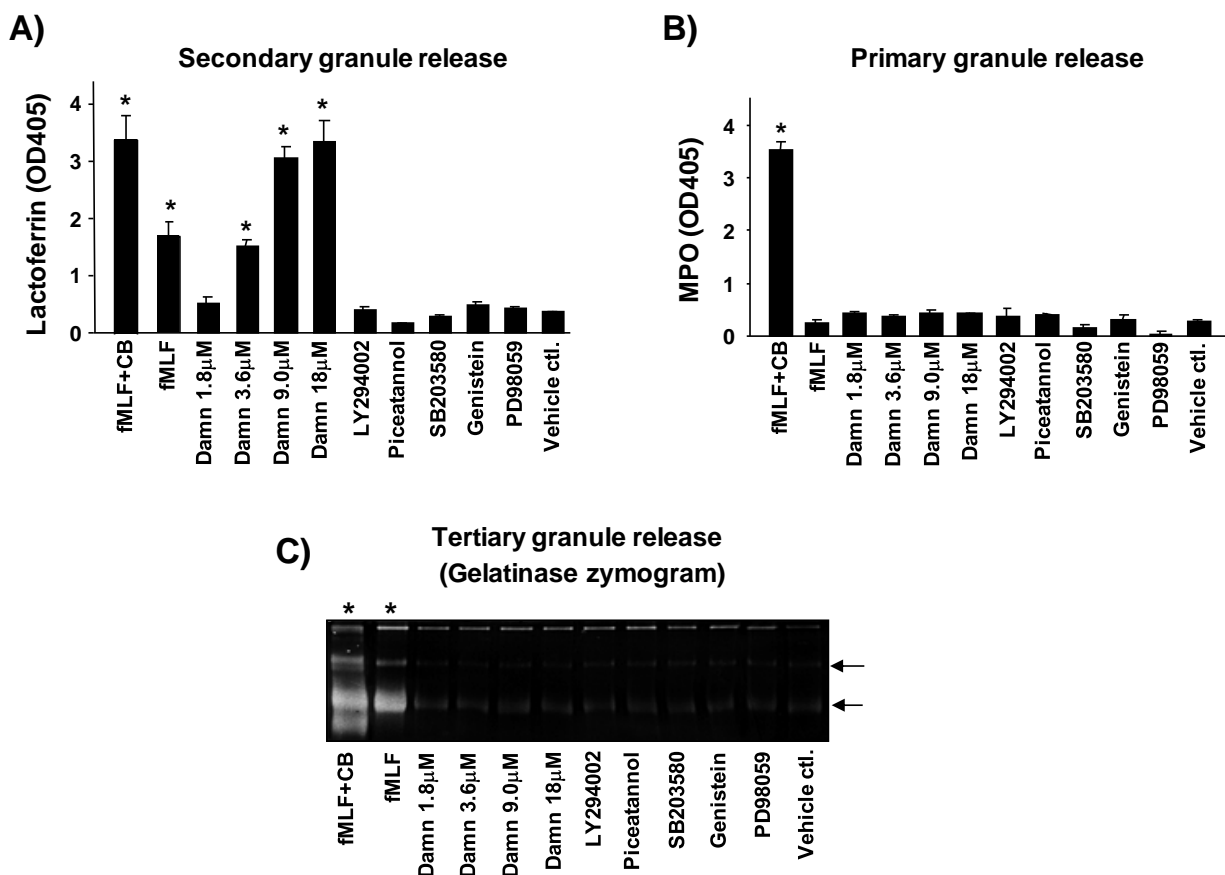


**Figure 3-1.** Damnacanth treatment induces specific release of PMN secondary granules. Freshly isolated PMN were treated with damnacanthal (Damn) of varied concentrations and other inhibitors for 15min at 25°C. A control treatment was performed using vehicle (DMSO) of the same dilution (0.1%). After centrifugation to pellet cells, PMN degranulation was assessed by assaying different granular markers in the cell-free supernatants. Positive degranulation controls were performed by stimulation of PMN with 1 $\mu$ M fMLF with and without an addition of 10 $\mu$ M cytochalasin B (CB). Concentrations of LY94002, Piceatannol, SB203580, genistein and PD98059 used in the treatment were the same as those in Table 1. A) Assaying secondary granule release by measuring lactoferrin in the supernatants. B) Assaying primary granule release by measuring MPO activity in the supernatants. C) Assaying tertiary granule release by zymogram detecting gelatinase in the supernatants. The arrows indicate the two major forms of gelatinase (92kD and 56kD, respectively) in PMN. As shown, damnacanthal (Damn.) specifically and dose-dependently induced secondary granule degranulation. Data (mean  $\pm$  SD) represent more than five independent experiments. Significant degranulation was marked by “\*”.

### **Damnacanthal treatment results in defect of PMN function.**

In general, PMN degranulation of secondary granules is triggered by chemoattractants binding to the cell surface receptors followed by signaling relays involving G protein and a series of downstream signaling molecules [208]. Since damnacanthal caused release of secondary granules in the absence of chemoattractant stimulation, I questioned whether this kind of “dysregulated” degranulation would affect PMN function and thus assayed chemoattractant-induced PMN transmigration and adhesion/spreading. As shown in Figure 3-2, in contrast to that PMN vigorously transmigrated towards fMLF in the control condition, damnacanthal dose-dependently inhibited PMN transmigration and completely abolished PMN migration at a concentration of 18 $\mu$ M. Also as shown in Figure 3-3A, compared to control PMN which responded to fMLF stimulation and quickly spread on collagen-coated surfaces displaying a polarized F-actin labeling pattern, damnacanthal treatment impaired PMN spreading. Indeed, PMN adhesion to collagen induced by fMLF was significantly weakened in the presence of damnacanthal (Figure 3-3B). Next I examined whether damnacanthal treatment affected cell surface protein function. Since CD47 and SIRP $\alpha$  are extracellular counter-ligands [68, 87], we thus tested cell surface CD47 direct binding to a SIRP $\alpha$  extracellular domain fusion protein, SIRP $\alpha$ 1.ex-Fc [70, 87]. As shown in Figure 3-4, although damnacanthal induced a significant increase of CD47 on PMN cell surface, these up-regulated CD47 were not binding to its ligand SIRP $\alpha$ . In contrast, CD47 was also increased on PMN surface after fMLF stimulation, and these CD47 directly bound to SIRP $\alpha$ 1.ex-Fc (Figure 3-4).

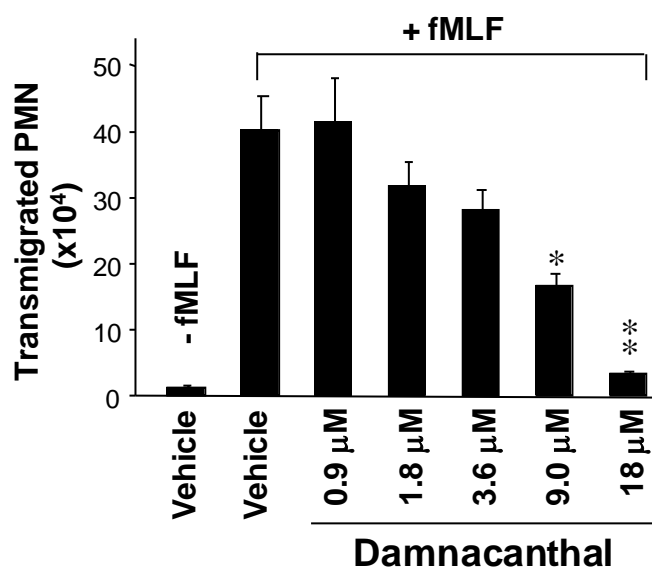


**Figure 3-2.** Damnacanthal inhibits chemoattractant-triggered PMN function. A) Damnacanthal inhibits PMN chemotaxis. PMN ( $10^6$ ) were treated with damnacanthal of varying concentrations for 15min at 25°C followed by assaying transmigration across collagen-coated filters towards fMLF (0.1μM) in 1h. Data (mean  $\pm$  SD) represent three independent experiments with triplicates in each condition (\*,  $p < 0.05$ , \*\*,  $p < 0.01$ ).

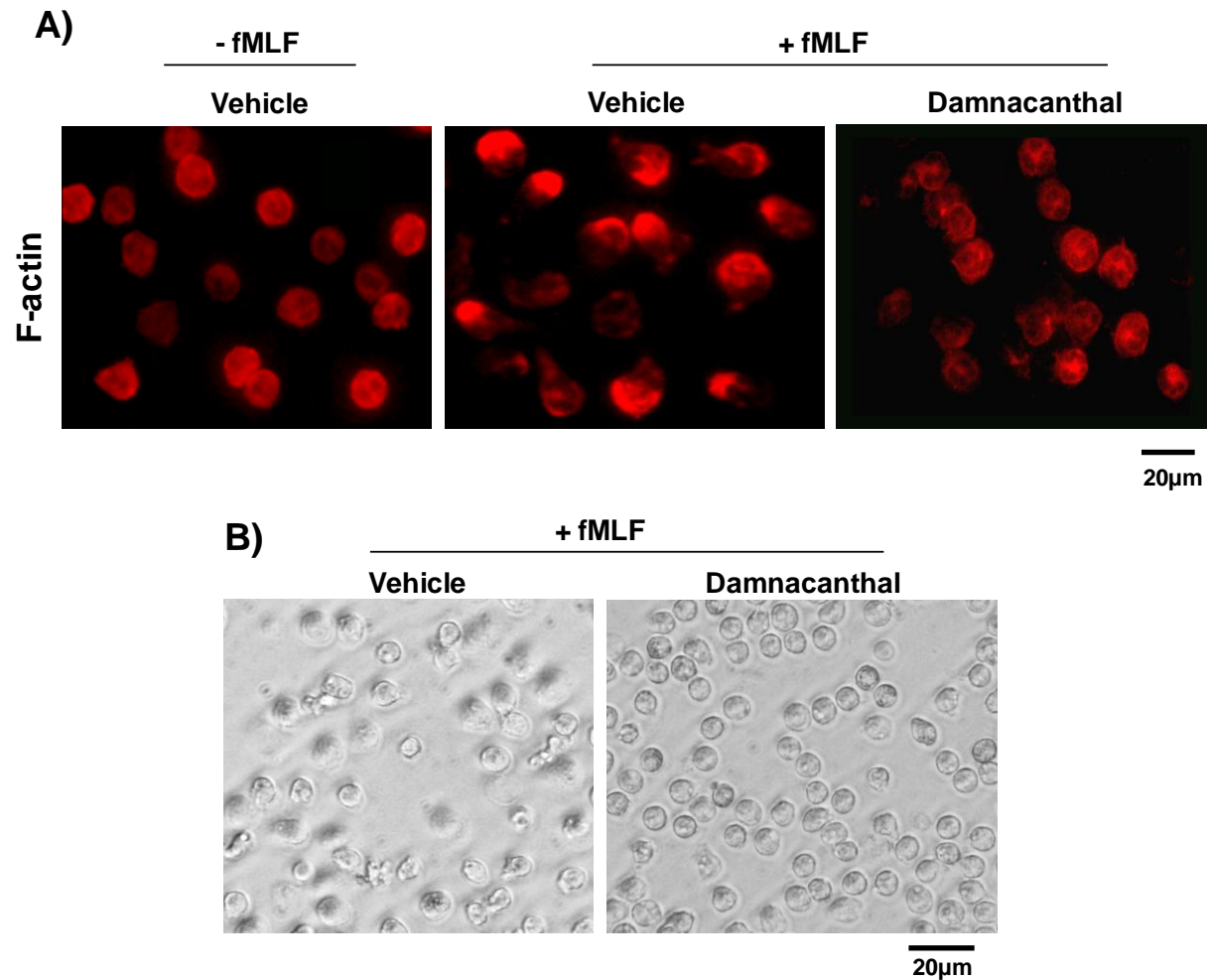


**Figure 3-3.** Damnacanthal inhibits chemoattractant-triggered PMN function. Damnacanthal inhibits PMN F-actin polarization (A) and spreading (B). PMN ( $10^6$ ), untreated or treated with damnacanthal (10  $\mu$ M), were stimulated with fMLF (1 $\mu$ M, 37°C) in collagen-coated wells followed by observation of PMN adhesion and spreading (phase-contrast images). After stimulation for 20min, the cells were then fixed and permeabilized followed by labeling F-actin with rhodamine-conjugated phalloidin.

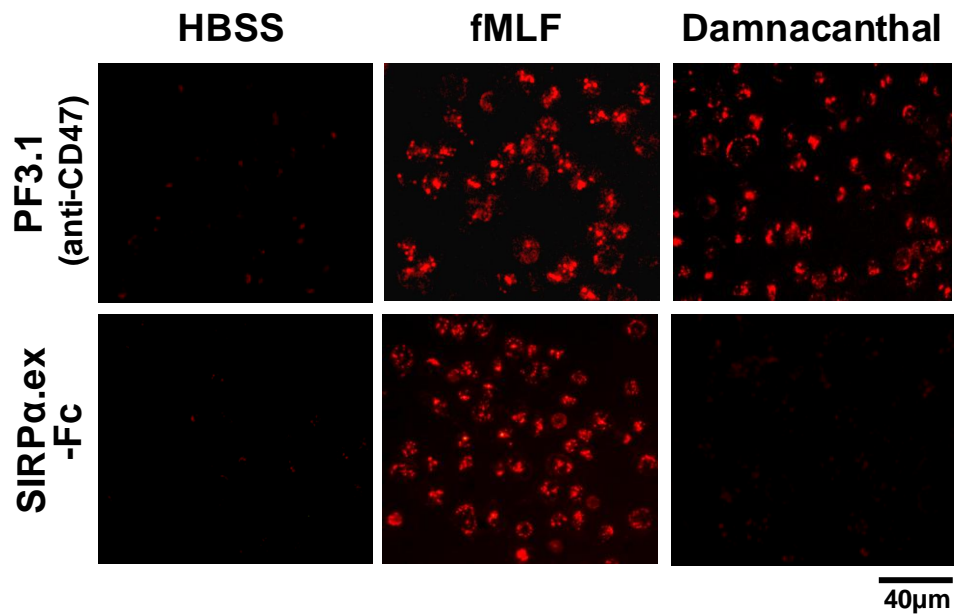


**Figure 3-4.** Damnacanthal inhibits chemoattractant-triggered PMN function. Cell surface CD47 binding to SIRP $\alpha$ . An extracellular domain fusion protein, SIRP $\alpha$ 1.ex-Fc, was used to test PMN cell surface CD47 binding after treatment with either fMLF (1 $\mu$ M) or damnacanthal (10 $\mu$ M). Total amount of CD47 on cell surface was confirmed by labeling non-permeabilized cells with anti-CD47 mAb PF3.1.



### **Identification of the specific GTPase associated with secondary granule release.**

Efforts have been made to identify the target molecule of damnacanthal that plays an important role in preventing secondary granule release in PMN prior to chemoattractant stimulation. We have found that, although damnacanthal is a potent inhibitor of the tyrosine kinase Lck, its effect on PMN degranulation was not through targeting Lck. In agreement with many studies by others, I observed that Lck is mainly expressed in T cells but not in PMN (Figure 3-5). In addition, Dr. Liu obtained Lck-knockout mice [209] from Dr. Tak Mak (Ontario Cancer Institute, Canada). Comparing PMN isolated from Lck knockout mice with the cells from their wild-type littermates yielded no difference in the levels of cell surface protein expression, PMN response to chemoattractant stimulation, degranulation and chemotactic transmigration (data not shown), suggesting that Lck is dispensable in PMN function. A previous study by Brumell et al. also indicated no Lck activity in PMN[210]. In addition to Lck, damnacanthal is also an established inhibitor of Ras family small GTPases [206-207]. Since some of these GTPases, such as Ras family member Ral, have been demonstrated to play important roles in vesicle transportation, thus it was likely that the effect of damnacanthal on PMN through inhibition of Ras family members.

The Ras family small GTPases are traditionally classified into three major subfamilies, Ras (H, R, etc.), Rap (1/2) and Ral (A/B) [211-213]. In addition, three new members of Ras family small GTPases have been identified recently including Rheb, Rin, and Rit [214]. To identify which is potentially involved in the degranulation of secondary granules, I screened the Ras members for activity changes before and after chemoattractant stimulation. Given that damnacanthal treatment caused secondary granule release in the absence of stimulation, I speculated that the candidate Ras member must be in its active form in resting PMN. Also, since chemoattractant stimulation

triggers secondary granule release, we reasoned that this specific Ras should be deactivated in order to coordinate secondary granule release. Based on this rationale, I assayed the activities of Ras, Rap and Ral in PMN before and after fMLF stimulation, and with or without damnacanthal treatment. As shown in Figure 3-6, Ras, Rap and Ral were all expressed in PMN. Among the three family members, Ras was found mainly in its inactive form in unstimulated PMN and was quickly activated after fMLF stimulation. Rap, on the other hand, showed minor activity changes before or after fMLF stimulation and, to our surprise, was insensitive to damnacanthal treatment (Figure 3-6). Therefore, neither Ras nor Rap was likely the candidate that regulates secondary granule release.

In contrast to Ras and Rap, Ral demonstrated a dynamic activity change that correlated with chemoattractant stimulation and PMN degranulation. As shown in Figure 3-6, Ral appeared to be in its active form in unstimulated PMN, and quickly became inactive following fMLF stimulation. Pull-down experiments using RalBP1, a downstream effector that specifically binds to active Ral, recovered significant amount of active Ral from resting PMN. On the other hand, stimulation with fMLF resulted in a quick diminishing of RalBP1 pull-down within 2-5min, a time course paralleled with secondary granule release that was assayed simultaneously (Figure 3-6, right). Same results of were obtained when PMN were stimulated by another chemoattractant IL-8 (Figure 3-7). Deactivation of Ral was also observed in PMN that had chemotactically transmigrated across collaged-coated filters towards fMLF (Figure 3-6, migrated). In addition, activity of Ral in resting PMN was inhibited after damnacanthal treatment (Figure 3-6), which correlated with damnacanthal-induced secondary granule release. Thus, these results suggested Ral to be the regulator that controls secondary granule release in PMN.

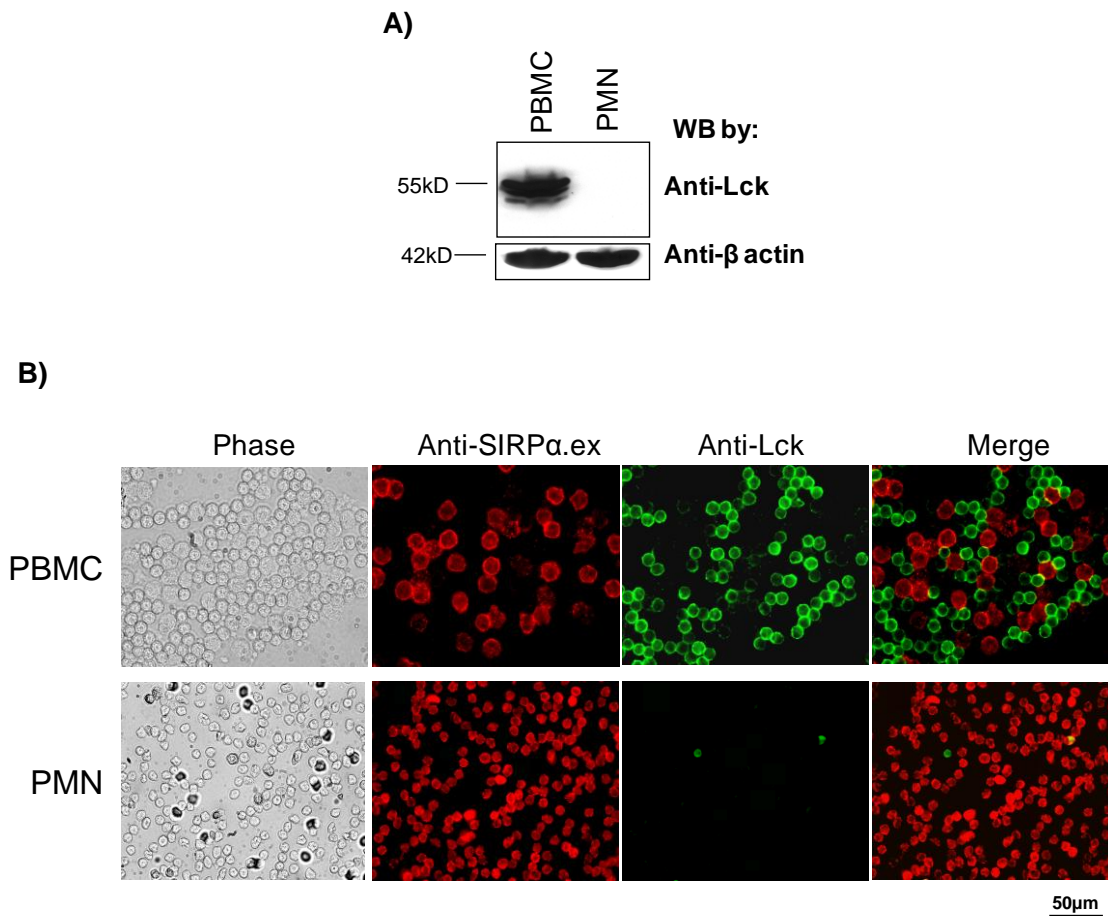


**Figure 3-5.** Lck is not expressed in neutrophils (PMN). A) Western blot detecting Lck in PMN and PBMC. B) Immunofluorescence labeling demonstrating that Lck is expressed in SIRP $\alpha$ -negative cells in PBMC, mainly lymphocytes, but not in SIRP $\alpha$ -positive monocytes or PMN. (Antibody against Lck was purchased from Cell Signaling Technology.) Note: SIRP $\alpha$  is restricted in myeloid lineages, including PMN, monocytes and dendritic cells, but not expressed in lymphocytes. Few Lck-positive cells detected in isolated PMN were likely due to an unavoidable contamination of PBMC. In general, PMN are separated from PBMC by Ficoll-Paque density gradient (used for this study) or gelatin sedimentation. The former method normally produces PMN of 90-95% purity while the latter method produces PMN of varied purity, between 70-90%. Expression of Lck in eosinophils was also reported (Stafford et al. The Journal of Immunology, 2002; Lynch et al. Blood, 2000) and may account for few Lck-positive cells in the preparation of PMN.

To further explore the mechanism that regulates Ral activity in PMN, the localization of RalGDS in PMN was investigated (Figure 4-1). The effect of  $\text{Ca}^{2+}$  and  $\text{Mg}^{2+}$  on Ral activity was examined (Figure 4-2, 4-3, 4-4). Results showed that  $\text{Mg}^{2+}$  was the potential regulator in controlling Ral activity.

To confirm my studies in PMN and verify the pull-down assays, in parallel experiments, I simultaneously assayed Ral activity in platelets. As shown in Figure 3-7B, RalBP1 pull-down results agreed with the previous report by others showing that Ral is inactive in resting platelets and activated after thrombin stimulation [163]. The different Ral activity profiles in PMN and platelets thus suggest that these cells employ distinctive signaling mechanisms to regulate Ral activity and that Ral may have different functional aspects in PMN and platelets.

In addition, Ral activity was also assayed in PMN isolated directly from the “buffy coat” (Figure 3-8) or isolated using lympholyte-poly (Figure 3-9, Figure 3-10) to further investigate the effects of Ral activity on PMN secondary granule release.

Comparing PMN isolated using DEAE-DEXTRAN with the cells isolated from the “buffy coat”, Ral demonstrated the same activity profile. As shown in Figure 3-8, Ral was in its active form in unstimulated PMN, and became inactive following fMLF stimulation.

Ral in PMN isolated using commercial separation chemical, lympholyte-poly, however, retained minimal activity in unstimulated cells (Figure 3-9 and Figure 3-10). fMLF stimulation (Figure 3-9) rendered a quick activation of Ral within 1 min, and a prompt diminishment of Ral activity

after 1 min. IL-8 stimulation (Figure 3-10), on the other hand, sustained Ral activity until 10 min, followed by the loss of activity after 15 min. The similar observation that Ral was inactive in unstimulated PMN was reported by another group [215]. The variation of Ral activity in unstimulated PMN was likely due to the distinct isolation method. In my study, I employed three isolation approaches to examine the activity of Ral in PMN before and after chemoattractant stimulation. Ral was only shown to be inactive in PMN isolated using lympholyte-poly. The results suggest that PMN isolated using DEAE-DEXTRAN may not represent the native status of PMN in the blood stream. Nonetheless, Ral lost activity following chemoattractant stimulation in PMN isolated using different methods, and Ral deactivation with time courses correlated with secondary granule release induced by either fMLF or IL-8. Thus, the results strongly suggest that Ral is likely the specific GTPase that regulates PMN granule mobilization, and in particular, plays an important role in controlling secondary granule release from PMN. Deactivation of Ral is likewise essential for PMN secondary granule release.

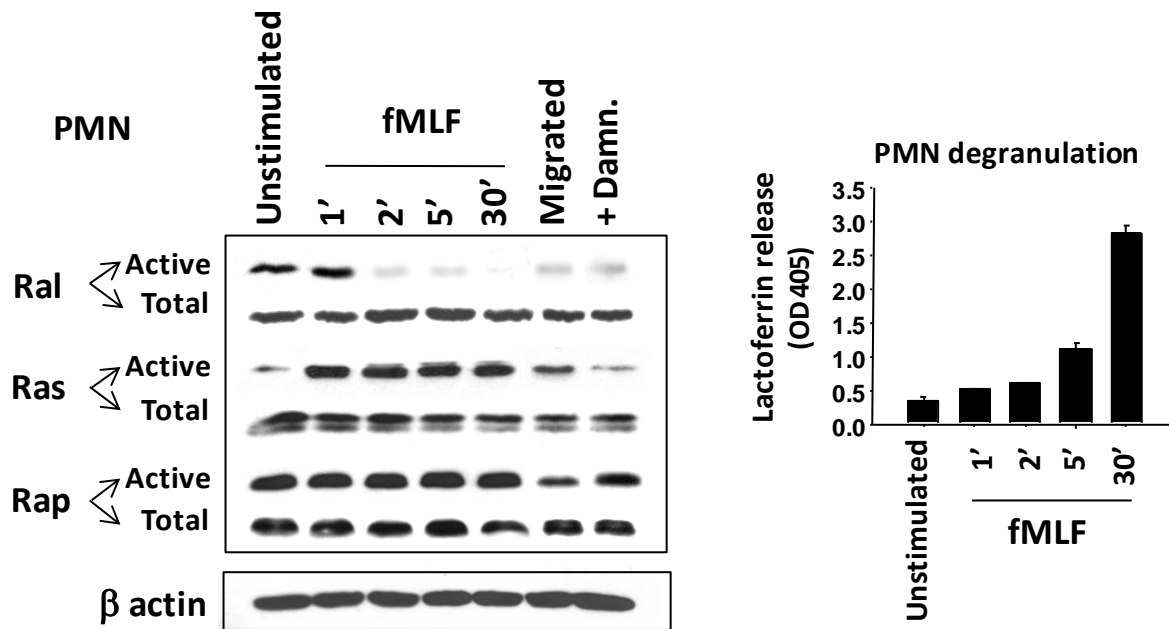


**Figure 3-6.** Ral deactivation correlates secondary granule release in PMN. Detecting activity changes of Ras family small GTPases including Ral, Ras and Rap in PMN. After time-course stimulation with fMLF (1 $\mu$ M), PMN were lysed and active Ras, Ral and Rap were pulled down using Raf-1 RBD, RalBP1 and RalGDS-RBD, respectively. In parallel, fMLF-induced PMN degranulation of secondary granules was assayed simultaneously by detecting lactoferrin in the cell-free supernatants (right panel). PMN that transmigrated across collagen-coated filters into the fMLF-containing lower chambers, or treated with damnacanthal were also assayed for active Ral, Ras and Rap. Cell lysates before pull-down were used to detect total Ral, Ras and Rap, as well as actin using antibodies against Ral, Ras, Rap and  $\beta$  actin.

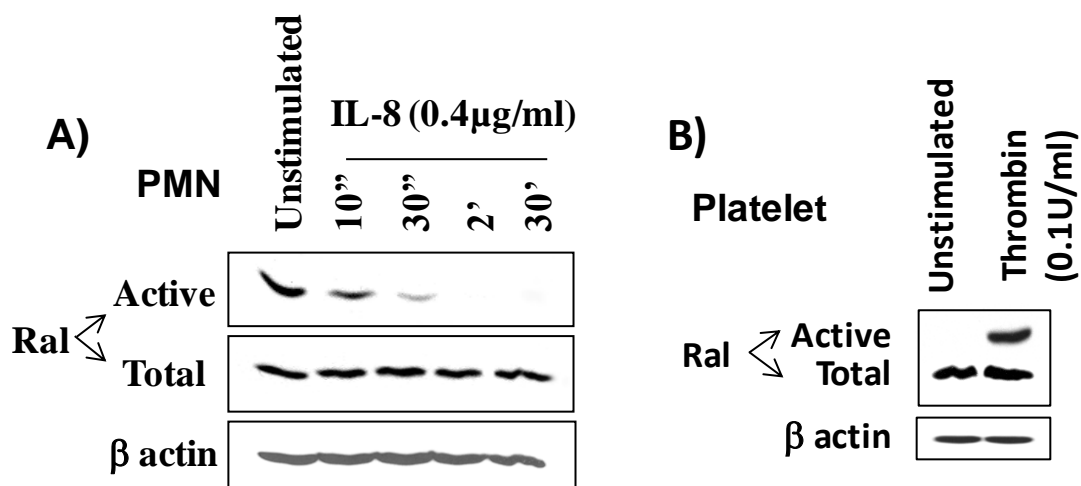


**Figure 3-7.** Ral deactivation correlates secondary granule release in PMN. A) Deactivation of Ral by IL-8 stimulation. Recombinant IL-8 (0.4μg/ml) (Sigma) was used to stimulate PMN for different time periods followed by RalBP1 pull-down to detect active Ral. B) Ral activities in unstimulated and thrombin (0.1U/ml) (Sigma)-stimulated platelets.

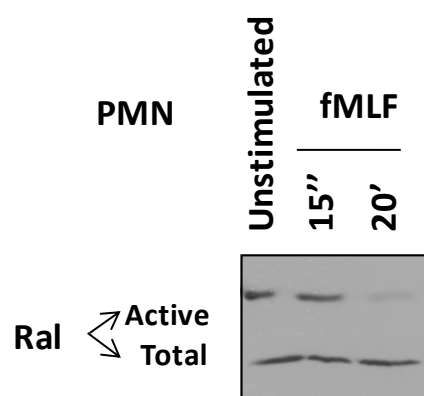


**Figure 3-8.** Detecting activity changes of Ral in PMN isolated directly from “buffy coat”. After time-course stimulation with fMLF (1 $\mu$ M), PMN were lysed and active Ral was pulled down using RalBP1.



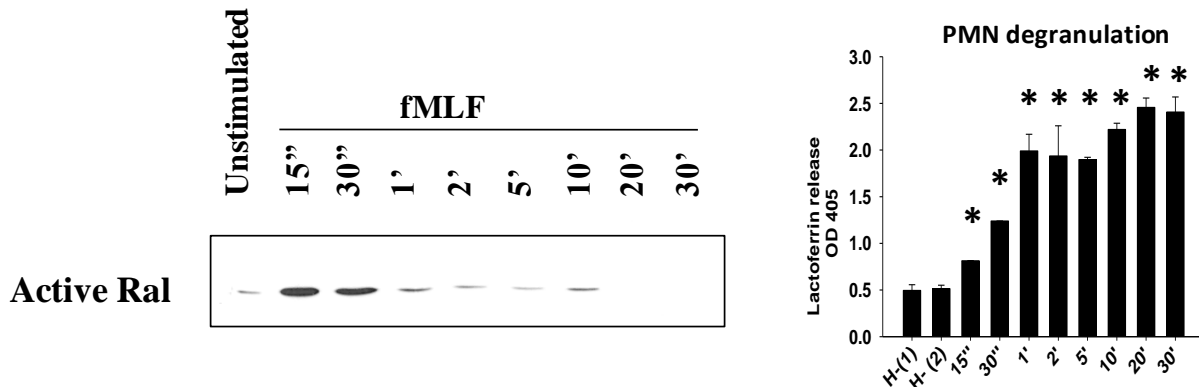


**Figure 3-9.** Ral deactivation correlates secondary granule release in PMN. Detecting activity changes of Ral in PMN isolated using lympholyte-poly. After time-course stimulation with fMLF (1 $\mu$ M), PMN were lysed and active Ral was pulled down using RalBP1. In parallel, fMLF-induced PMN degranulation of secondary granules was assayed simultaneously by detecting lactoferrin in the cell-free supernatants (right panel). All the posts were significantly higher than unstimulated (One-way ANOVA, repeated measures,  $p < 0.0001$  with Dunnett's post tests) \* indicates significant differences ( $p < 0.05$ ).

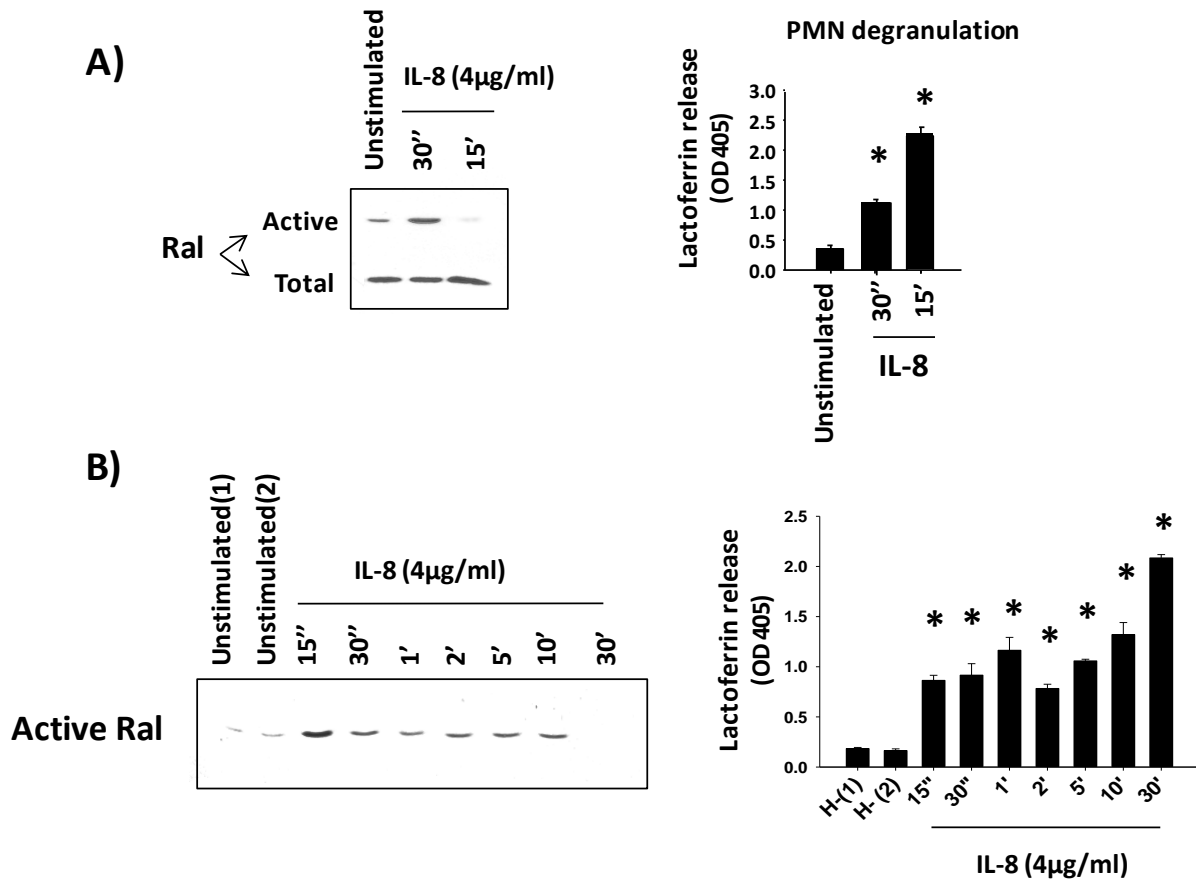


**Figure 3-10.** Ral deactivation correlates secondary granule release in PMN. Detecting activity changes of Ral in PMN isolated using lympholyte-poly. After time-course stimulation with recombinant IL-8 (0.4µg/ml) (Sigma), PMN were lysed and active Ral was pulled down using RalBP1. In parallel, fMLF-induced PMN degranulation of secondary granules was assayed simultaneously by detecting lactoferrin in the cell-free supernatants (right panel). All the posts were significantly higher than unstimulated (One-way ANOVA, repeated measures,  $p<0.0001$  with Dunnett's post tests) \* indicates significant differences ( $p<0.05$ ).

### **Active Ral blocks secondary granule release in PMN.**

To test that active Ral in resting PMN serves to prevent secondary granule release and that Ral deactivation in response to chemoattractant stimulation is required for degranulation, I designed experiments to over-express a constitutively active Ral, Ral23V, in PMN and tested its effect on fMLF-induced degranulation. Since freshly isolated PMN are short-lived and not suitable for protein expression by conventional gene transfection methods, I employed protein transduction technology and directly delivered purified recombinant Ral into PMN by tagging the proteins with an HIV Tat peptide (YGRKKRRQRRR) [54, 200, 216]. As demonstrated by previous studies, HIV Tat and other poly-arginine peptides have been widely used to transduce proteins of up to 120kD into live cells [54, 200, 216]. Although PMN are highly sensitive and difficult to handle, using HIV Tat to study important intracellular molecules has been very successful [54, 217-218]. In this study, three Tat-tagged Ral proteins were generated, including a wild-type Ral (WT), a constitutively active mutant Ral (Ral23V), and a dominant negative mutant Ral (Ral28N) [117, 167, 202]. As depicted in Figure 3-11, these proteins were first produced as recombinant GST fusions, followed by removal of GST and yielding Tat-tagged Ral. Figure 3-11B&C shows the stepwise production of Tat-tagged WT, Ral23V and Ral28N, and RalBP1 pull-down confirming that Ral23V was a constitutively active form.

To determine that Tat-tagged Ral proteins were capable of directly delivery into PMN, I chemically labeled the purified proteins with fluorescein (FITC), followed by incubation with PMN. As shown in Figure 3-12A, fluorescence microscopy revealed that the three Tat-tagged Ral proteins (Tat-WT, Tat-Ral23V and Tat-Ral28N) were all rapidly delivered into PMN after only a short incubation (10min) at a low temperature (4°C). Subsequent Western blot detected an over

two-folds increase of Ral in PMN after incubating with each Tat-tagged Ral protein (Figure 3-12B). I also performed RalBP1 pull-down assays to test Ral activity after delivery of each Tat-tagged Ral protein into PMN. As shown in Figure 3-13, transduction of exogenous Ral23V into PMN led to a sustained Ral activity in PMN even in the presence of fMLF stimulation, a condition that the endogenous Ral activity was completely diminished as that observed in the control, non-peptide transduction PMN. Transduction of WT Ral or Ral28N, on the other hand, only slightly (WT) or did not (Ral28N) increase Ral activity in PMN (Figure 3-13).

I next investigated whether Ral activity blocks fMLF-induced PMN degranulation. In these experiments, PMN were first loaded with Tat-tagged WT Ral, Ral23V or Ral28N, and then stimulated with fMLF. As shown in Figure 3-14A, no spontaneous PMN degranulation was detected by just loading Tat-tagged Ral proteins (unstimulated). Prominent release of secondary granules was induced by fMLF in PMN loaded with WT Ral or Ral28N, or without peptide delivery. On the contrary, transduction of the constitutively active Ral, Ral23V, into PMN strikingly blocked secondary granule release in the presence of fMLF. As shown in Figure 3-14, both lactoferrin release (Figure 3-14A) and CD47 translocation to the cell surface plasma membrane (Figure 3-14B) were inhibited by Ral23V in PMN in spite of fMLF stimulation. However, Ral23V had no effect on fMLF-induced tertiary granule release or the retention of primary granules (Figure 3-15A), further suggesting that Ral selectively regulates secondary granule mobilization.

Given that PMN degranulation of secondary granules is crucial for chemotaxis, I thus performed PMN transmigration assays and examined the effect of Ral23V. As shown in Figure 3-15B, as expected, transduction of Ral23V into PMN significantly reduced PMN transmigration towards

fMLF, while WT Ral or Ral28N had no inhibition. In conclusion, these results demonstrated that Ral activity blocks secondary granule release from PMN. Therefore chemoattractant-induced Ral deactivation is essential for PMN degranulation, activation and chemotaxis.

In order to further investigate whether active Ral inhibits fMLF-induced PMN secondary granule release regardless of what PMN isolation method is employed, transduction of Tat-tagged constitutively active Ral (Ral23V) into PMN isolated from “buffy coat” or using lympholyte-poly followed by assay of secondary granule release was carried out. In these experiments, PMN were first loaded with Tat-tagged WT Ral, Ral23V or Ral28N, and then stimulated with fMLF. As shown in Figure 3-16, 3-17, and 3-18, transduction of the constitutively active Ral, Ral23V, notably blocked both CD47 translocation to the cell surface plasma membrane (Figure 3-16 and Figure 3-17) and lactoferrin release (Figure 3-18) regardless of fMLF stimulation. Overexpression of active Ral in PMN isolated from the “buffy coat”, using lympholyte-poly, or using DEAE-DEXTRAN prevented secondary granule release, thus, further supporting the fact that active Ral serves as a gate-keeper for degranulation of secondary granules from PMN.

Considering that the *Ral* gene is composed of *RalA* and *RalB*, I further explored the role of the *Ral* gene in human PMN. As shown in Figure 3-19, studies of *Ral* expression in human leukocytes by RT-PCR detected both *RalA* and *RalB* in PMN. RalA and RalB are highly homologous proteins and share most (if not all) of the functional domains identified to date, as shown in Figure 1-11 and Figure 1-12. The possible Ral downstream effector proteins relevant to our study involved in receptor endocytosis, such as RalBP1/RLIP76, were found to bind to RalA and RalB at sites with an identical amino acid sequence (aa 37-56). Although RalA and RalB have over-

lapping functions, which have been reported by various studies, I further investigated the specific role of RalB in PMN secondary granule release. In these experiments, I generated a Tat-tagged constitutively active RalB (RalB23V) protein, followed by transduction of the protein into PMN, and assayed its effect on secondary granule release. Transduction of RalB23V into PMN also inhibited PMN mobilization of secondary granules shown by impaired lactoferrin release and blockage of CD47 translocation to plasma membrane (Figure 3-20).

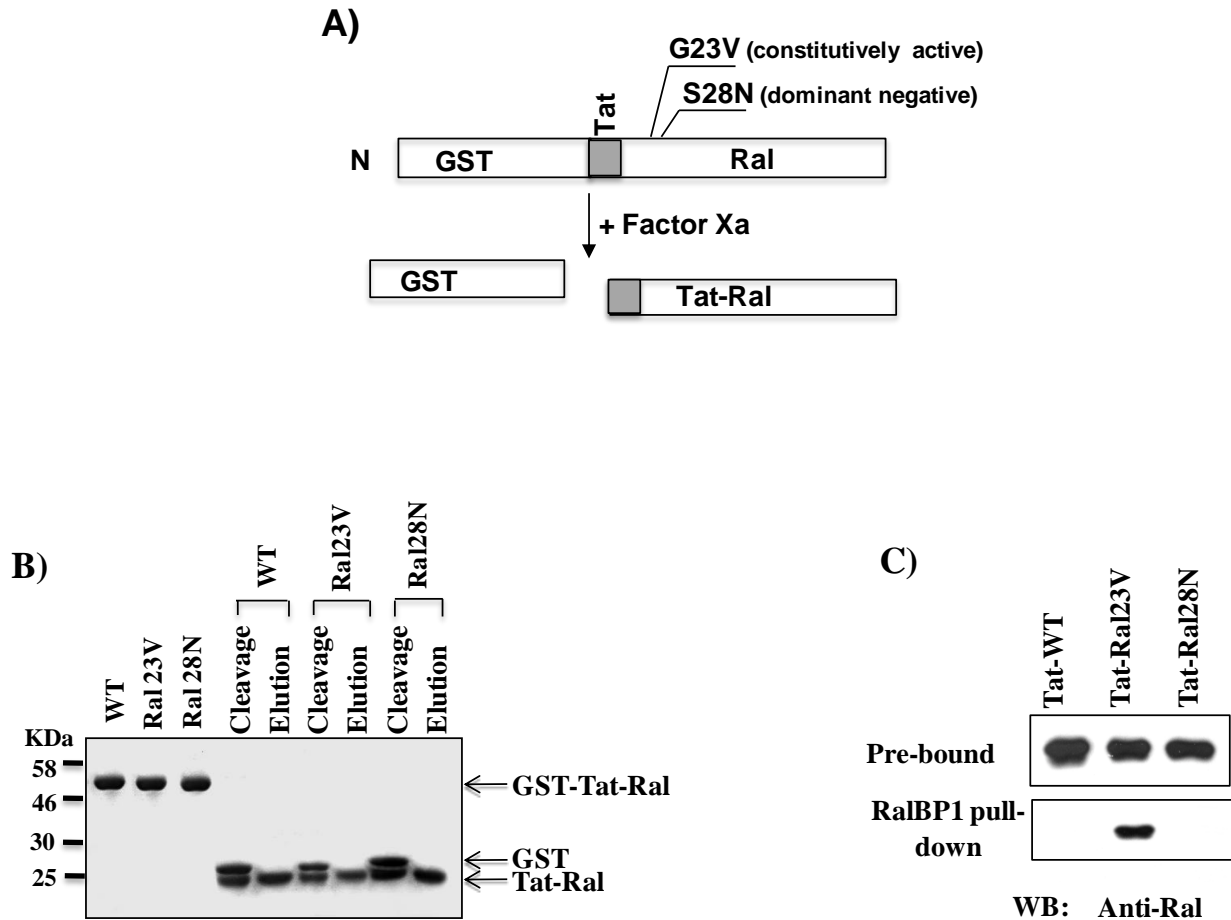


**Figure 3-11.** Generation of Tat-tagged wild-type Ral (WT), constitutively active Ral (Ral23V), and dominant negative Ral (28N) protein. A) A schematic depiction of Tat-tagged Ral production. The recombinant fusion proteins containing GST and Tat-Ral were produced, followed by cleavage of GST with Factor Xa to yield Tat-Ral peptides. The figure also shows that two point mutations, G23V and S28N, were created in Ral to produce constitutively active Ral (23V) and dominant negative Ral (28N). B) A stepwise analysis of Tat-tagged Ral protein production by SDS-PAGE and Coomassie blue staining. C) RalBP1 pull-down confirming that Tat-Ral23V was a constitutively active GTPase. Purified Tat-tagged wild-type Ral, Ral23V and Ral28N (0.2 $\mu$ g each) were incubated with GST-RalBP1 (1 $\mu$ g) and glutathione Sepharose in HBSS containing 5% non-fat dry milk, 2% BSA and 0.01% Tween 20 for 1h. After washing the precipitates, Western blot was performed to detect active Ral pulled down by RalBP1.

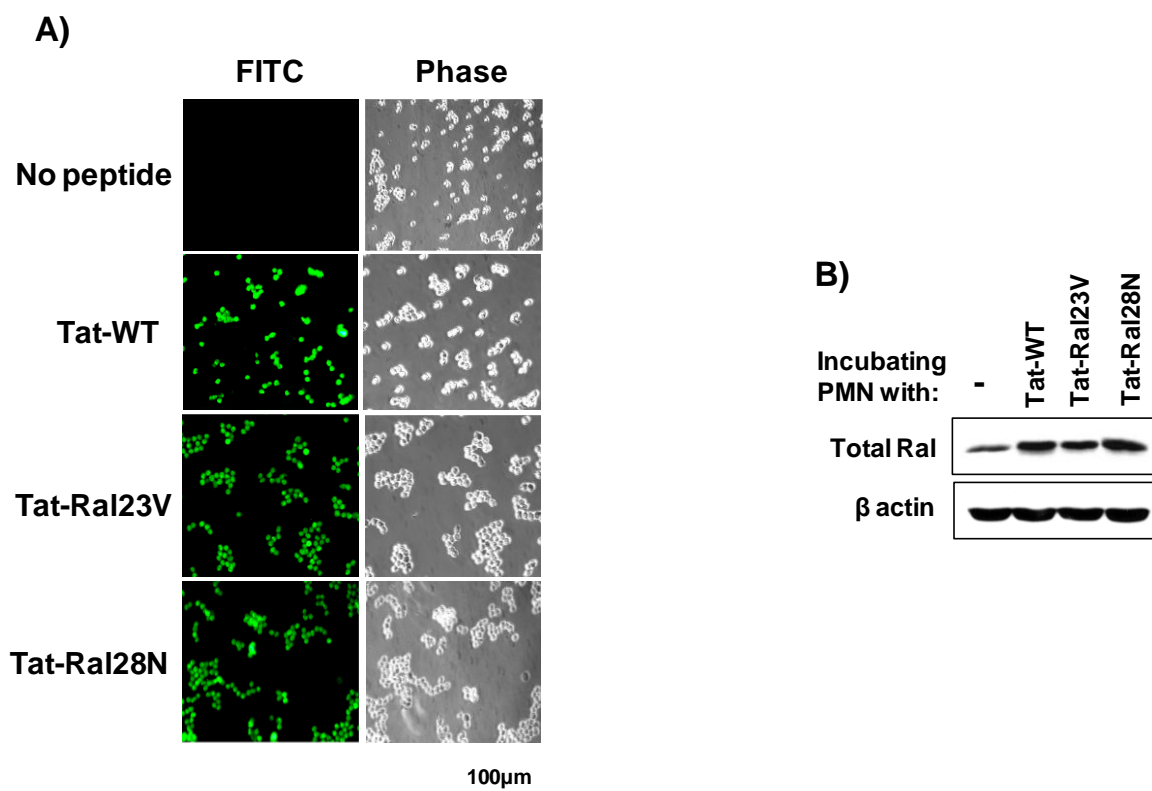


**Figure 3-12.** Transduction of Tat-tagged Ral proteins including wild-type Ral (WT), constitutively active Ral (Ral23V), and dominant negative Ral (28N) to PMN. A) Assaying Tat-tagged Ral transduction into PMN. Tat-tagged wild-type Ral (WT), Ral23V and Ral28N (0.1μM of each) were labeled with FITC followed by incubation with PMN for 10min at 4°C. B) Effective transduction into PMN was then analyzed by Western blot.



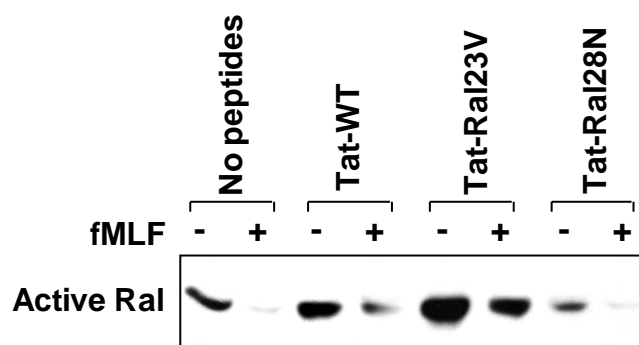


**Figure 3-13.** Tat-tagged constitutively active Ral sustained endogenous Ral activity in PMN. After transduction of Tat-tagged Ral into PMN, PMN were stimulated with fMLF (1 $\mu$ M) for 20min at 37°C followed by cell lysis. RalBP1 pull-down were then performed to detect active Ral. As shown, the result confirmed that transduction of Ral23V in PMN resulted in a sustained Ral activity even with fMLF stimulation.

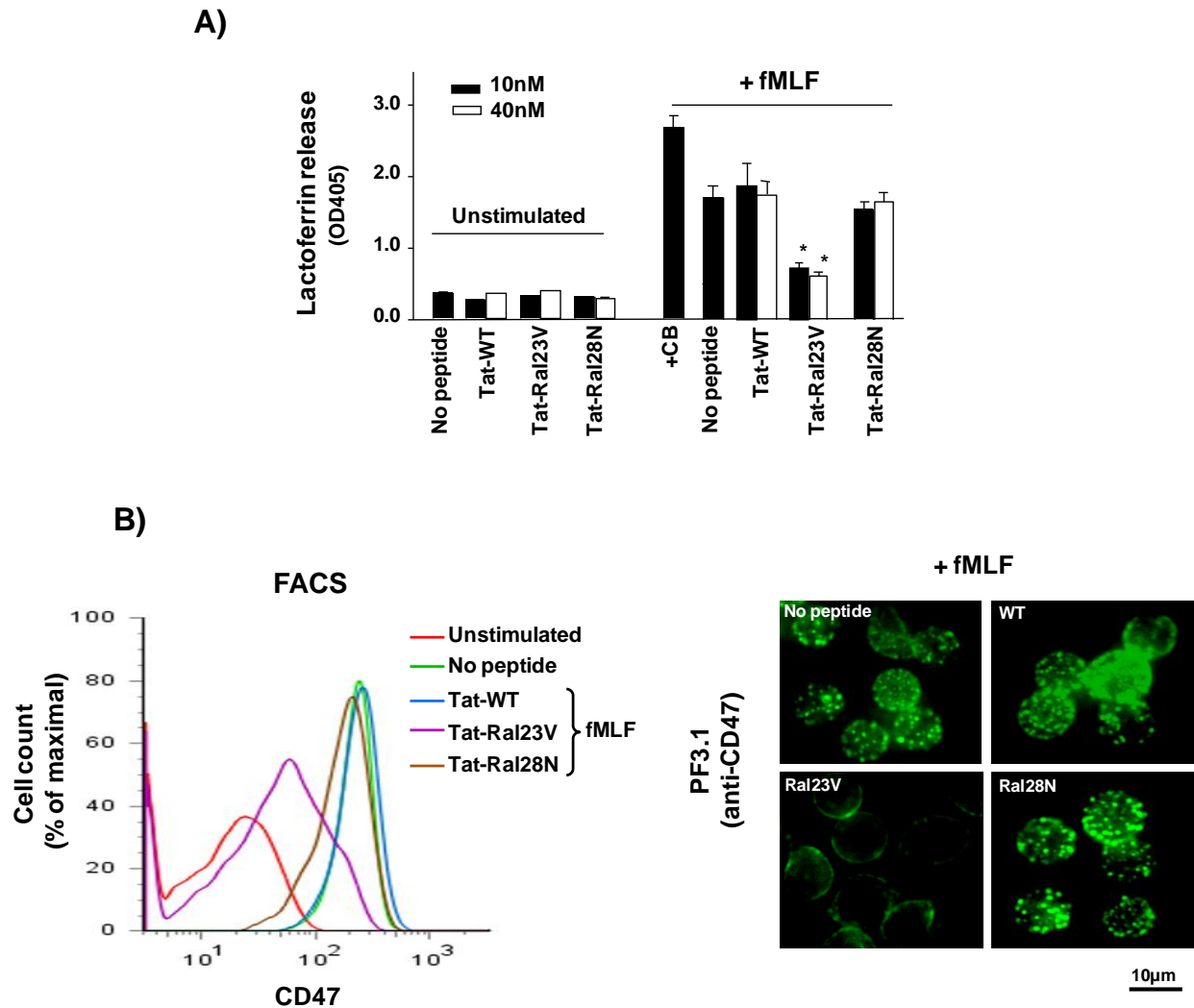


**Figure 3-14.** Constitutively active Ral (Ral23V) inhibits chemoattractant-induced secondary granule release in PMN. A) & B) Effects of Tat-tagged Ral proteins on fMLF-induced secondary granule release in PMN. PMN were incubated with purified Tat-tagged wild-type Ral (WT), the constitutive active Ral (Ral23V) and dominant negative Ral (Ral28N) at concentrations of 10nM and 40nM, or control buffer (No peptide) (30min, 4°C) followed by stimulation with fMLF (1µM) for 20min at 37°C. Degranulation of secondary granules was analyzed by measuring lactoferrin release in the cell-free supernatants (A) and cell surface labeling of CD47 by anti-CD47 antibody PF3.1 (B) followed by flow cytometry (FACS). The data were subjected to a one-way ANOVA (repeated measures,  $p < 0.0001$  with Dunnett's post tests). \* indicates significant differences in lactoferrin release from PMN with and without Tat-Ral23V transduction ( $p < 0.05$ ).

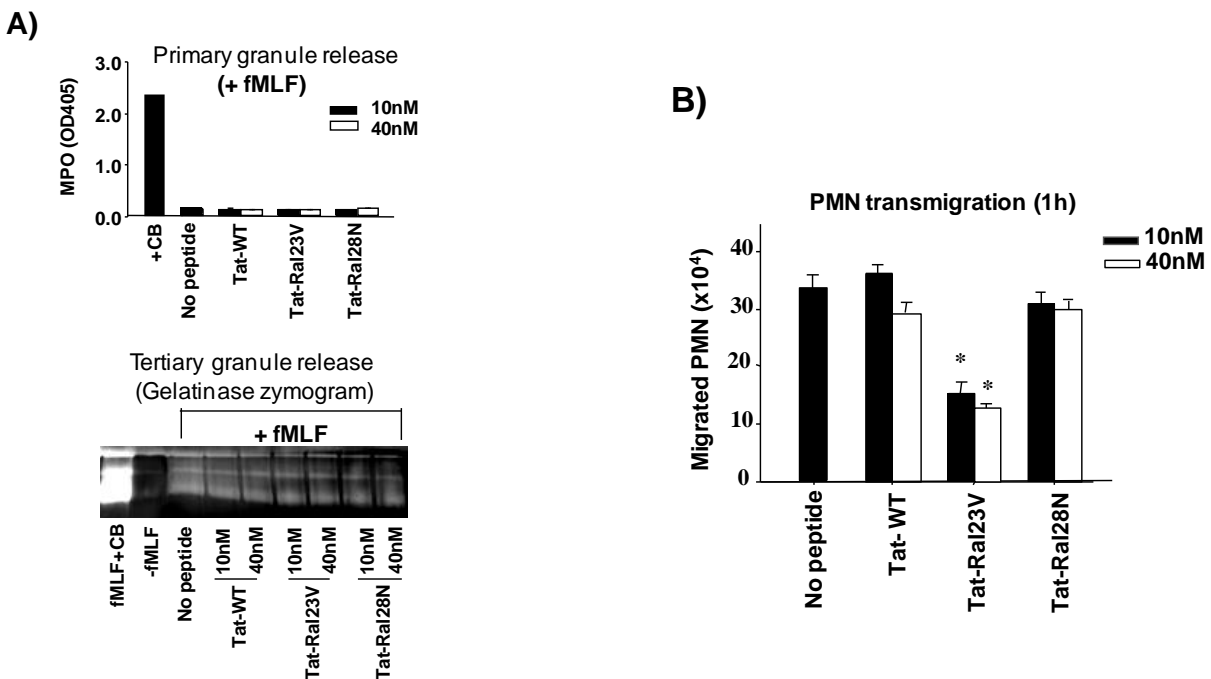


**Figure 3-15.** Specificity of Tat-tagged Ral proteins in PMN granule release. A) Tat-Ral23V has no effect on the mobilization of primary and tertiary granules. B) Transduction of Tat-Ral23V into PMN inhibited PMN chemotactic transmigration. Data (mean  $\pm$  SD) represent three independent experiments with triplicates in each condition. The data were subjected to a one-way ANOVA (repeated measures,  $p < 0.0001$  with Dunnett's post tests). \* indicates significant differences in cell number of migrated PMN with and without Tat-Ral23V transduction ( $p < 0.05$ )

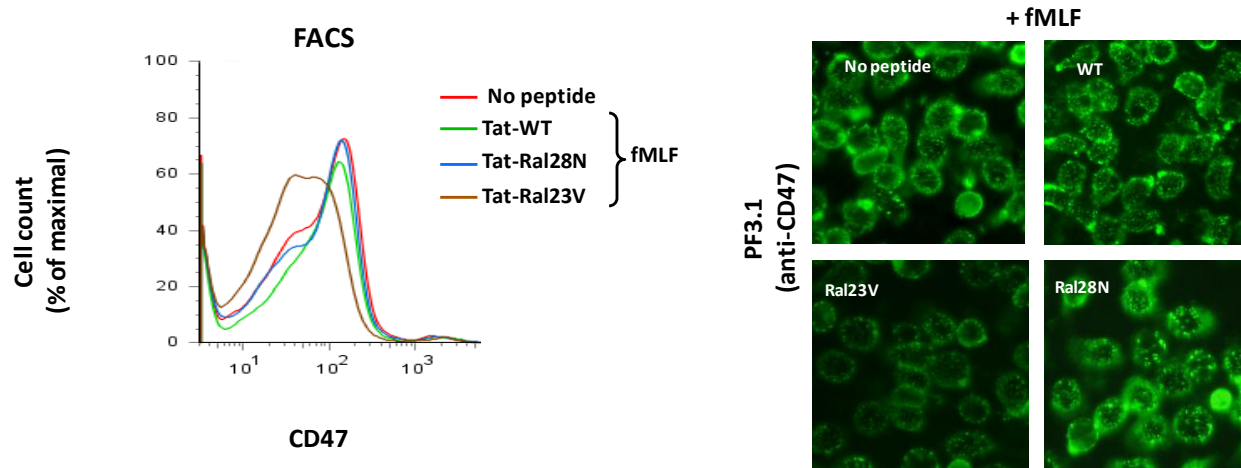


**Figure 3-16.** Constitutively active Ral (Ral23V) inhibits chemoattractant-induced secondary granule release in PMN isolated using lympholyte-poly. PMN were incubated with purified Tat-tagged wild-type Ral (WT), the constitutive active Ral (Ral23V) and dominant negative Ral (Ral28N) at concentration of 40nM, or control buffer (No peptide) (30min, 4°C) followed by stimulation with fMLF (1μM) for 20min at 37°C. Degranulation of secondary granules was analyzed by cell surface labeling of CD47 by anti-CD47 antibody PF3.1 (right panel) followed by flow cytometry (FACS) (left panel).

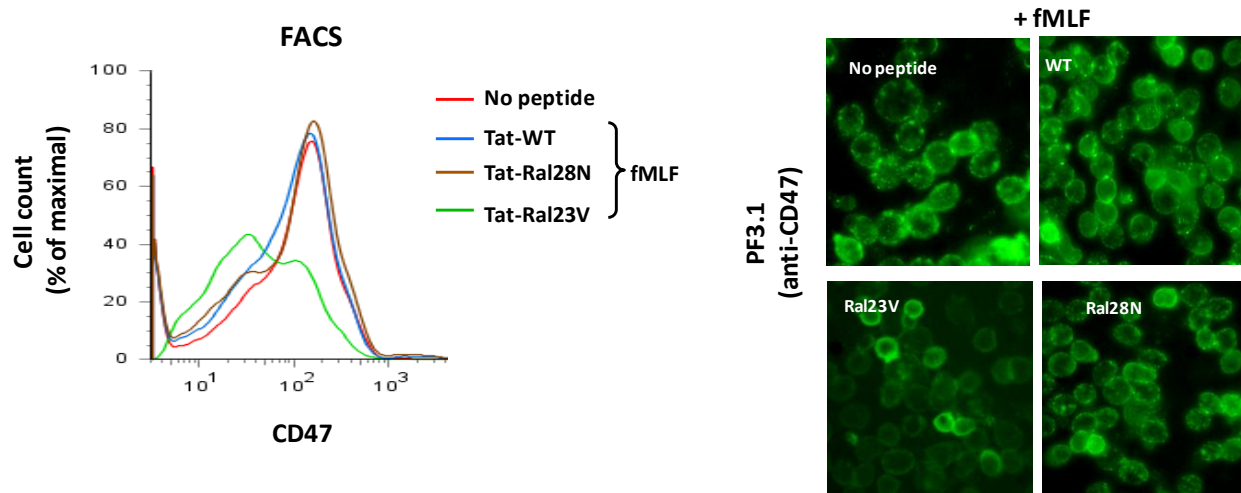


**Figure 3-17.** Constitutively active Ral (Ral23V) inhibits chemoattractant-induced secondary granule release in PMN isolated directly from “buffy coat”. PMN were incubated with purified Tat-tagged wild-type Ral (WT), the constitutive active Ral (Ral23V) and dominant negative Ral (Ral28N) at concentration of 40nM, or control buffer (No peptide) (30min, 4°C) followed by stimulation with fMLF (1μM) for 20min at 37°C. Degranulation of secondary granules was analyzed by cell surface labeling of CD47 by anti-CD47 antibody PF3.1 (right panel) followed by flow cytometry (FACS) (left panel).

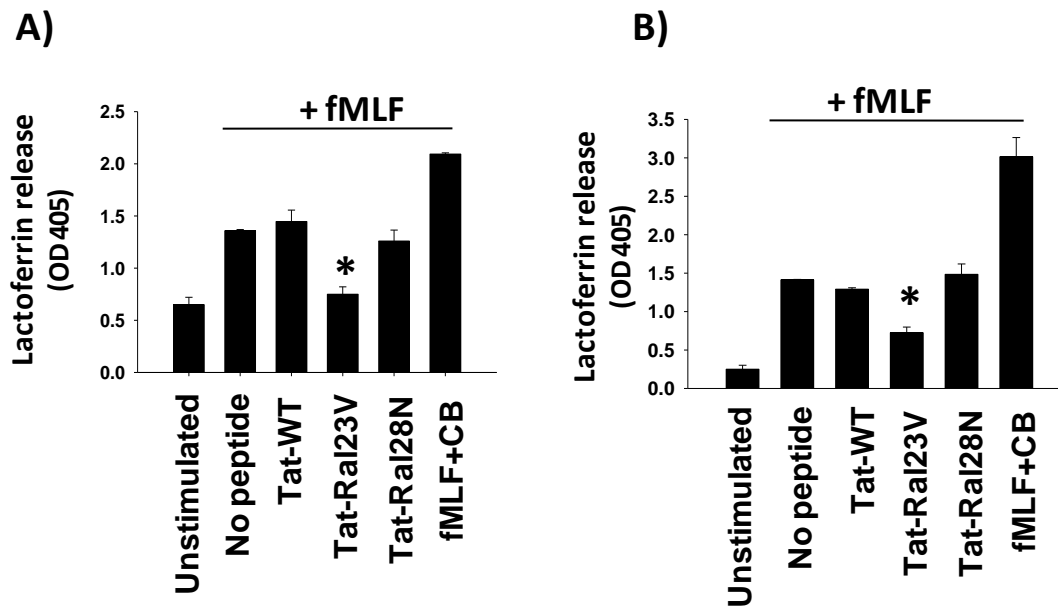


**Figure 3-18.** Constitutively active Ral (Ral23V) inhibits chemoattractant-induced secondary granule release in PMN isolated from “buffy coat” (A) and using lympholyte-poly (B). A) & B) Effects of Tat-tagged Ral proteins on fMLF-induced secondary granule release in PMN. PMN were incubated with purified Tat-tagged wild-type Ral (WT), the constitutive active Ral (Ral23V) and dominant negative Ral (Ral28N) at concentration of 40nM, or control buffer (No peptide) (30min, 4°C) followed by stimulation with fMLF (1μM) for 20min at 37°C. Degranulation of secondary granules was analyzed by measuring lactoferrin release in the cell-free supernatants. A) All the posts had significant difference compared with than no peptides (One-way ANOVA, repeated measures,  $p < 0.0002$  with Dunnett’s post tests) B) All the posts had significant difference compared with no peptide treatment (One-way ANOVA, repeated measures,  $p < 0.0001$  with Dunnett’s post tests) \* indicates significant differences in lactoferrin release from PMN with and without Tat-Ral23V transduction ( $p < 0.05$ ).

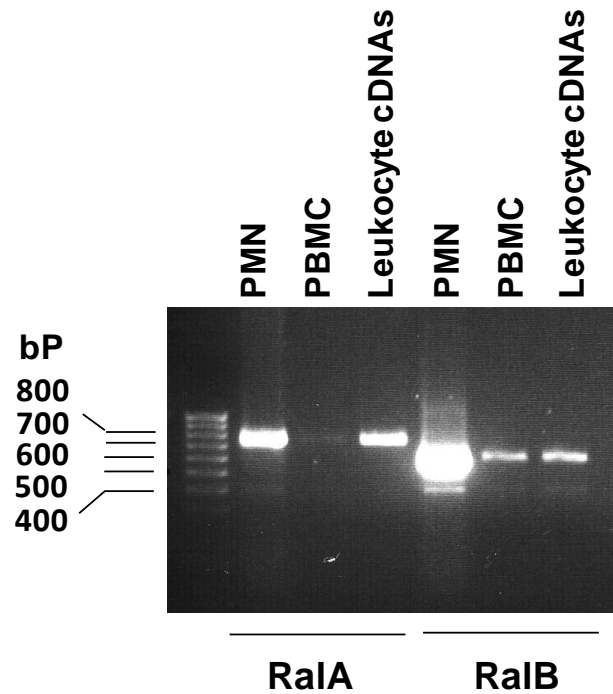


**Figure 3-19.** Detection of RalA and RalB in human leukocytes. The RalA-specific and the RalB-specific cDNA fragments, 777bps and 648bps, respectively, were RT-PCR amplified from freshly isolated PMN and PMBC. The same DNA fragments were also PCR amplified from a human leukocyte cDNA library (Marathon Ready cDNAs, Clontech). Given that RalA and RlaB are highly homologous, the PCR primers were specially chosen based on the most dissimilar regions of their cDNAs. The primers for amplifying RalA were 5-ttccaggcgacaaggaccg agta and 5-aagataagaaaggagtttggg. The primers for amplifying RalB were 5-atggctgccaacaagagtaag and 5-agctggcttcacgcgtcacctt. The amplified PCR fragments were DNA sequenced to confirm their identities.

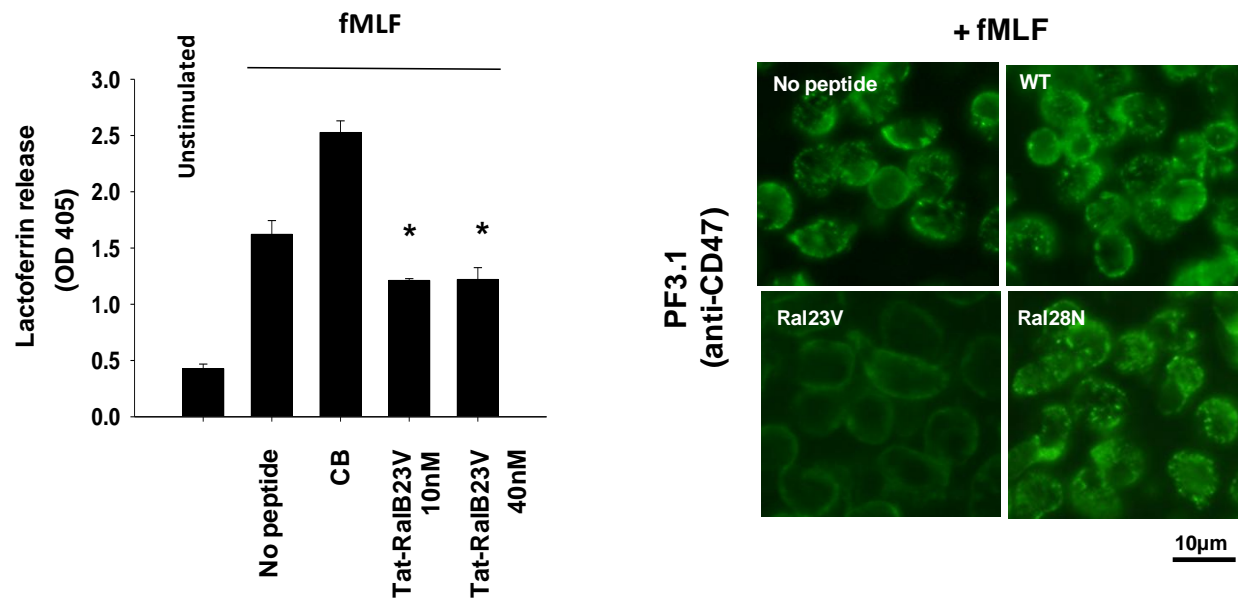


**Figure 3-20.** Constitutively active RalB (Ral23V) inhibits chemoattractant-induced secondary granule release. PMN were incubated with purified Tat-tagged wild-type RalB (WT), the constitutively active RalB (Ral23V) and dominant negative RalB (Ral28N) at concentration of 40nM or 10nM, or control buffer (No peptide) (30min, 4°C) followed by stimulation with fMLF (1μM) for 20min at 37°C. Degranulation of secondary granules was analyzed by lactoferrin release (left panel) and cell surface labeling of CD47 by anti-CD47 antibody PF3.1 (right panel). All the posts had significant difference compared with no peptide treatment (One-way ANOVA, repeated measures,  $p < 0.0001$  with Dunnett's post tests) \* indicates significant differences in lactoferrin release from PMN with and without Tat-Ral23V transduction ( $p < 0.05$ ).



### **Ral translocation between plasma membranes and secondary granules**

Like Ras family GTPases, Ral contains a lipid modification site at the carboxyl terminus, suggesting that Ral may be associated with the cell membranes. To test this, I separated PMN membranes from the cytosol by ultracentrifugation in the absence of detergent. As shown in Figure 10A, Western Blot indicated that Ral is exclusively associated with the cell membranes in PMN. To further localize Ral and define whether Ral is dynamically coupled with secondary granules, I performed subcellular fractionation using sucrose density gradients. As shown in Figure 3-21, the fractionations successfully separated PMN plasma membranes (alkaline phosphatase) from secondary granules (lactoferrin) and primary granules (MPO). To my surprise, detection of Ral in the fractions by western blots revealed that Ral is entirely associated with the plasma membrane in unstimulated PMN that is co-localized with another plasma membrane protein JAM-A. Stimulation with fMLF, on the other hand, resulted in translocation of a considerable amount of Ral to secondary granules (Figure 3-21B). In agreement with previous observation [68, 70], proteins initially stored in secondary granules, such as SIRP $\alpha$ , were redistributed to the plasma membrane after fMLF stimulation following degranulation. As predicted, RalBP1 pull-down recovered active Ral from the plasma membrane fractions of unstimulated PMN, but not from secondary granule-rich fractions (Figure 3-22). I also performed immunofluorescence labeling and observed that, as shown in Figure 3-23, Ral in unstimulated PMN was co-localized with the plasma membrane marker wheat germ agglutinin (WGA) [219]. Stimulation with fMLF induced a significant dissociation of Ral from WGA, suggesting Ral redistribution in PMN.

One major mechanism of plasma membrane internalization in PMN after chemoattractant stimulation is through clathrin-mediated cell surface receptor endocytosis [208, 220], and a previous

study demonstrated that a Ral effector is complexed with a component of clathrin pits [121]. Therefore, I examined whether fMLF-induced Ral translocation from the plasma membrane to intracellular granules followed this pathway.

Two inhibitors, dynasore [193] and a AP-2 binding Eps15 C-terminal peptide (Eps15-DIII)[194-195], which specifically act on the clathrin-dependent endocytosis were examined. As shown in Figure 3-24A, pre-treatment of PMN with dynasore (80  $\mu$ M) and recombinant Eps15-DIII (40 nM), or their combination, appeared to have no inhibition on Ral translocation to secondary granules after fMLF stimulation. Dynasore inhibits dynamin, an essential GTPase regulating clathrin-coated pit fission, while Eps15-DIII inhibits clathrin-mediated endocytosis through sequestration of AP-2 thus interferes formation of the clathrin coat. To effectively use Eps15-DIII in the study, this peptide was tagged with HIV-Tat, which significantly facilitated protein transduction into PMN (Figure 3-24B). I also confirmed the function of the Eps15-DIII by protein pull-down assays, which demonstrated that Eps15-DIII successfully co-precipitated AP-2 from PMN lysates (Figure 3-24C).

In addition to dynasore and a AP-2 binding Eps15 C-terminal peptide (Eps15-DIII), I also included several other traditional endocytosis inhibitors that act on the clathrin-dependent endocytosis including hypertonic sucrose (0.5M)[221], salt (0.76M NaCl)[222], phenylarsine oxide (POA)[223], chlorpromazine (CPZ)[196], and cytosolic acidification (succinic acid, pH5.5) [197-198]. As shown in Figure 3-25A, blocking clathrin-mediated endocytosis in PMN with classical inhibitors resulted in a partial or complete inhibition of fMLF-induced secondary granule release. Remarkably, as shown in Figure 3-25B, these reagents also abolished Ral deactiva-

tion after fMLF stimulation. In addition, contrary to the fact that dynasore and the Eps15 peptide failed to exhibit inhibitory effects, CPZ and succinic acid remarkably blocked Ral translocation. Subcellular fractionations demonstrated that, as shown in Figure 3-24A, blockage of clathrin-dependent endocytosis by CPZ [196] or cytosolic acidification (succinic acid, pH5.5) through inhibition of the pinching off of clathrin-coated pits [197-198] eliminated Ral translocation from plasma membranes to secondary granules in response to fMLF. These two inhibitors also effectively blocked fMLF-induced secondary granule release as indicated by a failure of translocation of secondary granule proteins (e.g. SIRP $\alpha$ ) to the plasma membrane (Figure 3-24A). As predicted, immunofluorescence labeling revealed a failure of Ral dissociation from the plasma membrane marker WGA in the presence of those two endocytic inhibitors (Figure 3-23, lower panel).

The results demonstrated that only classical inhibitors including CPZ and succinic acid were able to block Ral translocation from plasma membrane to secondary granules upon fMLF stimulation. Considering the nonspecificity of classical inhibitors for clathrin-mediated endocytosis, these results suggest that clathrin-mediated endocytosis might not be involved in Ral intracellular translocation and deactivation.

Considering that Ral deactivation and translation results in PMN secondary granule release, the role of Ral in damnacanth-mediated PMN secondary granule release was explored. Results, however, were not conclusive (Figure 4-5, 4-6, 4-7).

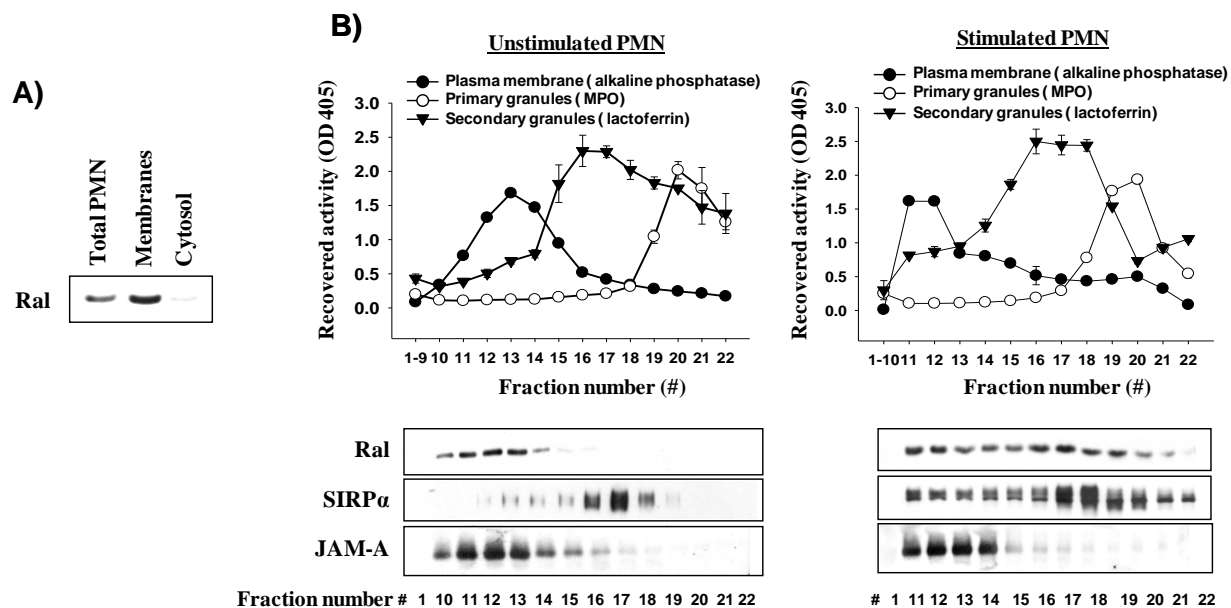


**Figure 3-21.** Localization of Ral in PMN. A) Ral is associated with membranes. PMN ( $2.5 \times 10^7$ ) were dounce-lysed followed by ultracentrifugation to separate cytosol from cell membranes. SDS-PAGE and Western blot were performed to detect Ral in the total lysate before centrifugation (total PMN) and in the separated cytosol and membranes. B) Subcellular localization of Ral in PMN. PMN ( $10^8$ /per condition), unstimulated and fMLF-stimulated, were lysed and subjected to sucrose density gradient centrifugation to separate the plasma membrane and intracellular granules followed by fractionation. Western blots (lower panel) were performed to detect Ral, SIRP $\alpha$  and JAM-A in the fractions using antibodies against Ral, anti-SIRP $\alpha$ .ex and anti-JAM-A.ex. JAM-A is a transmembrane protein consistently expressed in the plasma membranes.

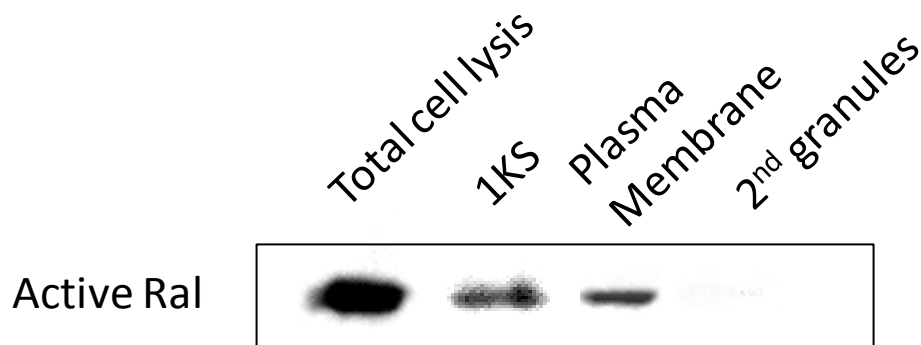


**Figure 3-22.** In unstimulated PMN, Ral is active in plasma membrane and inactive in secondary granules. PMN ( $10^8$ /per condition) were lysed and subjected to sucrose density gradient centrifugation to separate the plasma membrane and intracellular granules followed by fractionation. Active Ral was pulled down using RalBP1 from plasma membrane, secondary granules, 1KS (dounced lysate in the absence of detergent), and total cell lysate. SDS-PAGE and Western blot were performed to detect active Ral using antibody against Ral.

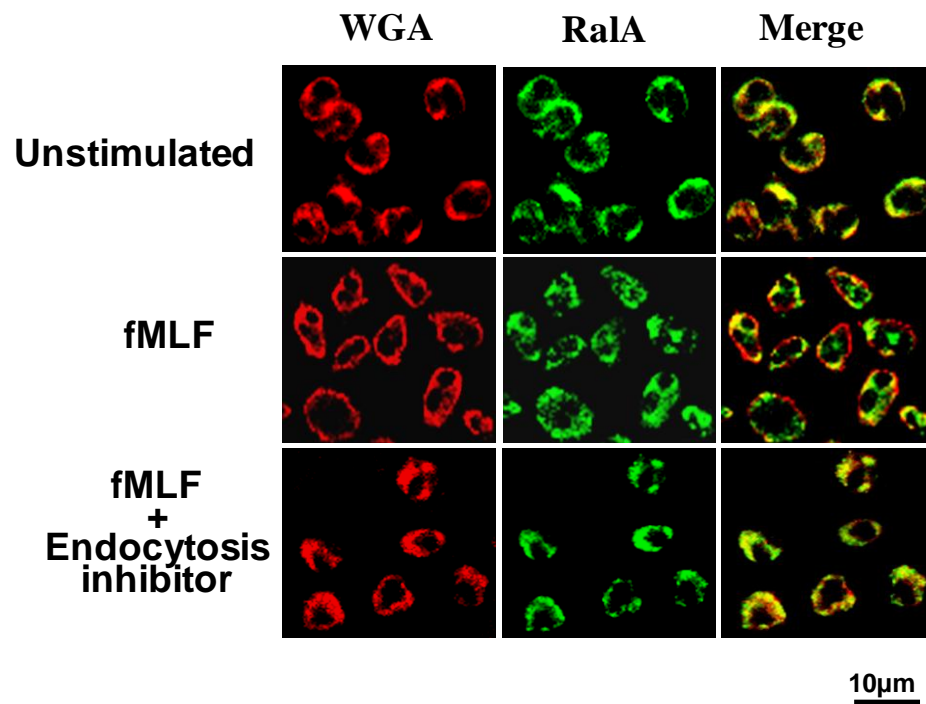


**Figure 3-23.** Localization of Ral in PMN. Immunofluorescence labeling of Ral in PMN. PMN, unstimulated and fMLF-stimulated, were fixed and permeabilized with 0.02% Triton X-100. After washing and blocking, cells were labeled with anti-Ral antibody (green) and plasma membrane marker wheat germ agglutinin (WGA) (red).

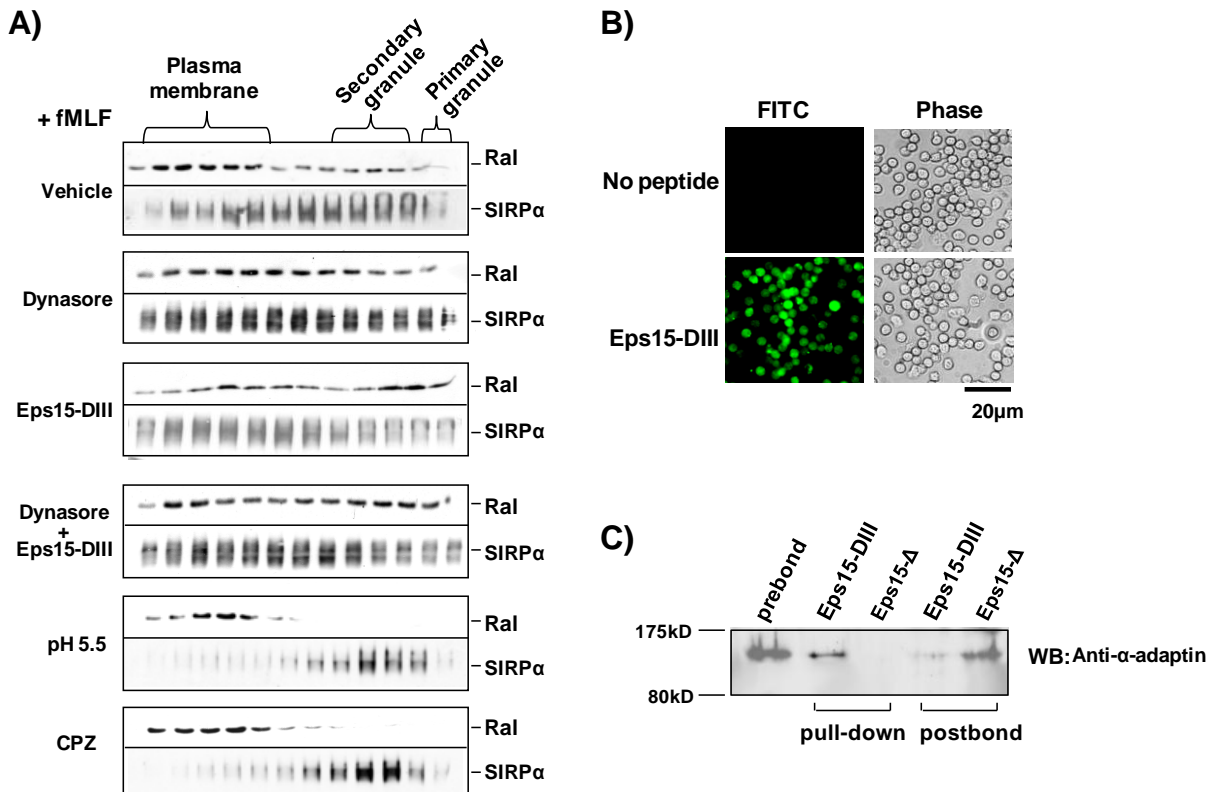


**Figure 3-24.** Ral translocation from the plasma membrane to secondary granules may follow fMLF-induced endocytic process. A) Effect of clathrin-dependent endocytic inhibitors on Ral redistribution in PMN. In these experiments, PMN were pre-incubated with dynasore (80μM), Tat-tagged Eps15 peptide (Eps15-DIII) (40nM), or a combination of the two reagents for 15min (25°C) before fMLF stimulation (20min at 37°C). After cell lysis, subcellular fractionation was performed followed by detection of Ral by Western blots. The effect of other endocytosis inhibitors, CPZ (50μM) and succinic acid (20mM, pH5.5), on Ral distribution was also tested. B) Protein transduction of Tat-tagged Eps15-DIII into PMN. Purified Tat-tagged Eps15-DIII was fluorescently labeled followed by incubating with PMN for 10min (4°C). The image shows that Eps15-DIII was successfully delivered into the cells. C) Pull-down assay confirmed that Eps15-DIII directly binds to AP-2 complexes. PMN ( $1.5 \times 10^7$ ) were lysed in a buffer containing 1% Triton X-100 and protease inhibitors followed by incubation with 10μg purified Tat-tagged Eps15-DIII in the form of GST fusion protein or its non-binding control peptide Tat-tagged Eps15-Δ for 3h (4°C). After pull-down with glutathione Sepharose, the precipitated protein complexes were washed and analyzed by western blot using antibody against α-adaptin, an important component of AP-2 complexes.

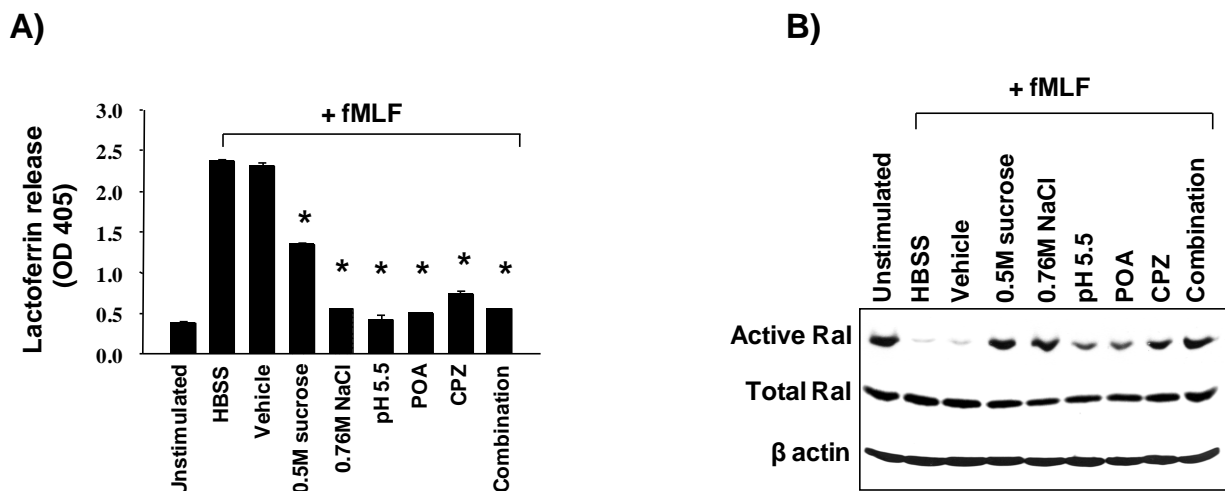


**Figure 3-25.** Blockage of clathrin-dependent endocytosis inhibits fMLF-induced secondary granule release (A), Ral deactivation (B) and Ral translocation (C). In these experiments, PMN were incubated with hypertonic solutions (0.5M sucrose and 0.76M NaCl), POA (20 $\mu$ M), CPZ (50 $\mu$ M), succinic acid (20mM, pH5.5), or a mixture of later three reagents (combination) for 5min (25°C) before fMLF stimulation (20min at 37°C). Release of lactoferrin into the supernatants was measured (A). Ral activity was detected by RalBP1 pull down assays (B). All the posts were significantly lower than HBSS and vehicle control (One-way ANOVA, repeated measures,  $p < 0.0001$  with Dunnett's post tests) \* indicates significant differences ( $p < 0.05$ ). There was no significant difference between HBSS and vehicle control ( $p > 0.05$ ).



## **CHAPTER IV:**

### **DISCUSSION**

As a type of highly specialized and fast responsive cells, PMN store a large number of functionally important molecules in the intracellular granules and vesicles. Upon stimulation, PMN promptly mobilize these granules/vesicles and rapidly release arrays of cell adhesion molecules, receptors, and proteases to the cell surfaces to facilitate PMN adhesion, chemotaxis and microbial killing. At least four types of granules and vesicles varied in size/shape and content have been identified in PMN [25, 96], but the mechanisms that control their mobilization and release during PMN response to inflammatory stimulation remain largely undefined. Among these granules and vesicles, secondary granules are defined as being mostly rich in leukocyte integrins and adhesive receptor-like proteins. Degranulation of secondary granules thus serves as a major means to furnish the cell surface plasma membrane with the essential cell adhesion and migration molecules. Here, we report our studies of PMN degranulation which reveal, for the first time, that the Ras family member, Ral, is a critical regulator specifically in the degranulation of secondary granules.

As shown by my results, Ral exists as an active GTPase in freshly isolated PMN and its activity plays a key role in keeping secondary granules in the cell. Inhibition of Ral in resting PMN by damnacanthal, a Ras family GTPase inhibitor with unclear mechanism [206-207], causes “premature” liberation of secondary granules in the absence of chemoattractant stimulation. However, this dysregulated degranulation has no benefit to, but instead impeded PMN function. As I observed, although damnacanthal increased cell surface integrins and adhesive molecules, these upregulated molecules failed to mediate effective PMN interactions, adhesion and migration. In

particular, my results (Figure 3-4) showed that, in contrast to fMLF-induced CD47 on the cell surface that mediates binding interactions with its extracellular ligand, damnacanthol-induced CD47 on PMN were incapable of binding interaction. Similarly, cell surface upregulated CD11b/CD18 by damnacanthol did not appear to mediate strong extracellular interactions, which count, in part, for the decrease of PMN adhesion and spreading in response to fMLF. Thus, these results suggest that a critical mechanism, which is generally elicited by chemoattractant stimulation, is required to control secondary granule degranulation and, along this process, also converts essential cell surface proteins to be functional and ready to mediate cell surface interactions. These studies thus further signify the important role of Ral in PMN. By preventing irregular degranulation in the absence of stimuli, the Ral-mediated mechanism preserves PMN functional capability for potent and effective response during inflammation.

In this study, I also obtained the important result that chemoattractant induces a rapid deactivation of Ral in PMN, which explains a dynamic regulation required for secondary granule release. In contrast, experimentally over-expression of a constitutively active Ral, Ral23V [117, 167, 202], into PMN to sustain Ral activity even in the presence of fMLF resulted in prohibition of secondary granule release, and hence hampered PMN chemotactic transmigration. While its role in secondary granule mobilization is evident, Ral has no control of the mobilization of primary and tertiary granules, and both damnacanthol and Ral23V only had effect on the degranulation of secondary granules.

The mechanism by which Ral regulates secondary granule storage and release is unclear. By subcellular fractionation, I found that Ral is associated with the plasma membrane under resting

conditions, while chemoattractant stimulation triggers a translocation of Ral to secondary granules. Presumably, chemoattractant-induced cell surface endocytosis plays an important role in Ral intracellular translocation, and thus PMN degranulation. Since PMN chemoattractant receptors are G protein-coupled, and clathrin-coated pits are generally employed to internalize these receptors after ligand binding, one possible hypothesis would be that Ral is in complex with the chemoattractant receptor and assembled into the clathrin pits after chemoattractant stimulation. However, testing this hypothesis using two inhibitors, dynasore and an AP-2 binding Eps15 peptide, both specific blockers of clathrin-dependent endocytosis, failed to inhibit Ral translocation to the pool of secondary granules. Interestingly, several other inhibitors that generally inhibit endocytosis, vesicle transportation and/or cytoskeleton structures blocked Ral intracellular translocation in the experiments.

In different cells, Ral has also been implicated in other types of vesicle transportation, including both endocytosis and exocytosis [117-121]. However, the detailed mechanism regulating Ral activity is not clearly understood.

In platelets, it was found that Ral is inactive under resting conditions but becomes activated after stimulation [163]. Contrary to our observation in this study, scientists in another study showed that Ral is inactive in resting PMN [215], a variation that was likely caused by different methods of cell preparation. In other studies, a guanine nucleotide dissociation stimulator, RalGDS, has been suggested to be important in regulating Ral [164, 224], and such regulation involves Ras. In particular, RalGDS was shown to directly bind to Ras, suggesting that Ral acts as a downstream effector in the Ras network [167, 225]. However, evidence obtained from my studies fall short of

supporting an important role of RalGDS in Ral-mediated degranulation in PMN. First, I found that the expression of RalGDS in PMN is trivial compared to many other cell types (Figure 4-1), and is also in no match for the abundance of Ral (Figure 4-1A). Second, subcellular fractionations detected no co-localization of RalGDS and Ral in PMN under either resting or fMLF-stimulated conditions. Contrary to Ral, which is translocated between plasma membrane and granules, RalGDS is consistently localized in the cytosolic fractions (Figure 4-1B). Studies of other cells have shown that RalGDS directly binds to Ras, suggesting that Ral acts as a downstream effector in the Ras network [201, 225]. However, I found that, in PMN, Ral has a completely different activity profile from that of Ras (Figure 3-6), suggesting a dissociation of Ral from the Ras pathway and a dispensable role for RalGDS in this regard.

While the mechanism of activation of Ral is vital, especially during PMN maturation, in order to restrain produced granules in PMN, my results suggest the later mechanism that deactivates Ral is also undoubtedly crucial for converting naive PMN into potent, functional inflammatory leukocytes. This mechanism, which is evidently important for PMN degranulation, remains unknown. Specific molecules that promote Ral deactivation, such as GTPase activating proteins (GAPs), are hardly detected in any cell types including PMN.

Previous studies have indicated a role of intracellular calcium in secondary granule release, the mechanism of how calcium functions is unclear. During chemoattractant (e.g. fMLF or IL-8) stimulation, the intracellular calcium concentration in neutrophils is generally increased to the peak ~10sec post-stimulation, followed by a quick decrease to the basal level (in the next ~1min) regardless of the continuous presence of the chemoattractant (Figure 4-2A). However, in the

same experimental setting, the robust release of secondary granules is observed approximately starting at ~1min and continuously to a much later time point (>30min) (Figure 4-2B). Thus, the time-course discrepancies of transient calcium increase in neutrophils versus the elongated release of secondary granule release after chemoattractant stimulation suggest that calcium likely serves as an important secondary messenger or a modulator, which activates downstream signaling molecules directly involved in the control of secondary granule release. Since inhibition of Ral by damnacanthal triggers neutrophil degranulation in the buffer without calcium (in HBSS (-)) (Table 1 & Figure. 3-1), I thus do not consider that damnacanthal-mediated downstream events (deactivation of Ral and secondary granule release) involve calcium or calcium signaling. However, my results did not exclude the possibility that calcium may regulate a step upstream of Ral deactivation. Indeed, Ral structurally contains a calmodulin binding site. Detailed studies of Ral activity at the very early phase of fMLF stimulation (within 1min) also sometimes showed a slight increase (10-20%) of Ral activity at 10-30sec (Figure 4-3A), a time-course correlating with the increase of intracellular calcium concentration. However, in vitro binding assays using the purified recombinant Ral and RalBP1 (one of the effectors of Ral) failed to demonstrate a direct involvement of calcium in Ral binding to this effector (Figure 4-3B).

Surprisingly, during my work, I found that  $Mg^{2+}$  inhibited Ral activity in PMN, as demonstrated by a pull-down assay (Figure 4-4). Ral activity was strikingly increased in the presence of 2 mM EDTA, while EDTA did not change Ral activity in resting platelets (Figure 4-4A and Figure 3-7B). Since EDTA is a chelator for both  $Ca^{2+}$  and  $Mg^{2+}$ , both cations are likely to be involved in regulating Ral activity. In order to dissect further which cation was the possible upstream inhibitor of Ral, I first stimulated PMN with fMLF in HBSS (-) buffer without  $Ca^{2+}$  and assayed Ral

activity by pull-down. As shown in Figure 4-4B, stimulation of PMN in HBSS (-) failed to inhibit Ral activity compared with stimulation of cells in HBSS (+). In addition, stimulation of PMN in the buffer supplemented with 5mM EGTA, a specific chelator for  $\text{Ca}^{2+}$ , did not have any effect on Ral activity change. These results agree with other results (Figure 4-3B) and suggest that  $\text{Ca}^{2+}$  is not a regulator of Ral activity.  $\text{Mg}^{2+}$ , however, inhibited Ral activity, which is shown in Figure 4-4C. Lysis of PMN in the presence of 30 mM  $\text{Mg}^{2+}$  abolished Ral activity. All of these results illustrate that  $\text{Mg}^{2+}$  is the potential upstream inhibitor of Ral in PMN.

Treatment of PMN with damnacanthal in the absence of chemoattractant stimulation results in secondary granule release. However, the detailed mechanisms underlying damnacanthal-mediated secondary granule release from PMN are unclear.

It is obvious that the effect of damnacanthal on PMN is different from that of CB. As shown in Figure 3-1, treatment of PMN with fMLF+CB triggered robust PMN degranulation of all the granules including primary, secondary and tertiary granules. Treatment of PMN with damnacanthal, with or without fMLF, affected only the release of secondary granules. In experiments, I observed that pre-treatment of PMN with low dose damnacanthal ( $< 10 \mu\text{M}$ ) followed by fMLF stimulation resulted in further degranulation in addition to the effect of damnacanthal alone (Figure 4-5). However, this manner of “synergistic” effect on secondary granule release was not observed with pre-treatment of PMN with higher doses of damnacanthal ( $>10 \mu\text{M}$ ), which alone triggered a near complete degranulation or complete degranulation without fMLF stimulation (Figure 3-1). Pretreatment of PMN with damnacanthal had no effect on fMLF-induced tertiary granule release (Figure 4-5). I further questioned whether receptor-mediated endocytosis in-

volves in damnacanthal-mediated PMN secondary granule release. As shown in Figure 4-6 and Figure 4-7, treatment of PMN with only the endocytosis inhibitors had no effect on Ral distribution. In addition, pretreatment with endocytosis inhibitors appeared to have no effect, or only partial effect on damnacanthal-induced secondary granule release and Ral translocation from the plasma membranes to the granules. These results, together with our other data (Figure 3-24), suggest that Ral deactivation might not be downstream of endocytosis or along the process of endocytic pathway.

Taking everything into consideration, our results demonstrate that it is important to elucidate Ral activation and its importance in PMN; however, the mechanism that deactivates Ral is crucial for PMN degranulation, thus converting to functional inflammatory leukocytes. Ral deactivation correlates with clathrin-mediated endocytosis. Further studies of the signaling pathways and the precise protein interactions involved in clathrin-dependent Ral translocation would provide clues to resolve Ral conformational changes. In addition to Ral, other small GTPases, such as Ras family members Ras and Rap, and Rho family members Rho, Rac and Cdc42 are also expressed in PMN [226-227] and some of these are found to be associated with granules [124, 131, 228]. Thus, detailed investigation of these small GTPases in PMN, and correlation of their activity changes with PMN activation and degranulation will shed new light on the understanding of PMN inflammatory functions. Given the critical role of PMN in innate immunity and inflammation, our findings illustrate a novel mechanism that modulates the PMN inflammatory response, which may provide a potential therapeutic target for treating various inflammatory conditions.

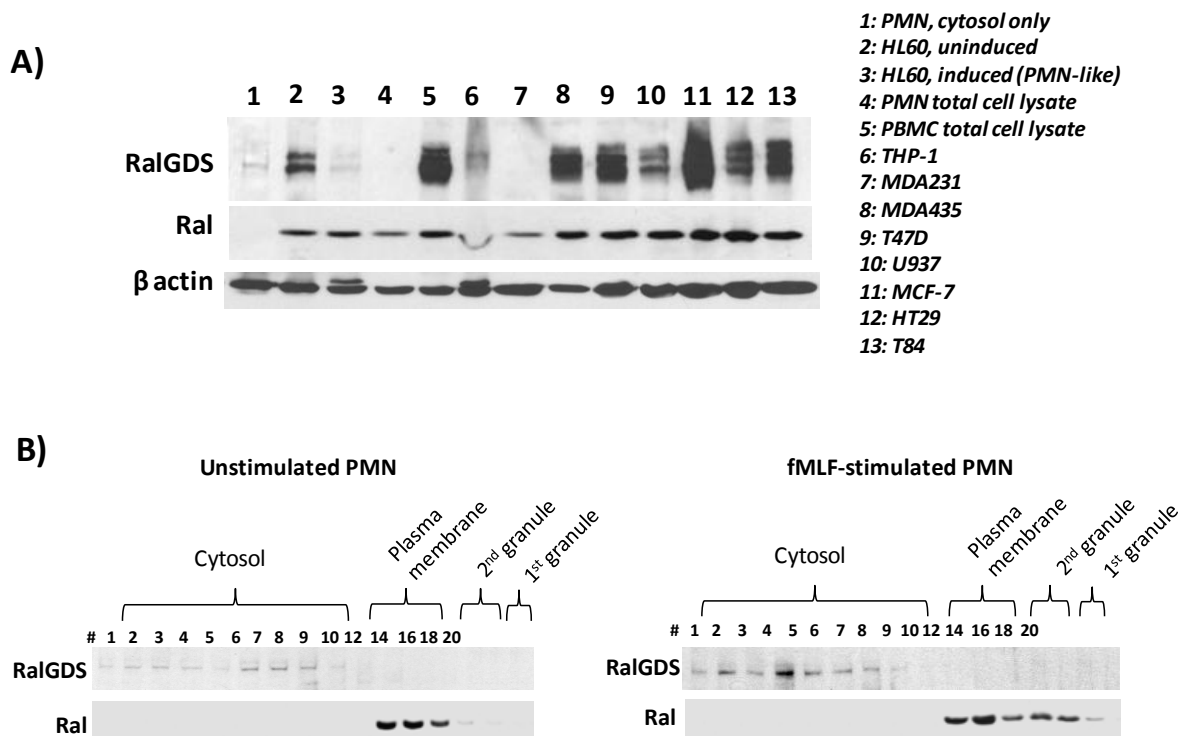


**Figure 4-1.** A) Expression of RalGDS in different cell types. Western blots were performed to detect RalGDS in the cytosol fraction of PMN (lane 1, same as Fig.5A) and total lysates of various cell types using an anti-RalGDS antibody (Millipore). As shown, only slight amount of RalGDS was detected in PMN cytosol, total PMN lysates or PMN-like, DMSO-induced HL-60 cell lysates. The same nitrocellulose membrane was re-blotted by anti-Ral antibody. The protein loading of each lane was normalized by detecting actin in the lysates. B) RalGDS localization in PMN. After subcellular fractionation, Western blots were performed to detect RalGDS and Ral in the cytosolic and membrane fractions. As shown in the figure, RalGDS was exclusively localized in the cytosolic fractions in both unstimulated and fMLF-stimulated PMN and had no co-localization with Ral which was associated with the plasma membrane and/or secondary granules.



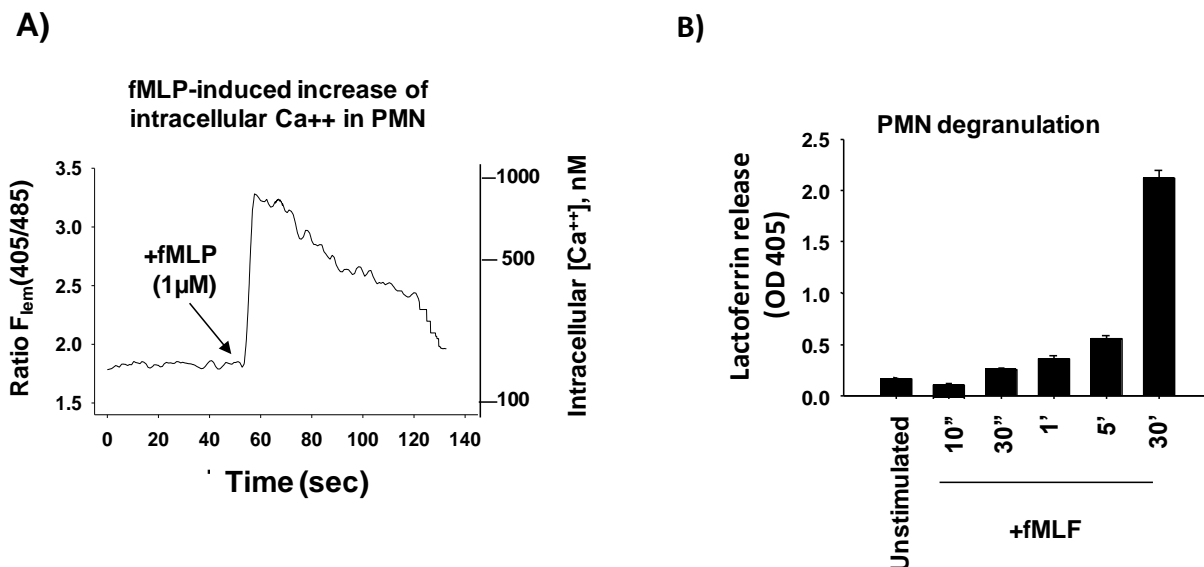


**Figure 4-2.** A study of chemoattractant stimulation-induced increase of intracellular calcium, secondary granule release and Ral activity changes in PMN. **A)** Chemoattractant stimulation induces an increase of intracellular calcium in PMN. Freshly isolated PMN ( $1 \times 10^6$ ) were loaded with the calcium indicator Indo-1 (Invitrogen) followed by washing. Labeled PMN in 1ml HBSS were transferred into a cuvette (Starstedt) and placed into the spectrofluorimeter that had been thermostated to 37°C. After equilibration, PMN were stimulated with 1  $\mu$ M fMLF (at 50sec position) and cytoplasmic  $[Ca^{2+}]$  changes were immediately recorded with fluorescence emission at 505nm and double excitation wavelengths of 340 nm and 380nm using an intracellular cation software (Hitachi). The concentrations of intracellular  $[Ca^{2+}]$  were calculated using the Grynciewicz equation  $(R-R_{min}) / (R_{max}-R) * K_d$  ( $K_d$  is  $2.54 \times 10^{-7}$  M in this experiment).  $R_{max}$  and  $R_{min}$  were measured by adding digitonin (10  $\mu$ M) and then EGTA (20mM) to Indo-1-loaded PMN. Autofluorescence was corrected by stimulation of non-Indo-1-loaded PMN. The method of detecting intracellular calcium in PMN was also described previously [192]. **B)** A parallel experiment detecting secondary granule release. PMN ( $2 \times 10^6$ ) were resuspended in 0.1ml HBSS and equilibrated to 37°C. Following stimulation with 1  $\mu$ M fMLF for different time periods, the cell-free supernatants were collected after centrifugation and the released lactoferrin was assayed by ELISA using an anti-lactoferrin antibody.

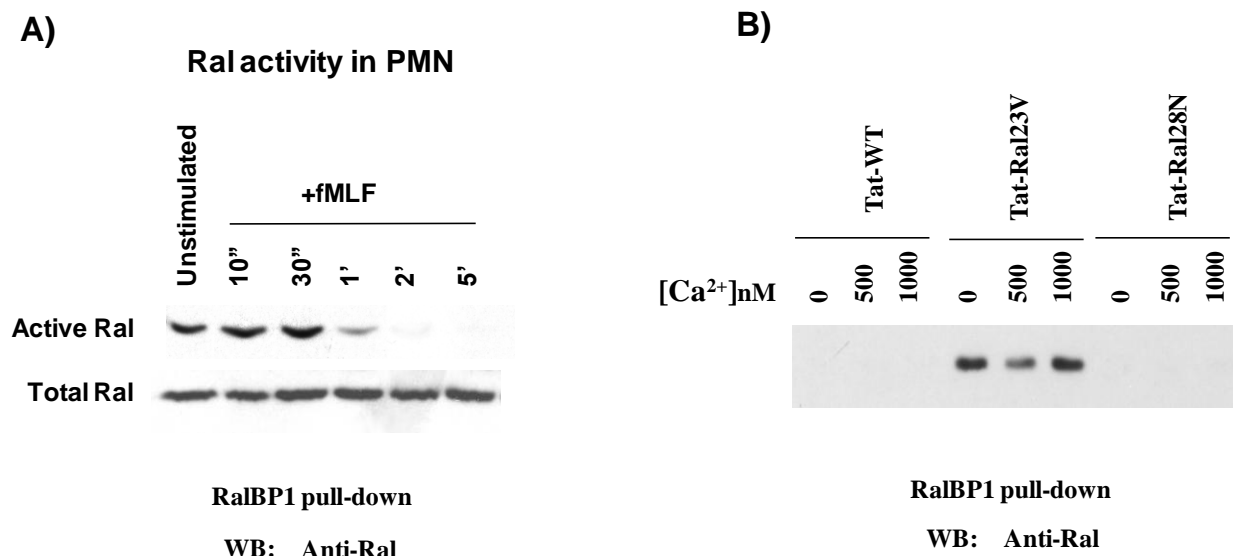


**Figure 4-3.** A study of chemoattractant stimulation-induced increase of intracellular calcium, secondary granule release and Ral activity changes in PMN. **A)** Ral activity changes in PMN after fMLF stimulation. In this experiment, PMN ( $1 \times 10^7$ ) were stimulated with  $1 \mu\text{M}$  fMLF at  $37^\circ\text{C}$  in HBSS for different time periods. After cell lysis, active Ral in PMN was recovered by RalBP1 pull-down followed by Western blot using an anti-Ral antibody. As can be seen in the figure, Ral activity was slightly increased (10-30%) immediately after fMLF stimulation (at ~10-30 second). **B)** Calcium concentrations have no effect on the direct binding of RalA to RalBP1. In these experiments recombinant GST-RalBP1 and Tat-tagged wild-type and mutant RalA were produced by expression in *E.coli* followed by protein purification. Pull-down assays were performed by incubation (30min,  $4^\circ\text{C}$ ) of GST-RalBP1 ( $1 \mu\text{g}$ ) with Tat-tagged Ral ( $0.2 \mu\text{g}$  each) in HBSS containing 5% non-fat dry milk, 2% BSA, 0.01% Tween 20 and different concentrations of  $\text{CaCl}_2$ . Glutathione-conjugated Sepharose ( $20 \mu\text{l}$ ) were also added. After washing, proteins pulled down by the Sepharose were analyzed by Western blot using an anti-Ral antibody. As can be seen in the figure, only the constitutively active Ral (Ral23V) was directly pulled down by RalBP1. Increasing calcium concentrations had no effect on the direct binding of Ral to RalBP1.

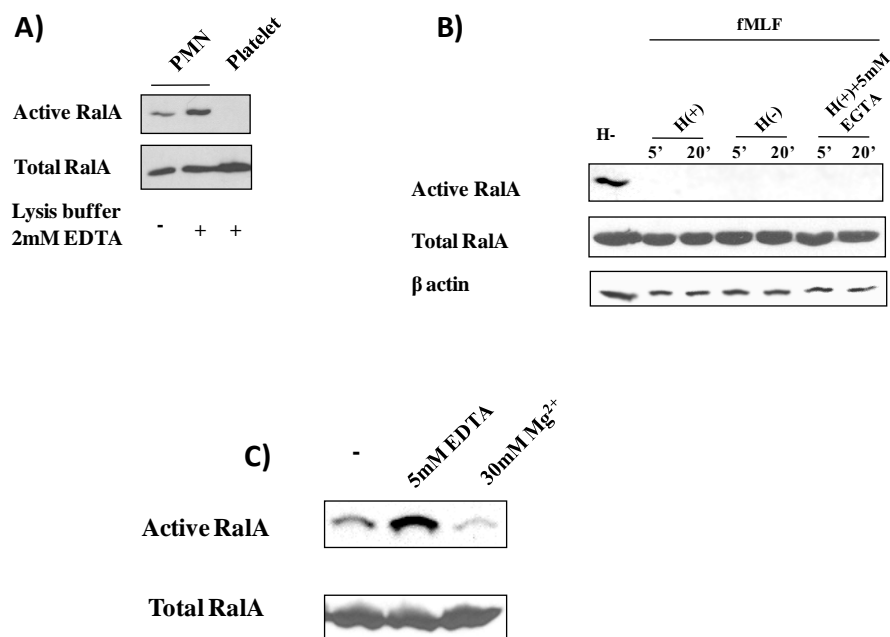


**Figure 4-4.**  $Mg^{2+}$  inhibits Ral activity in PMN. A) Ral activity in freshly isolated PMN was increased in the presence of EDTA. PMN were lysed in the presence or absence of 2mM EDTA, and active Ral was pulled down using RalBP1. In addition, resting platelets were lysed in the presence of 2mM EDTA, and active Ral was pulled down by RalBP1. B) Detecting activity changes of Ral in PMN. PMN were stimulated with fMLF (1 $\mu$ M) in HBSS (-), HBSS (+), or HBSS (+) supplemented with 5mM EGTA. After time-course stimulation, PMN were lysed, and active Ral was pulled down. Cell lysates before pull-down were used to detect total Ral as well as actin using antibodies against Ral and  $\beta$  actin. C) Detecting activity changes of Ral in PMN. PMN were lysed in the presence of 5mM EDTA or 30nM  $Mg^{2+}$ , and active Ral was detected by pull down assay.

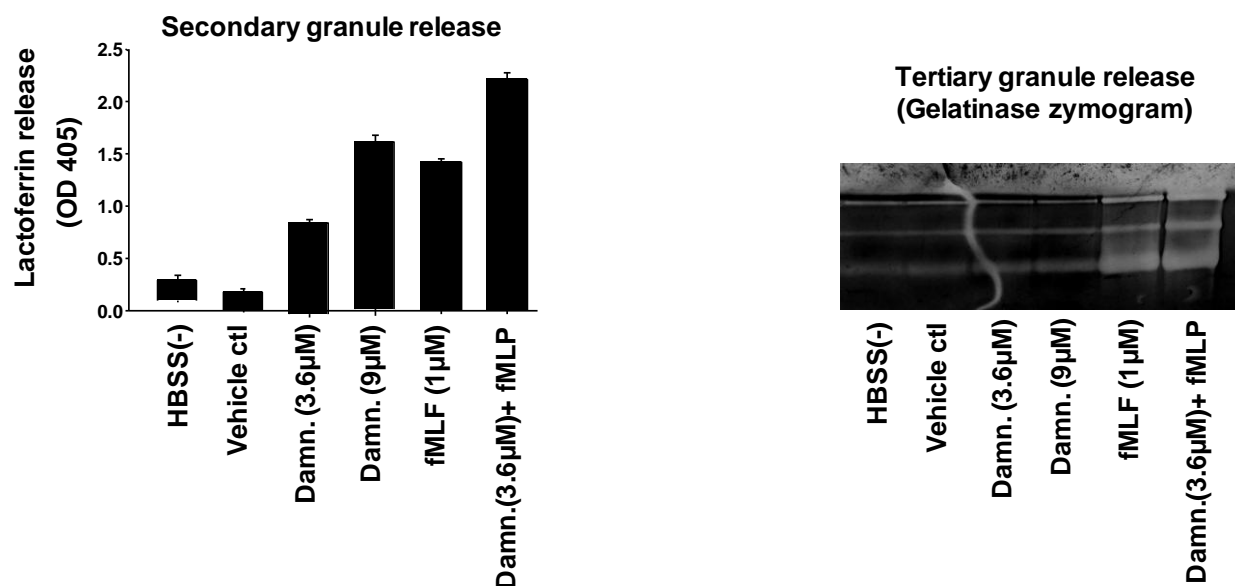


**Figure 4-5.** Effects of damnacanthal alone or in a combination with fMLF on PMN granule release. In these experiments, aliquots of freshly isolated PMN ( $1 \times 10^7$ ) were treated with vehicle (0.1% DMSO, 15min, 25°C), damnacanthal (3.6μM and 9μM, 15min, 25°C), fMLF (1μM, 15min, 37°C), or damnacanthal (3.6μM, 15min, 25°C) followed by fMLF (1μM, 15min, 37°C). An aliquot of PMN resuspended in HBSS(-) and kept at 25°C (15min) was also used as a control condition. After incubation, cell-free supernatants were collected after centrifugation and assayed for granule release. Left: assay of PMN secondary granule release by detecting lactoferrin in the supernatants. Right: Assay of PMN secondary granule release by zymogram detecting liberated gelatinase in the supernatants.

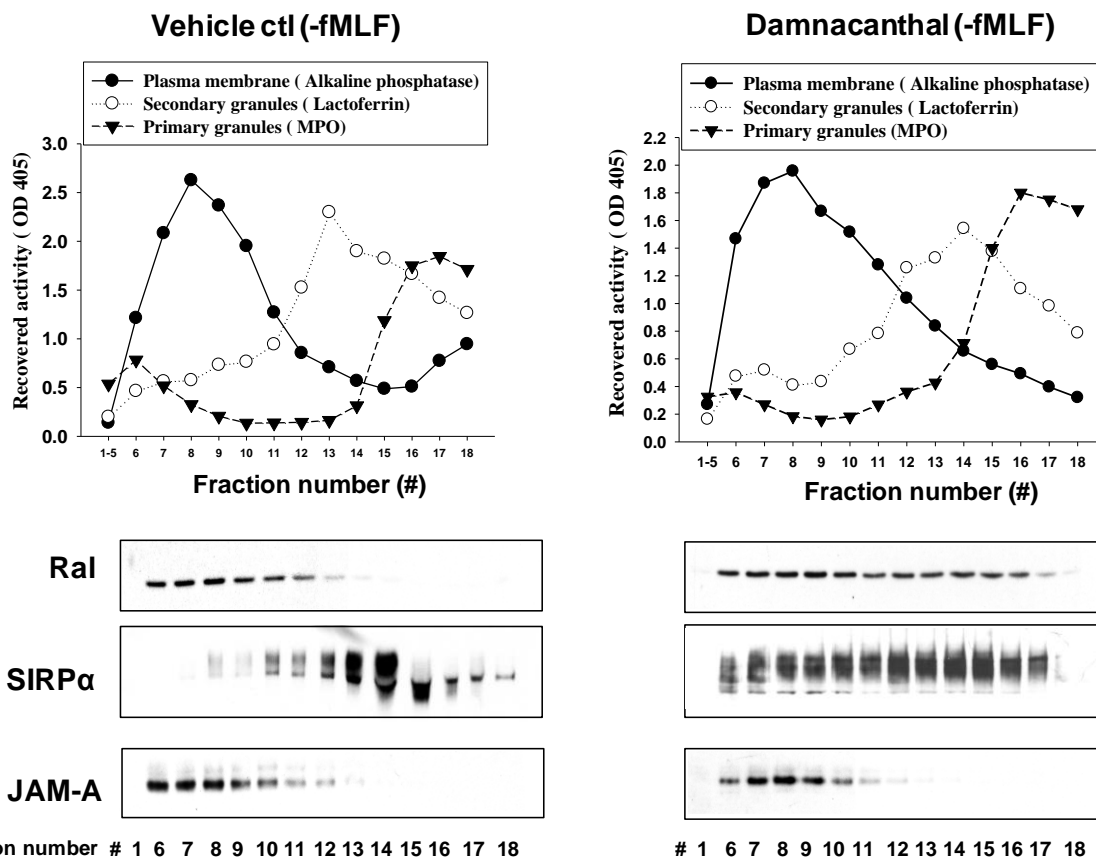


**Figure 4-6.** Subcellular fractionations studying the effects of damnacanthal and endocytosis inhibitors on Ral distribution in PMN. Damnacanthal triggers Ral redistribution from the plasma membranes into secondary granules. Freshly isolated PMN ( $1 \times 10^8$ /per condition) were treated with vehicle (0.1% DMSO) or damnacanthal (9  $\mu$ M) for 15 min (25°C) before lysis and subjected to sucrose density gradients to separate subcellular organelles. After fractionation, the localizations of plasma membranes and intracellular granules in respective fractions were determined by their specific marker proteins (upper panels). The lower panels show the Western blot results detecting Ral, SIRP $\alpha$  and JAM-A (junction adhesion molecule A) in the fractions. In PMN, SIRP $\alpha$  is mainly stored in secondary granules in the absence of stimulation, while JAM-A is consistently associated with the plasma membrane (unpublished data). As can be seen, a portion of Ral was redistributed from the plasma membranes into secondary granules after damnacanthal treatment. Given that damnacanthal induces secondary granule release, it was predictable to observe that a portion of SIRP $\alpha$  was translocated to the plasma membranes. The indifferent JAM-A localization demonstrated that plasma membrane integrity was not jeopardized by damnacanthal.

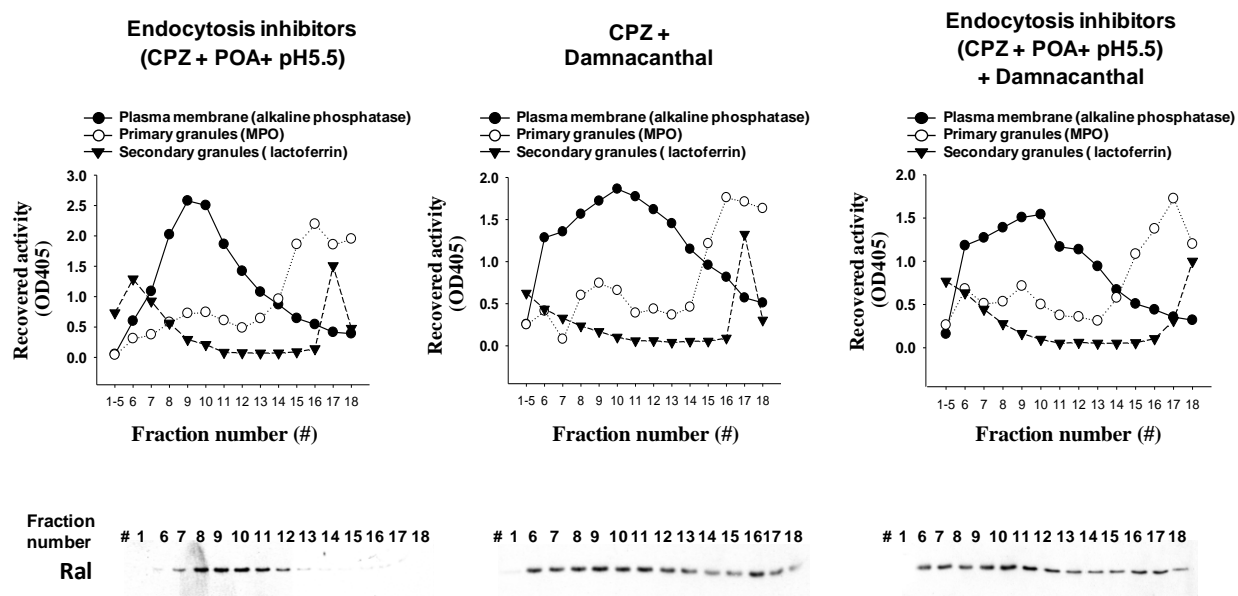


**Figure 4-7.** Subcellular fractionations studying the effects of damnacanthal and endocytosis inhibitors on Ral distribution in PMN. Inhibitors acting on clathrin-mediated endocytosis had no effect on damnacanthal-triggered Ral redistribution in PMN. In these experiments, PMN, pre-treated with an individual endocytosis inhibitor (e.g. CPZ, 50 $\mu$ M) or a combination of several inhibitors (50 $\mu$ M CPZ + 20 $\mu$ M POA + 20mM succinic acid (pH5.5)) (10min, 25°C), were either subjected or not subjected to further treatment with damnacanthal (9 $\mu$ M) (15min, 25°C). After treatment, the cells were lysed followed by sucrose density gradient centrifugation to separate subcellular organelles. After fractionation, Western blots were performed to detect Ral distribution in the fractions using an anti-Ral antibody. As shown in the figure, none of the endocytosis inhibitors markedly blocked damnacanthal-triggered Ral redistribution from the plasma membranes to secondary granules.

## CHAPTER V:

### APPENDICES (Data from other publications)

I. PUBLICATION: ZEN K, CHEN CX, CHEN YT, WILTON R, LIU Y. RECEPTOR FOR ADVANCED GLYCATION ENDPRODUCTS MEDIATES NEUTROPHIL MIGRATION ACROSS INTESTINAL EPITHELIUM. J IMMUNOL. 2007 FEB 15; 178(4):2483-90.

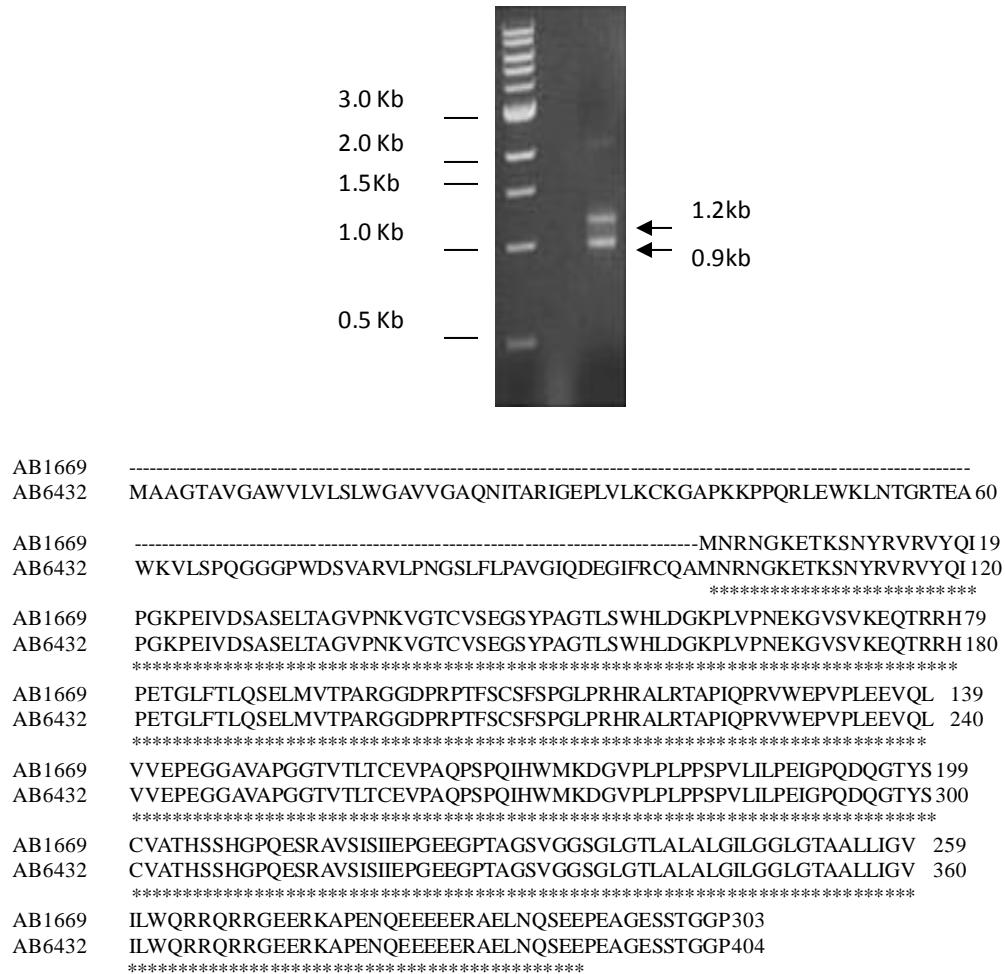


**Figure 5-1.** RAGE was amplified from human intestinal epithelial cells by RT-PCR. Results showed that two fragments were amplified. Sequencing results showed that the longer fragment was 1.2kb matching the full-length RAGE (GeneBank # AB036432) and the shorter fragment was 0.9kb matching a N-terminal truncated RAGE form (GeneBank # AB061669).

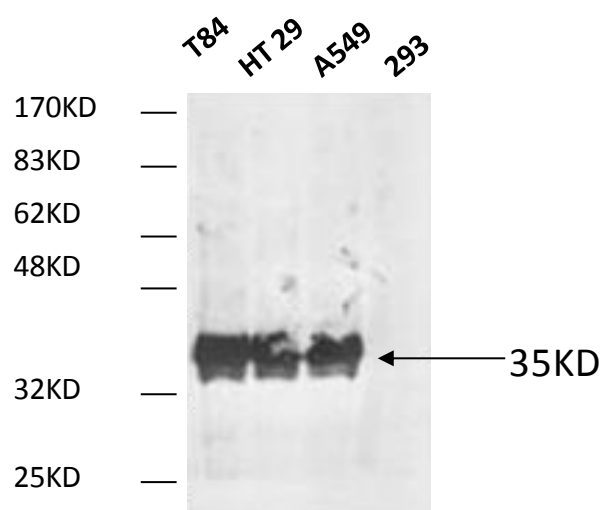


**Figure 5-2.** RAGE was detected from epithelial cell lines by western blot. RAGE was detected from human colonic epithelial cells lines including T84 and HT29. RAGE was also detected from epithelial cell A549.



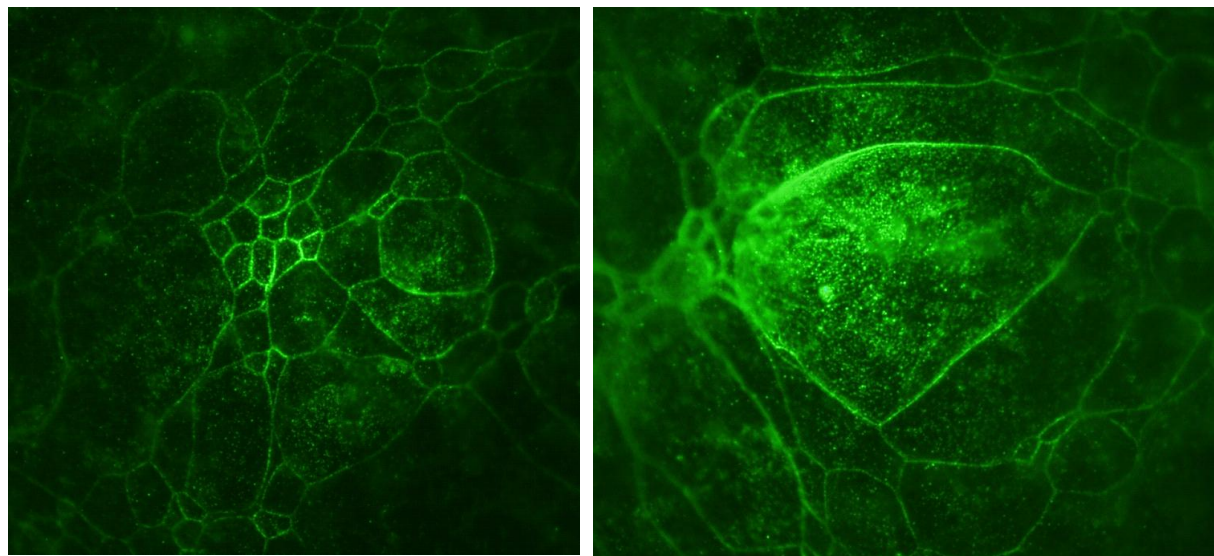


**Figure 5-3.** RAGE was detected in intestinal epithelial cells by immunofluorescence staining. Confluent T84 intestinal epithelial monolayers were quickly permeabilized and fixed with methanol (10min, 4°C) followed by blocking with 5% normal goat serum. RAGE was detected using anti-RAGE antibody followed by labeling with FITC-conjugated goat anti-mouse IgG (H+L). Imaging was analyzed by confocal microscope (Zeiss).

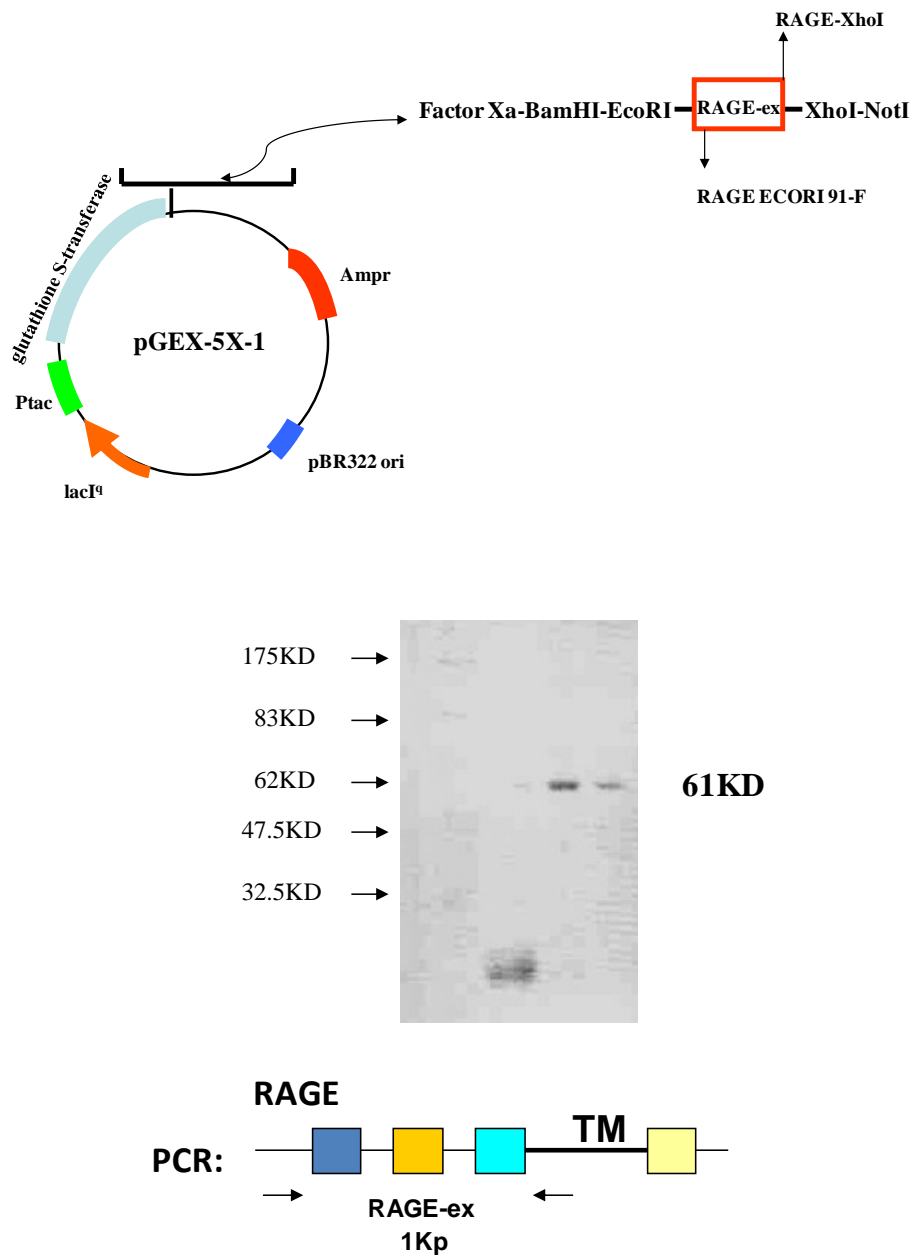


**Figure 5-4.** Generation of GST-exRAGE fusion protein. RAGE was amplified from the plasmid pcDNA3-RAGE-GST using the primers RAGE ECORI 91-F (ATATGAATTCGCTCAAAA-CATCACAGCCCCGGATT) and RAGE-XhoI (ATATCTCGAGTGGTTCGAT-GATGCTGATGCT) and cloned into the vector (pGEX-5X1) through ECORI and XhoI, respectively. GST-exRAGE fusion protein (61KD) was produced in the same way described in 2.7.1.

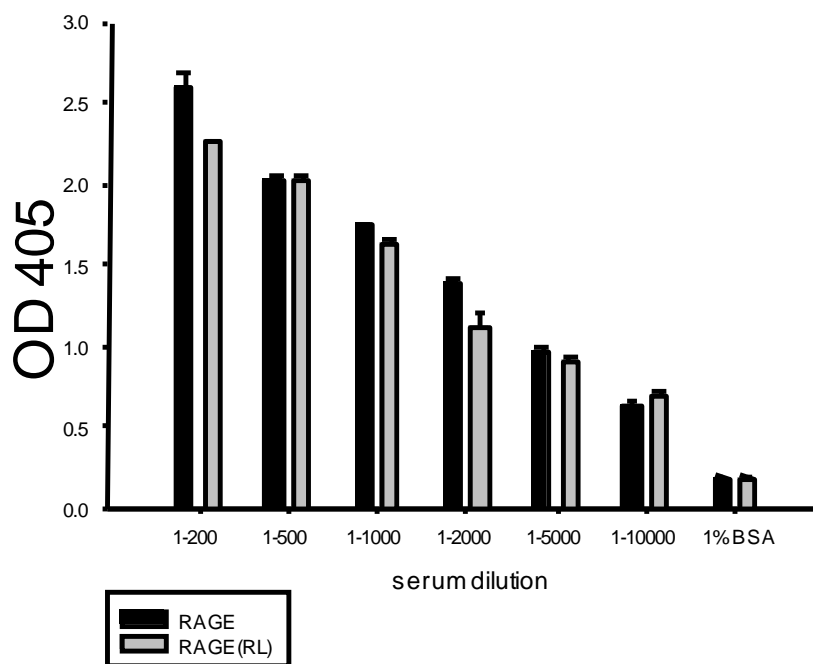


**Figure 5-5.** RAGE antibody titer test by ELISA. 96-well microtiter plate wells were coated with RAGE-ex/GST fusion proteins (5 $\mu$ g/ml each) overnight at 4°C. After blocking with 1% BSA (30min, 25°C), the wells were incubated with serum (1:200; 1:500; 1:1000; 1:2000; 1:5000; 1:100000) for 30min. After washing, fusion protein binding to the antibody (serum) was detected by peroxidase conjugated goat anti-mouse Fc antibody.

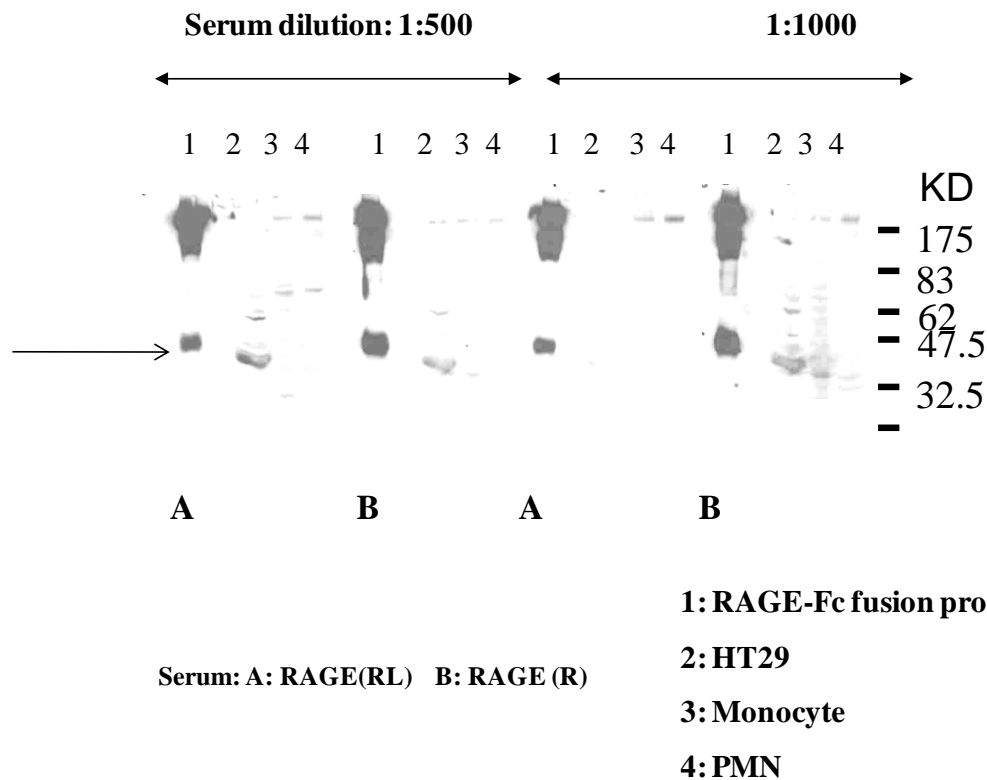


**Figure 5-6.** RAGE antibody titer test by western blot. The serum from the mouse RAGE-ex(RL) and RAGE-ex(R) recognized the RAGE-Fc fusion protein, including the nonreducing form (A) and reducing form. (B). Antibody also picked the band from the HT29, PMN and monocyte. After immunization for 5 times, the serum was used for WB at 1:1000 dilution.

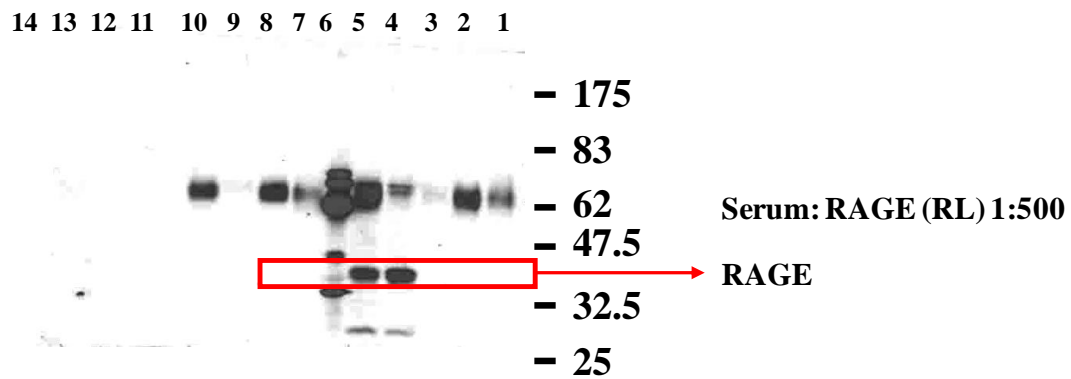


**Figure 5-7.** RAGE detection from human PMN. RAGE was detected from human PMN using RAGE-ex serum. 3 samples out of 12 samples were RAGE positive.

II. Guo YL, Bai R, Chen CX, Liu DQ, Liu Y, Zhang CY, Zen K. Role of junctional adhesion molecule-like protein in mediating monocyte transendothelial migration. *Arterioscler Thromb Vasc Biol.* 2009 Jan;29(1):75-83

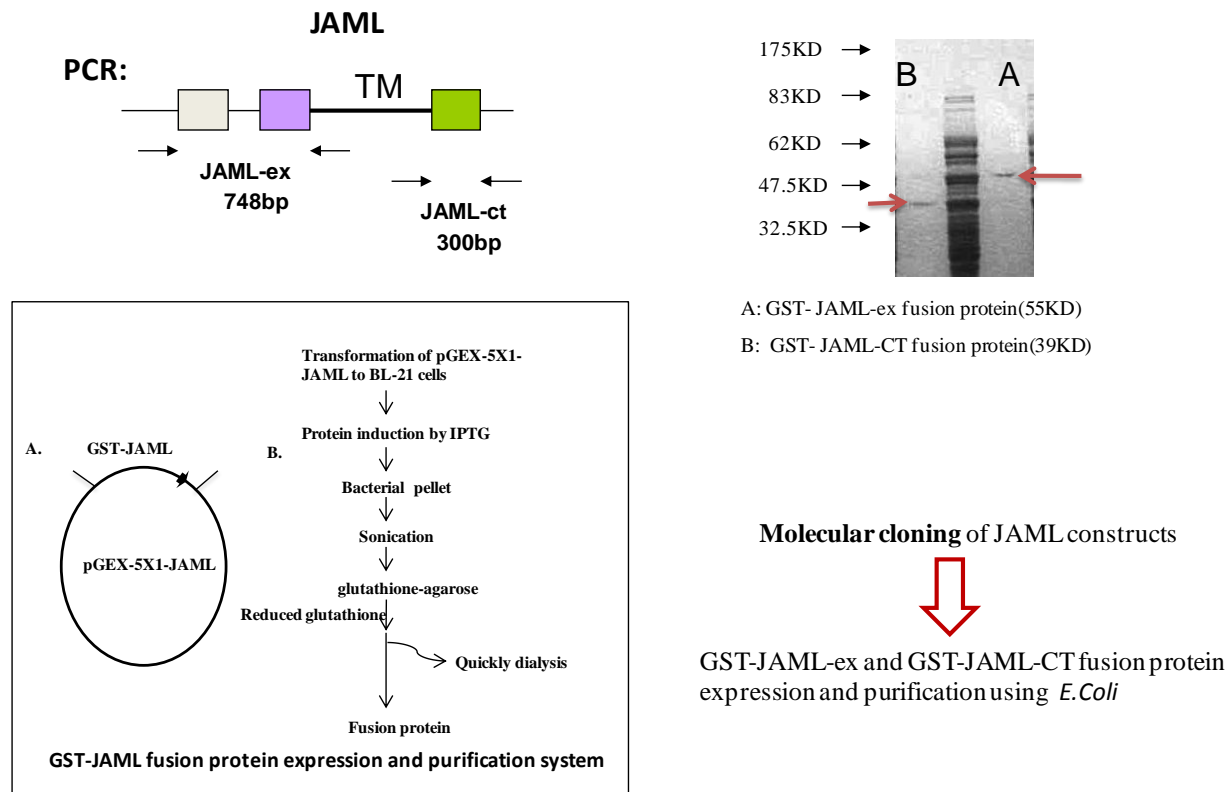


**Figure 5-8.** Generation of GST-JAML fusion protein. JAML-ex (AJ515553) was amplified from the Leukocyte cDNA library with the primers JAML-151-BamH I (ATAT GGATCC TGAAT-GACTTGAATGTTTCC) and JAML-898-Xho I (ATAT CTCGAG CAACTGATTACCACC-CAAGAC) and cloned into the vector (pGEX-5X1) through BamH I and Xho I, respectively. JAML-CT was amplified from the leukocyte cDNA library with the primers JAML-979-BamH I (ATATGGATCCTGGTGAAGAAGACCTGTGGAAAT) and JAML-1278-XhoI (ATATCTCGAGAAGGGACTCTCCATTCTTCT) and cloned into the vector (pGEX-5X1) through BamH I and Xho I, respectively.

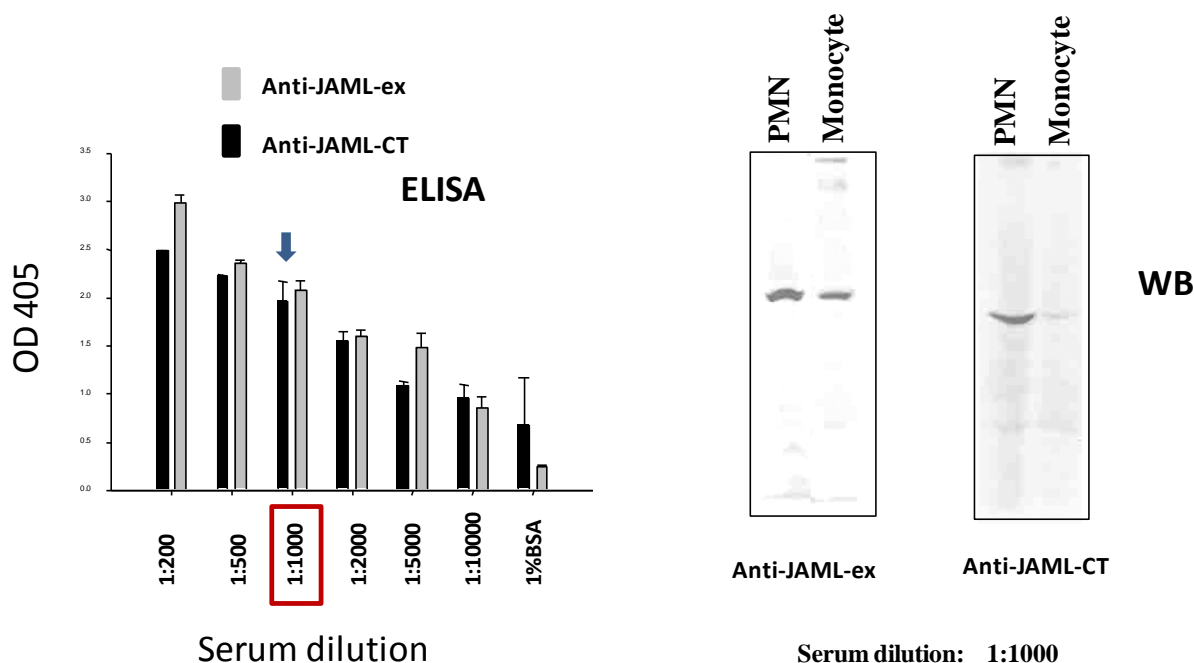


**Figure 5-9.** JAML antibody titer test by ELISA and western blot. 96-well microtiter plate wells were coated with RAGE-ex/GST fusion proteins (5 $\mu$ g/ml each) overnight at 4°C. After blocking with 1% BSA (30min, 25°C), the wells were incubated with serum (1:200; 1:500; 1:1000; 1:2000; 1:5000; 1:100000) for 30min. After washing, fusion protein binding to the antibody (serum) was detected by peroxidase conjugated goat anti-mouse Fc antibody. JAML was detected from human PMN and monocytes using anti-JAML-ex serum and anti-JAML-CT serum at 1:1000 dilution.

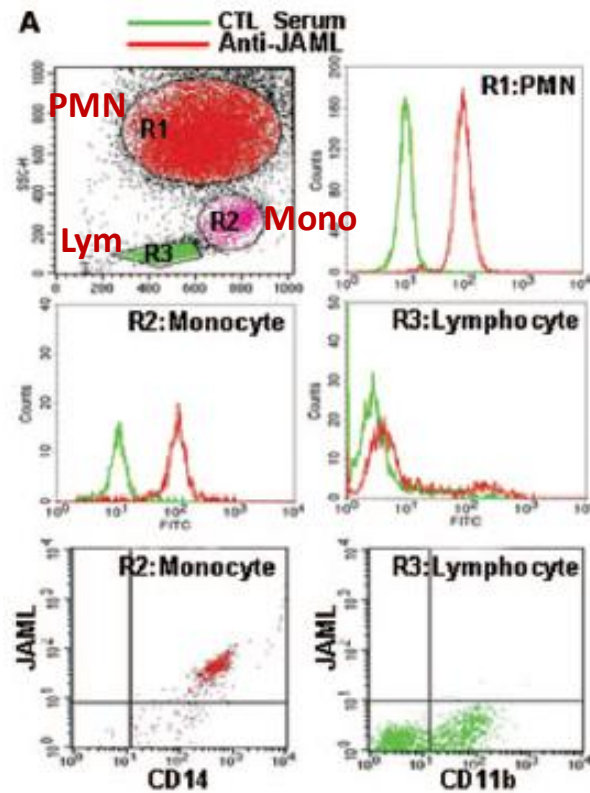


**Figure 5-10.** JAML was expressed on PMN and monocytes. Human whole leukocytes were surface labeled using anti-JAML-ex serum and anti-JAML-CT serum (control), respectively. RAGE expression was detected from PMN (R1 group) and monocytes (R2 group), but no lymphocytes (R3 group).



III. PUBLICATION: Liu Y, Tong Q, Zhou Y, Lee HW, Yang JJ, Bühring HJ, Chen YT, Ha B, Chen CX, Yang Y, Zen K. Functional elements on SIRP $\alpha$  IgV domain mediate cell surface binding to CD47. *J Mol Biol.* 2007 Jan 19;365(3):680-93

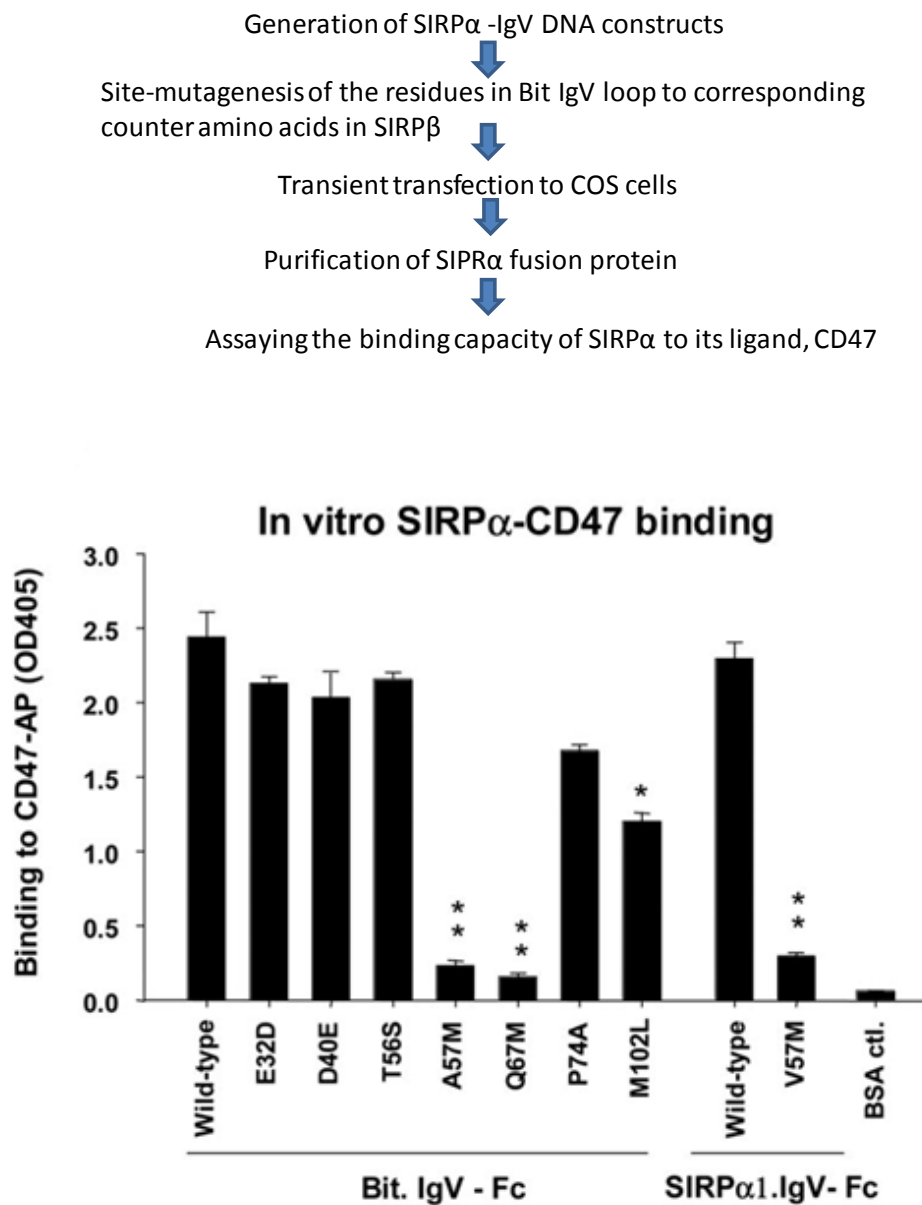


**Figure 5-11.** Ala57, Gln67, and Val57 were key amino acid residues mediating binding interaction of SIRP $\alpha$  to CD47.

## **REFERENCES**

1. Zychlinsky, A., Y. Weinrauch, and J. Weiss, *Introduction: Forum in immunology on neutrophils*. Microbes Infect, 2003. **5**(14): p. 1289-91.
2. Parham, P., *The immune system*. 2009(3rd edition): Garland Science.
3. Borregaard, N., *Neutrophils, from marrow to microbes*. Immunity, 2010. **33**(5): p. 657-70.
4. Gordy, C., et al., *Regulation of steady-state neutrophil homeostasis by macrophages*. Blood, 2011. **117**(2): p. 618-29.
5. Christopher, M.J. and D.C. Link, *Regulation of neutrophil homeostasis*. Curr Opin Hematol, 2007. **14**(1): p. 3-8.
6. Weinmann, P., et al., *A role for apoptosis in the control of neutrophil homeostasis in the circulation: insights from CD18-deficient mice*. Blood, 2003. **101**(2): p. 739-46.
7. Lieschke, G.J., et al., *Mice lacking granulocyte colony-stimulating factor have chronic neutropenia, granulocyte and macrophage progenitor cell deficiency, and impaired neutrophil mobilization*. Blood, 1994. **84**(6): p. 1737-46.
8. Schwarzenberger, P., et al., *Requirement of endogenous stem cell factor and granulocyte-colony-stimulating factor for IL-17-mediated granulopoiesis*. J Immunol, 2000. **164**(9): p. 4783-9.
9. Hernandez, P.A., et al., *Mutations in the chemokine receptor gene CXCR4 are associated with WHIM syndrome, a combined immunodeficiency disease*. Nat Genet, 2003. **34**(1): p. 70-4.

10. Broxmeyer, H.E., et al., *Rapid mobilization of murine and human hematopoietic stem and progenitor cells with AMD3100, a CXCR4 antagonist*. J Exp Med, 2005. **201**(8): p. 1307-18.
11. Nagasawa, T., et al., *Defects of B-cell lymphopoiesis and bone-marrow myelopoiesis in mice lacking the CXC chemokine PBSF/SDF-1*. Nature, 1996. **382**(6592): p. 635-8.
12. Zou, Y.R., et al., *Function of the chemokine receptor CXCR4 in haematopoiesis and in cerebellar development*. Nature, 1998. **393**(6685): p. 595-9.
13. Kawabata, K., et al., *A cell-autonomous requirement for CXCR4 in long-term lymphoid and myeloid reconstitution*. Proc Natl Acad Sci U S A, 1999. **96**(10): p. 5663-7.
14. Liles, W.C., et al., *Mobilization of hematopoietic progenitor cells in healthy volunteers by AMD3100, a CXCR4 antagonist*. Blood, 2003. **102**(8): p. 2728-30.
15. Suratt, B.T., et al., *Role of the CXCR4/SDF-1 chemokine axis in circulating neutrophil homeostasis*. Blood, 2004. **104**(2): p. 565-71.
16. Ma, Q., et al., *Impaired B-lymphopoiesis, myelopoiesis, and derailed cerebellar neuron migration in CXCR4- and SDF-1-deficient mice*. Proc Natl Acad Sci U S A, 1998. **95**(16): p. 9448-53.
17. Ma, Q., D. Jones, and T.A. Springer, *The chemokine receptor CXCR4 is required for the retention of B lineage and granulocytic precursors within the bone marrow microenvironment*. Immunity, 1999. **10**(4): p. 463-71.
18. Link, D.C., *Neutrophil homeostasis: a new role for stromal cell-derived factor-1*. Immunol Res, 2005. **32**(1-3): p. 169-78.

19. Lee, A., M.K. Whyte, and C. Haslett, *Inhibition of apoptosis and prolongation of neutrophil functional longevity by inflammatory mediators*. J Leukoc Biol, 1993. **54**(4): p. 283-8.
20. Liles, W.C. and S.J. Klebanoff, *Regulation of apoptosis in neutrophils--Fas track to death?* J Immunol, 1995. **155**(7): p. 3289-91.
21. Luo, H.R. and F. Loison, *Constitutive neutrophil apoptosis: mechanisms and regulation*. Am J Hematol, 2008. **83**(4): p. 288-95.
22. Doerschuk, C.M., et al., *Marginated pool of neutrophils in rabbit lungs*. J Appl Physiol, 1987. **63**(5): p. 1806-15.
23. Saverymuttu, S.H., et al., *The kinetics of <sup>111</sup>indium distribution following injection of <sup>111</sup>indium labelled autologous granulocytes in man*. Br J Haematol, 1985. **61**(4): p. 675-85.
24. Suratt, B.T., et al., *Neutrophil maturation and activation determine anatomic site of clearance from circulation*. Am J Physiol Lung Cell Mol Physiol, 2001. **281**(4): p. L913-21.
25. Kobayashi, S.D., J.M. Voyich, and F.R. DeLeo, *Regulation of the neutrophil-mediated inflammatory response to infection*. Microbes Infect, 2003. **5**(14): p. 1337-44.
26. Kelly, M., J.M. Hwang, and P. Kubes, *Modulating leukocyte recruitment in inflammation*. J Allergy Clin Immunol, 2007. **120**(1): p. 3-10.
27. Nathan, C., *Neutrophils and immunity: challenges and opportunities*. Nat Rev Immunol, 2006. **6**(3): p. 173-82.
28. Ryan, G.B. and G. Majno, *Acute inflammation. A review*. Am J Pathol, 1977. **86**(1): p. 183-276.

29. Murphy, P.M., *The molecular biology of leukocyte chemoattractant receptors*. Annu Rev Immunol, 1994. **12**: p. 593-633.
30. Zlotnik, A. and O. Yoshie, *Chemokines: a new classification system and their role in immunity*. Immunity, 2000. **12**(2): p. 121-7.
31. Witko-Sarsat, V., et al., *Neutrophils: molecules, functions and pathophysiological aspects*. Lab Invest, 2000. **80**(5): p. 617-53.
32. Ali, H., et al., *Chemoattractant receptor cross-desensitization*. J Biol Chem, 1999. **274**(10): p. 6027-30.
33. Sogawa, Y., et al., *Formyl peptide receptor 1 and 2 dual agonist inhibits human neutrophil chemotaxis by the induction of chemoattractant receptor cross-desensitization*. J Pharmacol Sci. **115**(1): p. 63-8.
34. Sabroe, I., et al., *Chemoattractant cross-desensitization of the human neutrophil IL-8 receptor involves receptor internalization and differential receptor subtype regulation*. J Immunol, 1997. **158**(3): p. 1361-9.
35. Foxman, E.F., J.J. Campbell, and E.C. Butcher, *Multistep navigation and the combinatorial control of leukocyte chemotaxis*. J Cell Biol, 1997. **139**(5): p. 1349-60.
36. Kitayama, J., et al., *Contrasting responses to multiple chemotactic stimuli in transendothelial migration: heterologous desensitization in neutrophils and augmentation of migration in eosinophils*. J Immunol, 1997. **158**(5): p. 2340-9.
37. Foxman, E.F., E.J. Kunkel, and E.C. Butcher, *Integrating conflicting chemotactic signals. The role of memory in leukocyte navigation*. J Cell Biol, 1999. **147**(3): p. 577-88.
38. Selvatici, R., et al., *Signal transduction pathways triggered by selective formylpeptide analogues in human neutrophils*. Eur J Pharmacol, 2006. **534**(1-3): p. 1-11.

39. Rabiet, M.J., E. Huet, and F. Boulay, *The N-formyl peptide receptors and the anaphylatoxin C5a receptors: an overview*. Biochimie, 2007. **89**(9): p. 1089-106.
40. Putney, J.W., Jr. and C.M. Ribeiro, *Signaling pathways between the plasma membrane and endoplasmic reticulum calcium stores*. Cell Mol Life Sci, 2000. **57**(8-9): p. 1272-86.
41. Hofer, A.M. and E.M. Brown, *Extracellular calcium sensing and signalling*. Nat Rev Mol Cell Biol, 2003. **4**(7): p. 530-8.
42. Nowycky, M.C. and A.P. Thomas, *Intracellular calcium signaling*. J Cell Sci, 2002. **115**(Pt 19): p. 3715-6.
43. Gerthoffer, W.T., *Mechanisms of vascular smooth muscle cell migration*. Circ Res, 2007. **100**(5): p. 607-21.
44. Ginis, I. and A.I. Tauber, *Activation mechanisms of adherent human neutrophils*. Blood, 1990. **76**(6): p. 1233-9.
45. Merrill, J.T., et al., *Two pathways of CD11b/CD18-mediated neutrophil aggregation with different involvement of protein kinase C-dependent phosphorylation*. J Immunol, 1990. **145**(8): p. 2608-15.
46. Panaro, M.A. and V. Mitolo, *Cellular responses to FMLP challenging: a mini-review*. Immunopharmacol Immunotoxicol, 1999. **21**(3): p. 397-419.
47. Pongracz, J. and J.M. Lord, *Superoxide production in human neutrophils: evidence for signal redundancy and the involvement of more than one PKC isoenzyme class*. Biochem Biophys Res Commun, 1998. **247**(3): p. 624-9.
48. Fontayne, A., et al., *Phosphorylation of p47phox sites by PKC alpha, beta II, delta, and zeta: effect on binding to p22phox and on NADPH oxidase activation*. Biochemistry, 2002. **41**(24): p. 7743-50.

49. Dekker, L.V., et al., *Protein kinase C-beta contributes to NADPH oxidase activation in neutrophils*. Biochem J, 2000. **347 Pt 1**: p. 285-9.
50. Li, Z., et al., *Roles of PLC-beta2 and -beta3 and PI3Kgamma in chemoattractant-mediated signal transduction*. Science, 2000. **287**(5455): p. 1046-9.
51. Merlot, S. and R.A. Firtel, *Leading the way: Directional sensing through phosphatidylinositol 3-kinase and other signaling pathways*. J Cell Sci, 2003. **116**(Pt 17): p. 3471-8.
52. Rickert, P., et al., *Leukocytes navigate by compass: roles of PI3Kgamma and its lipid products*. Trends Cell Biol, 2000. **10**(11): p. 466-73.
53. Wymann, M.P., et al., *Lipids on the move: phosphoinositide 3-kinases in leukocyte function*. Immunol Today, 2000. **21**(6): p. 260-4.
54. Bruyninckx, W.J., et al., *Phosphoinositide 3-kinase modulation of beta(3)-integrin represents an endogenous "braking" mechanism during neutrophil transmatrix migration*. Blood, 2001. **97**(10): p. 3251-8.
55. Sasaki, T., et al., *Function of PI3Kgamma in thymocyte development, T cell activation, and neutrophil migration*. Science, 2000. **287**(5455): p. 1040-6.
56. Sadhu, C., et al., *Essential role of phosphoinositide 3-kinase delta in neutrophil directional movement*. J Immunol, 2003. **170**(5): p. 2647-54.
57. Wang, F., et al., *Lipid products of PI(3)Ks maintain persistent cell polarity and directed motility in neutrophils*. Nat Cell Biol, 2002. **4**(7): p. 513-8.
58. Iannone, M.A., G. Wolberg, and T.P. Zimmerman, *Chemotactic peptide induces cAMP elevation in human neutrophils by amplification of the adenylate cyclase response to endogenously produced adenosine*. J Biol Chem, 1989. **264**(34): p. 20177-80.

59. Harvath, L., et al., *cAMP and human neutrophil chemotaxis. Elevation of cAMP differentially affects chemotactic responsiveness.* J Immunol, 1991. **146**(1): p. 224-32.
60. Derian, C.K., et al., *Inhibition of chemotactic peptide-induced neutrophil adhesion to vascular endothelium by cAMP modulators.* J Immunol, 1995. **154**(1): p. 308-17.
61. Borregaard, N. and J.B. Cowland, *Granules of the human neutrophilic polymorphonuclear leukocyte.* Blood, 1997. **89**(10): p. 3503-21.
62. Borregaard, N., O.E. Sorensen, and K. Theilgaard-Monch, *Neutrophil granules: a library of innate immunity proteins.* Trends Immunol, 2007. **28**(8): p. 340-5.
63. Faurschou, M. and N. Borregaard, *Neutrophil granules and secretory vesicles in inflammation.* Microbes Infect, 2003. **5**(14): p. 1317-27.
64. Nourshargh, S. and F.M. Marelli-Berg, *Transmigration through venular walls: a key regulator of leukocyte phenotype and function.* Trends Immunol, 2005. **26**(3): p. 157-65.
65. Ley, K., et al., *Getting to the site of inflammation: the leukocyte adhesion cascade updated.* Nat Rev Immunol, 2007. **7**(9): p. 678-89.
66. Mayadas, T.N. and X. Cullere, *Neutrophil beta2 integrins: moderators of life or death decisions.* Trends Immunol, 2005. **26**(7): p. 388-95.
67. Parkos, C.A., *Cell adhesion and migration. I. Neutrophil adhesive interactions with intestinal epithelium.* Am J Physiol, 1997. **273**(4 Pt 1): p. G763-8.
68. Liu, Y., et al., *Signal regulatory protein (SIRPalpha), a cellular ligand for CD47, regulates neutrophil transmigration.* J Biol Chem, 2002. **277**(12): p. 10028-36.
69. Liu, Y., et al., *The role of CD47 in neutrophil transmigration. Increased rate of migration correlates with increased cell surface expression of CD47.* J Biol Chem, 2001. **276**(43): p. 40156-66.



70. Liu, Y., et al., *SIRPbeta1 is expressed as a disulfide-linked homodimer in leukocytes and positively regulates neutrophil transepithelial migration*. J Biol Chem, 2005. **280**(43): p. 36132-40.
71. Parkos, C.A., et al., *CD47 mediates post-adhesive events required for neutrophil migration across polarized intestinal epithelia*. J Cell Biol, 1996. **132**(3): p. 437-50.
72. Kubes, P. and S.M. Kerfoot, *Leukocyte recruitment in the microcirculation: the rolling paradigm revisited*. News Physiol Sci, 2001. **16**: p. 76-80.
73. Diamond, M.S., et al., *ICAM-1 (CD54): a counter-receptor for Mac-1 (CD11b/CD18)*. J Cell Biol, 1990. **111**(6 Pt 2): p. 3129-39.
74. Sengelov, H., et al., *Subcellular localization and dynamics of Mac-1 (alpha m beta 2) in human neutrophils*. J Clin Invest, 1993. **92**(3): p. 1467-76.
75. Pohlman, T.H., et al., *An endothelial cell surface factor(s) induced in vitro by lipopolysaccharide, interleukin 1, and tumor necrosis factor-alpha increases neutrophil adherence by a CDw18-dependent mechanism*. J Immunol, 1986. **136**(12): p. 4548-53.
76. Zimmerman, G.A. and T.M. McIntyre, *Neutrophil adherence to human endothelium in vitro occurs by CDw18 (Mo1, MAC-1/LFA-1/GP 150,95) glycoprotein-dependent and -independent mechanisms*. J Clin Invest, 1988. **81**(2): p. 531-7.
77. Wallis, W.J., et al., *Human monocyte adherence to cultured vascular endothelium: monoclonal antibody-defined mechanisms*. J Immunol, 1985. **135**(4): p. 2323-30.
78. Smith, C.W., et al., *Cooperative interactions of LFA-1 and Mac-1 with intercellular adhesion molecule-1 in facilitating adherence and transendothelial migration of human neutrophils in vitro*. J Clin Invest, 1989. **83**(6): p. 2008-17.

79. Ding, Z.M., et al., *Relative contribution of LFA-1 and Mac-1 to neutrophil adhesion and migration*. J Immunol, 1999. **163**(9): p. 5029-38.
80. Zen, K. and C.A. Parkos, *Leukocyte-epithelial interactions*. Curr Opin Cell Biol, 2003. **15**(5): p. 557-64.
81. Petri, B. and M.G. Bixel, *Molecular events during leukocyte diapedesis*. FEBS J, 2006. **273**(19): p. 4399-407.
82. Cooper, D., et al., *Transendothelial migration of neutrophils involves integrin-associated protein (CD47)*. Proc Natl Acad Sci U S A, 1995. **92**(9): p. 3978-82.
83. Parkos, C.A., *Molecular events in neutrophil transepithelial migration*. Bioessays, 1997. **19**(10): p. 865-73.
84. Lindberg, F.P., et al., *Decreased resistance to bacterial infection and granulocyte defects in IAP-deficient mice*. Science, 1996. **274**(5288): p. 795-8.
85. Miyashita, M., et al., *Promotion of neurite and filopodium formation by CD47: roles of integrins, Rac, and Cdc42*. Mol Biol Cell, 2004. **15**(8): p. 3950-63.
86. Yoshida, H., et al., *Integrin-associated protein/CD47 regulates motile activity in human B-cell lines through CDC42*. Blood, 2000. **96**(1): p. 234-41.
87. Liu, Y., et al., *Functional elements on SIRPalpha IgV domain mediate cell surface binding to CD47*. J Mol Biol, 2007. **365**(3): p. 680-93.
88. Luscinskas, F.W., et al., *Leukocyte transendothelial migration: a junctional affair*. Semin Immunol, 2002. **14**(2): p. 105-13.
89. Ozaki, H., et al., *Cutting edge: combined treatment of TNF-alpha and IFN-gamma causes redistribution of junctional adhesion molecule in human endothelial cells*. J Immunol, 1999. **163**(2): p. 553-7.

90. Ostermann, G., et al., *JAM-1 is a ligand of the beta(2) integrin LFA-1 involved in transendothelial migration of leukocytes*. Nat Immunol, 2002. **3**(2): p. 151-8.
91. Libby, P., *Inflammatory mechanisms: the molecular basis of inflammation and disease*. Nutr Rev, 2007. **65**(12 Pt 2): p. S140-6.
92. Simon, S.I. and C.E. Green, *Molecular mechanics and dynamics of leukocyte recruitment during inflammation*. Annu Rev Biomed Eng, 2005. **7**: p. 151-85.
93. Lawrence, T. and D.W. Gilroy, *Chronic inflammation: a failure of resolution?* Int J Exp Pathol, 2007. **88**(2): p. 85-94.
94. Ayala, A., et al., *Mechanisms of immune resolution*. Crit Care Med, 2003. **31**(8 Suppl): p. S558-71.
95. Simon, H.U., *Neutrophil apoptosis pathways and their modifications in inflammation*. Immunol Rev, 2003. **193**: p. 101-10.
96. Butterfield, T.A., T.M. Best, and M.A. Merrick, *The dual roles of neutrophils and macrophages in inflammation: a critical balance between tissue damage and repair*. J Athl Train, 2006. **41**(4): p. 457-65.
97. Baniyash, M., *Chronic inflammation, immunosuppression and cancer: new insights and outlook*. Semin Cancer Biol, 2006. **16**(1): p. 80-8.
98. Terui, T., M. Ozawa, and H. Tagami, *Role of neutrophils in induction of acute inflammation in T-cell-mediated immune dermatosis, psoriasis: a neutrophil-associated inflammation-boosting loop*. Exp Dermatol, 2000. **9**(1): p. 1-10.
99. Gullberg, U., et al., *Processing and targeting of granule proteins in human neutrophils*. J Immunol Methods, 1999. **232**(1-2): p. 201-10.

100. Pham, C.T., *Neutrophil serine proteases: specific regulators of inflammation*. Nat Rev Immunol, 2006. **6**(7): p. 541-50.
101. Pham, C.T., *Neutrophil serine proteases fine-tune the inflammatory response*. Int J Biochem Cell Biol, 2008. **40**(6-7): p. 1317-33.
102. Abbott, R.E., et al., *Augmented inflammatory responses and altered wound healing in cathepsin G-deficient mice*. Arch Surg, 1998. **133**(9): p. 1002-6.
103. Olsson, I., et al., *Biosynthesis and processing of lactoferrin in bone marrow cells, a comparison with processing of myeloperoxidase*. Blood, 1988. **71**(2): p. 441-7.
104. Klebanoff, S.J., *Myeloperoxidase*. Proc Assoc Am Physicians, 1999. **111**(5): p. 383-9.
105. Rainger, G.E., A.F. Rowley, and G.B. Nash, *Adhesion-dependent release of elastase from human neutrophils in a novel, flow-based model: specificity of different chemotactic agents*. Blood, 1998. **92**(12): p. 4819-27.
106. Champagne, B., et al., *Proteolytic cleavage of ICAM-1 by human neutrophil elastase*. J Immunol, 1998. **161**(11): p. 6398-405.
107. Levesque, J.P., et al., *Vascular cell adhesion molecule-1 (CD106) is cleaved by neutrophil proteases in the bone marrow following hematopoietic progenitor cell mobilization by granulocyte colony-stimulating factor*. Blood, 2001. **98**(5): p. 1289-97.
108. Ginzberg, H.H., et al., *Neutrophil-mediated epithelial injury during transmigration: role of elastase*. Am J Physiol Gastrointest Liver Physiol, 2001. **281**(3): p. G705-17.
109. Masson, P.L., J.F. Heremans, and E. Schonke, *Lactoferrin, an iron-binding protein in neutrophilic leukocytes*. J Exp Med, 1969. **130**(3): p. 643-58.

110. Gallin, J.I., et al., *Human neutrophil-specific granule deficiency: a model to assess the role of neutrophil-specific granules in the evolution of the inflammatory response*. *Blood*, 1982. **59**(6): p. 1317-29.
111. Gallin, J.I., *Neutrophil specific granule deficiency*. *Annu Rev Med*, 1985. **36**: p. 263-74.
112. Pei, D., *Leukolysin/MMP25/MT6-MMP: a novel matrix metalloproteinase specifically expressed in the leukocyte lineage*. *Cell Res*, 1999. **9**(4): p. 291-303.
113. Borregaard, N., et al., *Stimulus-dependent secretion of plasma proteins from human neutrophils*. *J Clin Invest*, 1992. **90**(1): p. 86-96.
114. Cannarozzi, N.A. and S.E. Malawista, *Phagocytosis by human blood leukocytes measured by the uptake of <sup>131</sup>I-labeled human serum albumin: inhibitory and stimulatory effects of cytochalasin B*. *Yale J Biol Med*, 1973. **46**(3): p. 177-89.
115. Garwicz, D., A. Lindmark, and U. Gullberg, *Human cathepsin G lacking functional glycosylation site is proteolytically processed and targeted for storage in granules after transfection to the rat basophilic/mast cell line RBL or the murine myeloid cell line 32D*. *J Biol Chem*, 1995. **270**(47): p. 28413-8.
116. Liu, Y., et al., *The role of CD47 in neutrophil transmigration. Increased rate of migration correlates with increased cell surface expression of CD47*. *J Biol Chem*, 2001. **276**(43): p. 40156-66.
117. Vitale, N., et al., *The Small GTPase RalA controls exocytosis of large dense core secretory granules by interacting with ARF6-dependent phospholipase D1*. *J Biol Chem*, 2005. **280**(33): p. 29921-8.
118. Polzin, A., et al., *Ral-GTPase influences the regulation of the readily releasable pool of synaptic vesicles*. *Mol Cell Biol*, 2002. **22**(6): p. 1714-22.

119. Brymora, A., et al., *The brain exocyst complex interacts with RalA in a GTP-dependent manner: identification of a novel mammalian Sec3 gene and a second Sec15 gene*. J Biol Chem, 2001. **276**(32): p. 29792-7.
120. Balasubramanian, N., et al., *RalA-exocyst complex regulates integrin-dependent membrane raft exocytosis and growth signaling*. Curr Biol. **20**(1): p. 75-9.
121. Jullien-Flores, V., et al., *RLIP76, an effector of the GTPase Ral, interacts with the AP2 complex: involvement of the Ral pathway in receptor endocytosis*. J Cell Sci, 2000. **113** (Pt 16): p. 2837-44.
122. Matozaki, T., H. Nakanishi, and Y. Takai, *Small G-protein networks: their crosstalk and signal cascades*. Cell Signal, 2000. **12**(8): p. 515-24.
123. Takai, Y., T. Sasaki, and T. Matozaki, *Small GTP-binding proteins*. Physiol Rev, 2001. **81**(1): p. 153-208.
124. Abdel-Latif, D., et al., *Rac2 is critical for neutrophil primary granule exocytosis*. Blood, 2004. **104**(3): p. 832-9.
125. Abdel-Latif, D., M. Steward, and P. Lacy, *Neutrophil primary granule release and maximal superoxide generation depend on Rac2 in a common signalling pathway*. Can J Physiol Pharmacol, 2005. **83**(1): p. 69-75.
126. Ambruso, D.R., et al., *Human neutrophil immunodeficiency syndrome is associated with an inhibitory Rac2 mutation*. Proc Natl Acad Sci U S A, 2000. **97**(9): p. 4654-9.
127. Williams, D.A., et al., *Dominant negative mutation of the hematopoietic-specific Rho GTPase, Rac2, is associated with a human phagocyte immunodeficiency*. Blood, 2000. **96**(5): p. 1646-54.

128. Munafo, D.B., et al., *Rab27a is a key component of the secretory machinery of azurophilic granules in granulocytes*. Biochem J, 2007. **402**(2): p. 229-39.
129. Brzezinska, A.A., et al., *The Rab27a effectors JFC1/Slp1 and Munc13-4 regulate exocytosis of neutrophil granules*. Traffic, 2008. **9**(12): p. 2151-64.
130. Johnson, J.L., et al., *Rab27a and Rab27b regulate neutrophil azurophilic granule exocytosis and NADPH oxidase activity by independent mechanisms*. Traffic, 2010. **11**(4): p. 533-47.
131. Maridonneau-Parini, I. and J. de Gunzburg, *Association of rap1 and rap2 proteins with the specific granules of human neutrophils. Translocation to the plasma membrane during cell activation*. J Biol Chem, 1992. **267**(9): p. 6396-402.
132. Zhong, B., et al., *Human neutrophils utilize a Rac/Cdc42-dependent MAPK pathway to direct intracellular granule mobilization toward ingested microbial pathogens*. Blood, 2003. **101**(8): p. 3240-8.
133. Mitchell, T., et al., *Primary granule exocytosis in human neutrophils is regulated by Rac-dependent actin remodeling*. Am J Physiol Cell Physiol, 2008. **295**(5): p. C1354-65.
134. Lanzetti, L., *Actin in membrane trafficking*. Curr Opin Cell Biol, 2007. **19**(4): p. 453-8.
135. Mocsai, A., et al., *Kinase pathways in chemoattractant-induced degranulation of neutrophils: the role of p38 mitogen-activated protein kinase activated by Src family kinases*. J Immunol, 2000. **164**(8): p. 4321-31.
136. Jog, N.R., et al., *The actin cytoskeleton regulates exocytosis of all neutrophil granule subsets*. Am J Physiol Cell Physiol, 2007. **292**(5): p. C1690-700.
137. Rothwell, S.W., J. Nath, and D.G. Wright, *Interactions of cytoplasmic granules with microtubules in human neutrophils*. J Cell Biol, 1989. **108**(6): p. 2313-26.

138. Jahn, R. and R.H. Scheller, *SNAREs--engines for membrane fusion*. Nat Rev Mol Cell Biol, 2006. **7**(9): p. 631-43.
139. Stow, J.L., A.P. Manderson, and R.Z. Murray, *SNAREing immunity: the role of SNAREs in the immune system*. Nat Rev Immunol, 2006. **6**(12): p. 919-29.
140. Duman, J.G. and J.G. Forte, *What is the role of SNARE proteins in membrane fusion?* Am J Physiol Cell Physiol, 2003. **285**(2): p. C237-49.
141. Martin-Martin, B., et al., *Involvement of SNAP-23 and syntaxin 6 in human neutrophil exocytosis*. Blood, 2000. **96**(7): p. 2574-83.
142. Logan, M.R., et al., *A critical role for vesicle-associated membrane protein-7 in exocytosis from human eosinophils and neutrophils*. Allergy, 2006. **61**(6): p. 777-84.
143. Mollinedo, F., et al., *Role of vesicle-associated membrane protein-2, through Q-soluble N-ethylmaleimide-sensitive factor attachment protein receptor/R-soluble N-ethylmaleimide-sensitive factor attachment protein receptor interaction, in the exocytosis of specific and tertiary granules of human neutrophils*. J Immunol, 2003. **170**(2): p. 1034-42.
144. Barlic, J., et al., *Regulation of tyrosine kinase activation and granule release through beta-arrestin by CXCR1*. Nat Immunol, 2000. **1**(3): p. 227-33.
145. Mohn, H., et al., *The src-family protein-tyrosine kinase p59hck is located on the secretory granules in human neutrophils and translocates towards the phagosome during cell activation*. Biochem J, 1995. **309** ( Pt 2): p. 657-65.
146. Gutkind, J.S. and K.C. Robbins, *Translocation of the FGR protein-tyrosine kinase as a consequence of neutrophil activation*. Proc Natl Acad Sci U S A, 1989. **86**(22): p. 8783-7.



147. Mocsai, A., et al., *Adhesion-dependent degranulation of neutrophils requires the Src family kinases Fgr and Hck*. J Immunol, 1999. **162**(2): p. 1120-6.
148. Sengelov, H., L. Kjeldsen, and N. Borregaard, *Control of exocytosis in early neutrophil activation*. J Immunol, 1993. **150**(4): p. 1535-43.
149. Laudanna, C., et al., *Sulfatides trigger increase of cytosolic free calcium and enhanced expression of tumor necrosis factor-alpha and interleukin-8 mRNA in human neutrophils. Evidence for a role of L-selectin as a signaling molecule*. J Biol Chem, 1994. **269**(6): p. 4021-6.
150. Ng-Sikorski, J., et al., *Calcium signaling capacity of the CD11b/CD18 integrin on human neutrophils*. Exp Cell Res, 1991. **195**(2): p. 504-8.
151. Fuortes, M., W.W. Jin, and C. Nathan, *Adhesion-dependent protein tyrosine phosphorylation in neutrophils treated with tumor necrosis factor*. J Cell Biol, 1993. **120**(3): p. 777-84.
152. Berton, G., et al., *Beta 2 integrin-dependent protein tyrosine phosphorylation and activation of the FGR protein tyrosine kinase in human neutrophils*. J Cell Biol, 1994. **126**(4): p. 1111-21.
153. Agwu, D.E., et al., *Choline-linked phosphoglycerides. A source of phosphatidic acid and diglycerides in stimulated neutrophils*. J Biol Chem, 1989. **264**(3): p. 1405-13.
154. Fallman, M., et al., *Complement receptor-mediated phagocytosis is associated with accumulation of phosphatidylcholine-derived diglyceride in human neutrophils. Involvement of phospholipase D and direct evidence for a positive feedback signal of protein kinase*. J Biol Chem, 1992. **267**(4): p. 2656-63.

155. Sjolín, C., O. Stendahl, and C. Dahlgren, *Calcium-induced translocation of annexins to subcellular organelles of human neutrophils*. Biochem J, 1994. **300** ( Pt 2): p. 325-30.
156. Francis, J.W., et al., *Human neutrophil annexin I promotes granule aggregation and modulates Ca(2+)-dependent membrane fusion*. J Clin Invest, 1992. **90**(2): p. 537-44.
157. Shirakawa, R., et al., *Tuberous sclerosis tumor suppressor complex-like complexes act as GTPase-activating proteins for Ral GTPases*. J Biol Chem, 2009. **284**(32): p. 21580-8.
158. Wolthuis, R.M., et al., *Ras-dependent activation of the small GTPase Ral*. Curr Biol, 1998. **8**(8): p. 471-4.
159. Murai, H., et al., *Characterization of Ral GDP dissociation stimulator-like (RGL) activities to regulate c-fos promoter and the GDP/GTP exchange of Ral*. J Biol Chem, 1997. **272**(16): p. 10483-90.
160. Wolthuis, R.M., et al., *Stimulation of gene induction and cell growth by the Ras effector Rlf*. EMBO J, 1997. **16**(22): p. 6748-61.
161. Urano, T., R. Emkey, and L.A. Feig, *Ral-GTPases mediate a distinct downstream signaling pathway from Ras that facilitates cellular transformation*. EMBO J, 1996. **15**(4): p. 810-6.
162. Hofer, F., R. Berdeaux, and G.S. Martin, *Ras-independent activation of Ral by a Ca(2+)-dependent pathway*. Curr Biol, 1998. **8**(14): p. 839-42.
163. Wolthuis, R.M., et al., *Activation of the small GTPase Ral in platelets*. Mol Cell Biol, 1998. **18**(5): p. 2486-91.
164. Bhattacharya, M., et al., *Beta-arrestins regulate a Ral-GDS Ral effector pathway that mediates cytoskeletal reorganization*. Nat Cell Biol, 2002. **4**(8): p. 547-55.

165. Chardin, P. and A. Tavitian, *Coding sequences of human ralA and ralB cDNAs*. Nucleic Acids Res, 1989. **17**(11): p. 4380.
166. Jilkina, O. and R.P. Bhullar, *Generation of antibodies specific for the RalA and RalB GTP-binding proteins and determination of their concentration and distribution in human platelets*. Biochim Biophys Acta, 1996. **1314**(1-2): p. 157-66.
167. Hinoi, T., et al., *Post-translational modifications of Ras and Ral are important for the action of Ral GDP dissociation stimulator*. J Biol Chem, 1996. **271**(33): p. 19710-6.
168. van Dam, E.M. and P.J. Robinson, *Ral: mediator of membrane trafficking*. Int J Biochem Cell Biol, 2006. **38**(11): p. 1841-7.
169. Lipschutz, J.H. and K.E. Mostov, *Exocytosis: the many masters of the exocyst*. Curr Biol, 2002. **12**(6): p. R212-4.
170. He, B. and W. Guo, *The exocyst complex in polarized exocytosis*. Curr Opin Cell Biol, 2009. **21**(4): p. 537-42.
171. Camonis, J.H. and M.A. White, *Ral GTPases: corrupting the exocyst in cancer cells*. Trends Cell Biol, 2005. **15**(6): p. 327-32.
172. Moskalenko, S., et al., *Ral GTPases regulate exocyst assembly through dual subunit interactions*. J Biol Chem, 2003. **278**(51): p. 51743-8.
173. Moskalenko, S., et al., *The exocyst is a Ral effector complex*. Nat Cell Biol, 2002. **4**(1): p. 66-72.
174. Cascone, I., et al., *Distinct roles of RalA and RalB in the progression of cytokinesis are supported by distinct RalGEFs*. EMBO J, 2008. **27**(18): p. 2375-87.
175. Kawato, M., et al., *Regulation of platelet dense granule secretion by the Ral GTPase-exocyst pathway*. J Biol Chem, 2008. **283**(1): p. 166-74.

176. Rosse, C., et al., *RalB mobilizes the exocyst to drive cell migration*. Mol Cell Biol, 2006. **26**(2): p. 727-34.
177. Shipitsin, M. and L.A. Feig, *RalA but not RalB enhances polarized delivery of membrane proteins to the basolateral surface of epithelial cells*. Mol Cell Biol, 2004. **24**(13): p. 5746-56.
178. Nakashima, S., et al., *Small G protein Ral and its downstream molecules regulate endocytosis of EGF and insulin receptors*. EMBO J, 1999. **18**(13): p. 3629-42.
179. Rosse, C., et al., *RLIP, an effector of the Ral GTPases, is a platform for Cdk1 to phosphorylate epsin during the switch off of endocytosis in mitosis*. J Biol Chem, 2003. **278**(33): p. 30597-604.
180. Gundelfinger, E.D., M.M. Kessels, and B. Qualmann, *Temporal and spatial coordination of exocytosis and endocytosis*. Nat Rev Mol Cell Biol, 2003. **4**(2): p. 127-39.
181. Smith, S.C., et al., *Expression of ral GTPases, their effectors, and activators in human bladder cancer*. Clin Cancer Res, 2007. **13**(13): p. 3803-13.
182. Lim, K.H., et al., *Divergent roles for RalA and RalB in malignant growth of human pancreatic carcinoma cells*. Curr Biol, 2006. **16**(24): p. 2385-94.
183. Oxford, G., et al., *RalA and RalB: antagonistic relatives in cancer cell migration*. Cancer Res, 2005. **65**(16): p. 7111-20.
184. Falsetti, S.C., et al., *Geranylgeranyltransferase I inhibitors target RalB to inhibit anchorage-dependent growth and induce apoptosis and RalA to inhibit anchorage-independent growth*. Mol Cell Biol, 2007. **27**(22): p. 8003-14.
185. Chien, Y., et al., *RalB GTPase-mediated activation of the IkappaB family kinase TBK1 couples innate immune signaling to tumor cell survival*. Cell, 2006. **127**(1): p. 157-70.

186. Jenkins, G.M. and M.A. Frohman, *Phospholipase D: a lipid centric review*. Cell Mol Life Sci, 2005. **62**(19-20): p. 2305-16.
187. Vitale, N., et al., *Phospholipase D1: a key factor for the exocytotic machinery in neuroendocrine cells*. EMBO J, 2001. **20**(10): p. 2424-34.
188. Caumont, A.S., et al., *Regulated exocytosis in chromaffin cells. Translocation of ARF6 stimulates a plasma membrane-associated phospholipase D*. J Biol Chem, 1998. **273**(3): p. 1373-9.
189. Vitale, N., S. Chasserot-Golaz, and M.F. Bader, *Regulated secretion in chromaffin cells: an essential role for ARF6-regulated phospholipase D in the late stages of exocytosis*. Ann N Y Acad Sci, 2002. **971**: p. 193-200.
190. Cantor, S.B., T. Urano, and L.A. Feig, *Identification and characterization of Ral-binding protein 1, a potential downstream target of Ral GTPases*. Mol Cell Biol, 1995. **15**(8): p. 4578-84.
191. Zen, K., et al., *Response to genistein: assaying the activation status and chemotaxis efficacy of isolated neutrophils*. J Immunol Methods, 2006. **309**(1-2): p. 86-98.
192. Zen, K. and Y. Liu, *Role of different protein tyrosine kinases in fMLP-induced neutrophil transmigration*. Immunobiology, 2008. **213**(1): p. 13-23.
193. Macia, E., et al., *Dynasore, a cell-permeable inhibitor of dynamin*. Dev Cell, 2006. **10**(6): p. 839-50.
194. van Bergen En Henegouwen, P.M., *Eps15: a multifunctional adaptor protein regulating intracellular trafficking*. Cell Commun Signal, 2009. **7**: p. 24.
195. Benmerah, A., et al., *AP-2/Eps15 interaction is required for receptor-mediated endocytosis*. J Cell Biol, 1998. **140**(5): p. 1055-62.

196. Wang, L.H., K.G. Rothberg, and R.G. Anderson, *Mis-assembly of clathrin lattices on endosomes reveals a regulatory switch for coated pit formation*. J Cell Biol, 1993. **123**(5): p. 1107-17.
197. Sandvig, K., et al., *Acidification of the cytosol inhibits endocytosis from coated pits*. J Cell Biol, 1987. **105**(2): p. 679-89.
198. Sandvig, K., et al., *Inhibition of endocytosis from coated pits by acidification of the cytosol*. J Cell Biochem, 1988. **36**(1): p. 73-81.
199. Joliot, A. and A. Prochiantz, *Transduction peptides: from technology to physiology*. Nat Cell Biol, 2004. **6**(3): p. 189-96.
200. Schwarze, S.R. and S.F. Dowdy, *In vivo protein transduction: intracellular delivery of biologically active proteins, compounds and DNA*. Trends Pharmacol Sci, 2000. **21**(2): p. 45-8.
201. Schwarze, S.R., K.A. Hruska, and S.F. Dowdy, *Protein transduction: unrestricted delivery into all cells?* Trends Cell Biol, 2000. **10**(7): p. 290-5.
202. Kawai, M., et al., *Ral GDP dissociation stimulator and Ral GTPase are involved in myocardial hypertrophy*. Hypertension, 2003. **41**(4): p. 956-62.
203. Liu, Y., et al., *Human junction adhesion molecule regulates tight junction resealing in epithelia*. J Cell Sci, 2000. **113** ( Pt 13): p. 2363-74.
204. de Vries, H.E., et al., *Signal-regulatory protein alpha-CD47 interactions are required for the transmigration of monocytes across cerebral endothelium*. J Immunol, 2002. **168**(11): p. 5832-9.
205. Faltynek, C.R., et al., *Damnacanthal is a highly potent, selective inhibitor of p56lck tyrosine kinase activity*. Biochemistry, 1995. **34**(38): p. 12404-10.

206. Hiramatsu, T., et al., *Induction of normal phenotypes in ras-transformed cells by damnacanthol from Morinda citrifolia*. Cancer Lett, 1993. **73**(2-3): p. 161-6.
207. Hiwasa, T., et al., *GDNF-induced neurite formation was stimulated by protein kinase inhibitors and suppressed by Ras inhibitors*. Neurosci Lett, 1997. **238**(3): p. 115-8.
208. Liu, Y., et al., *Regulation of leukocyte transmigration: cell surface interactions and signaling events*. J Immunol, 2004. **172**(1): p. 7-13.
209. Molina, T.J., et al., *Profound block in thymocyte development in mice lacking p56lck*. Nature, 1992. **357**(6374): p. 161-4.
210. Brumell, J.H., et al., *Endogenous reactive oxygen intermediates activate tyrosine kinases in human neutrophils*. J Biol Chem, 1996. **271**(3): p. 1455-61.
211. Colicelli, J., *Human RAS superfamily proteins and related GTPases*. Sci STKE, 2004. **2004**(250): p. RE13.
212. Macaluso, M., et al., *Ras family genes: an interesting link between cell cycle and cancer*. J Cell Physiol, 2002. **192**(2): p. 125-30.
213. Oxford, G. and D. Theodorescu, *Ras superfamily monomeric G proteins in carcinoma cell motility*. Cancer Lett, 2003. **189**(2): p. 117-28.
214. Reuther, G.W. and C.J. Der, *The Ras branch of small GTPases: Ras family members don't fall far from the tree*. Curr Opin Cell Biol, 2000. **12**(2): p. 157-65.
215. M'Rabet, L., et al., *Differential fMet-Leu-Phe- and platelet-activating factor-induced signaling toward Ral activation in primary human neutrophils*. J Biol Chem, 1999. **274**(31): p. 21847-52.
216. Schwarze, S.R., et al., *In vivo protein transduction: delivery of a biologically active protein into the mouse*. Science, 1999. **285**(5433): p. 1569-72.

217. Choi, M., et al., *Inhibition of NF-kappaB by a TAT-NEMO-binding domain peptide accelerates constitutive apoptosis and abrogates LPS-delayed neutrophil apoptosis.* Blood, 2003. **102**(6): p. 2259-67.
218. Gao, X.P., et al., *Blockade of class IA phosphoinositide 3-kinase in neutrophils prevents NADPH oxidase activation- and adhesion-dependent inflammation.* J Biol Chem, 2007. **282**(9): p. 6116-25.
219. Chang, K.J., V. Bennett, and P. Cuatrecasas, *Membrane receptors as general markers for plasma membrane isolation procedures. The use of 125-I-labeled wheat germ agglutinin, insulin, and cholera toxin.* J Biol Chem, 1975. **250**(2): p. 488-500.
220. Wolfe, B.L. and J. Trejo, *Clathrin-dependent mechanisms of G protein-coupled receptor endocytosis.* Traffic, 2007. **8**(5): p. 462-70.
221. Heuser, J.E. and R.G. Anderson, *Hypertonic media inhibit receptor-mediated endocytosis by blocking clathrin-coated pit formation.* J Cell Biol, 1989. **108**(2): p. 389-400.
222. Manara, F.S., J. Chin, and D.L. Schneider, *Role of degranulation in activation of the respiratory burst in human neutrophils.* J Leukoc Biol, 1991. **49**(5): p. 489-98.
223. Gibson, A.E., et al., *Phenylarsine oxide inhibition of endocytosis: effects on asialofetuin internalization.* Am J Physiol, 1989. **257**(2 Pt 1): p. C182-4.
224. Albright, C.F., et al., *Characterization of a guanine nucleotide dissociation stimulator for a ras-related GTPase.* EMBO J, 1993. **12**(1): p. 339-47.
225. Jullien-Flores, V., et al., *Bridging Ral GTPase to Rho pathways. RLIP76, a Ral effector with CDC42/Rac GTPase-activating protein activity.* J Biol Chem, 1995. **270**(38): p. 22473-7.



226. Makino, A., et al., *Control of neutrophil pseudopods by fluid shear: role of Rho family GTPases*. Am J Physiol Cell Physiol, 2005. **288**(4): p. C863-71.
227. Cicchetti, G., P.G. Allen, and M. Glogauer, *Chemotactic signaling pathways in neutrophils: from receptor to actin assembly*. Crit Rev Oral Biol Med, 2002. **13**(3): p. 220-8.
228. Mollinedo, F., et al., *Localization of rap1 and rap2 proteins in the gelatinase-containing granules of human neutrophils*. FEBS Lett, 1993. **326**(1-3): p. 209-14.

Sarah Crespi <screspi@asbmb.org>  
from

hide details Apr 25  
(1 day ago)

to Celia Xiaojing Chen <celiachen.chen@gmail.com>

date Mon, Apr 25, 2011 at 4:06 PM

subject RE: citation (JBC Feedback Form)

Greetings,

As the author of the paper, you may include any or all of it in your dissertation. Please cite the original publication according to the style outlines on our permissions page: [http://www.jbc.org/site/misc/Copyright\\_Permission.xhtml](http://www.jbc.org/site/misc/Copyright_Permission.xhtml)

Congratulations on your impending graduation,

Sarah Crespi  
- Hide quoted text -

-----Original Message-----

From: Celia Xiaojing Chen [mailto:[celiachen.chen@gmail.com](mailto:celiachen.chen@gmail.com)]  
Sent: Monday, April 25, 2011 4:06 PM  
To: [jbc-feedback@highwire.stanford.edu](mailto:jbc-feedback@highwire.stanford.edu)  
Cc: [celiachen.chen@gmail.com](mailto:celiachen.chen@gmail.com)  
Subject: citation (JBC Feedback Form)

-----  
Comments sent via JBC Feedback Page  
-----

NAME: Celia Xiaojing Chen USER NAME: libnhm  
EMAIL: [celiachen.chen@gmail.com](mailto:celiachen.chen@gmail.com)  
IP ADDRESS: 131.96.39.122  
HOSTNAME: [CeliaChen-PC.gsu.edu](http://CeliaChen-PC.gsu.edu)  
PREVIOUS PAGE: <http://www.jbc.org/>  
BROWSER: Mozilla/5.0 (Windows; U; Windows NT 6.1; en-US) AppleWebKit/534.16 (KHTML, like Gecko) Chrome/10.0.648.205 Safari/534.16, JBC  
PROMOTIONAL USE: Granted  
SESSION ID: W6odokyITFzGLtqeUZsltA  
-----

COMMENTS:

Dear JBC Editor,  
I am a Ph.D student from Georgia State University, Department of Biology. I want to get the permission from JBC to cite my own paper (first author) for my dissertation writing.

paper information:

Control of Secondary Granule Release in Neutrophils by Ral GTPase.  
J Biol Chem. 2011 Apr 1;286(13):11724-33. Epub 2011 Jan 31  
Chen CX, Soto I, Guo YL, Liu Y.  
Thank you so much!

## Copyright Permission Policy

These guidelines apply to the reuse of articles, figures, charts and photos in the *Journal of Biological Chemistry*, *Molecular & Cellular Proteomics* and the *Journal of Lipid Research*.

### **For authors reusing their own material:**

Authors need **NOT** contact the journal to obtain rights to reuse their own material. They are automatically granted permission to do the following:

- Reuse the article in print collections of their own writing.
- Present a work orally in its entirety.
- Use an article in a thesis and/or dissertation.
- Reproduce an article for use in the author's courses. (If the author is employed by an academic institution, that institution also may reproduce the article for teaching purposes.)
- Reuse a figure, photo and/or table in future commercial and noncommercial works.
- Post a copy of the paper in PDF that you submitted via BenchPress.
  - Only authors who published their papers under the "Author's Choice" option may post the final edited PDFs created by the publisher to their own/departamental/university Web sites.
  - All authors may link to the journal site containing the final edited PDFs created by the publisher.

Please note that authors must include the following citation when using material that appeared in an ASBMB journal:

"This research was originally published in Journal Name. Author(s). Title. *Journal Name*. Year; Vol:pp-pp. © the American Society for Biochemistry and Molecular Biology."

### **For other parties using material for noncommercial use:**

Other parties are welcome to copy, distribute, transmit and adapt the work — at no cost and without permission — for noncommercial use as long as they attribute the work to the original source using the citation above.

Examples of noncommercial use include:

- Reproducing a figure for educational purposes, such as schoolwork or lecture presentations, with attribution.
- **Appending a reprinted article to a Ph.D. dissertation, with attribution.**

### **For other parties using material for commercial use:**

Navigate to the article of interest and click the "Request Permissions" button on the middle navigation bar. (See diagram at right.) It will walk you through the steps for obtaining permission for reuse.

Examples of commercial use by parties other than authors include:

- Reproducing a figure in a book published by a commercial publisher.
- Reproducing a figure in a journal article published by a commercial publisher.

Updated Nov. 10, 2009

[http://www.jbc.org/site/misc/Copyright\\_Permission.xhtml](http://www.jbc.org/site/misc/Copyright_Permission.xhtml)